Performance of Pile Supported Sign Structures
Final Report

Andrew Boeckmann, P.E., Research Engineer
Minh Uong, Graduate Research Assistant
J. Erik Loehr, Ph.D., P.E., Associate Professor

University of Missouri
Department of Civil and Environmental Engineering

WisDOT ID no. 0092-14-02
January 2015

RESEARCH & LIBRARY UNIT

WISCONSIN HIGHWAY RESEARCH PROGRAM

WISCONSIN DOT
PUTTING RESEARCH TO WORK

Disclaimer

This research was funded through the Wisconsin Highway Research Program by the Wisconsin Department of Transportation and the Federal Highway Administration under Project 0092-14-02. The contents of this report reflect the views of the authors who are responsible for the facts and accuracy of the data presented herein. The contents do not necessarily reflect the official views of the Wisconsin Department of Transportation or the Federal Highway Administration at the time of publication.

Technical Report Documentation Page

1. Report No.	2. Government Accession No	3. Recipient's Catalog No
4. Title and Subtitle Performance of Pile Supported Sign Structures		5. Report Date 6. Performing Organization Code
7. Authors Andrew Boeckmann, Minh Uong, J. Erik Loehr		8. Performing Organization Report No.
9. Performing Organization Name and Address University of Missouri Civil and Environmental Engineering E2509 Lafferre Hall Columbia, MO 65211-2200		10. Work Unit No. (TRAIS) 11. Contract or Grant No. 0092-14-02
12. Sponsoring Agency Name and Address Wisconsin Department of Transportation Research & Library Unit 4802 Sheboygan Ave. Rm 104 Madison, WI 53707		13. Type of Report and Period Covered 14. Sponsoring Agency Code
15. Supplementary Notes		

16. Abstract

Foundations for sign structures are subjected primarily to overturning loads, but published methods for designing driven pile groups only address groups subjected either to compression or uplift, not both simultaneously. A lateral load test of two four-pile groups therefore was conducted to evaluate load transfer among the piles, especially as the groups approach failure, and to evaluate potential design implications. The test consisted of pulling together two four-pile groups: one constructed with HP 10x42 H-piles and the other with 10.75-in. diameter closed-end steel pipe piles backfilled with concrete (CIP piles).

Load test measurements indicate the tension piles in both groups failed in geotechnical uplift before the test was terminated. Axial load and bending moment profiles along the length of the piles were created from strain gage and ShapeArrayAccel (SAA) measurements. Interpretation of the results suggests initial resistance to overturning is provided primarily by the axial force couple that develops in the compression and tension piles. As the axial load in the tension piles approaches the ultimate uplift resistance, the contribution of pile head bending to resisting the applied overturning moment appears to become more significant. These observations were examined by creating models of the pile groups using Ensoft *GROUP*. The calibrated models confirm the observed trends and suggest additional overturning capacity for the pile groups potentially can be realized by considering the contribution of pile head bending moments.

17. Key Words	18. Distribution Statement
Sign structure; overturning; driven pile; pile group; lateral load test	No restriction. This document is available to the public through the National Technical Information Service 5285 Port Royal Road Springfield VA 22161

19. Security Classif.(of this report)	19. Security Classif. (of this page)	20. No. of Pages	21. Price
Unclassified	Unclassified		

Form DOT F 1700.7 (8-72) Reproduction of completed page authorized

Acknowledgements

Financial Support

Wisconsin Department of Transportation

WisDOT Personnel

Robert Arndorfer
Jeff Horsfall
Thao Vu
Andrew Zimmer

University Students, Faculty, and Staff

Dan Ding
Gunnar Goslin
Sajid Iqbal
Eric Lindsey
Aaron Schoen

Special Thanks

C&M Manufacturing Co., Curt Moore, President – for donating centralizers for the CIP piles

Geokon / John Flynn, Sales Engineer – for outstanding technical support with instrumentation during the load test.

Missouri Department of Transportation / Jen Harper, Research Engineer – for donating use of load test site.

Missouri University of Science and Technology / Ronaldo Luna – for donating use of vibrating wire DAQ

Executive Summary

Background

Sign structures in Wisconsin are often founded on groups of driven piles. Published methods for design of driven pile groups subjected to axial compression or uplift are readily available. However, overturning loads are predominant for sign foundations, where some piles are subjected to compression and others uplift. Currently available design methods do not address this condition. A lateral load test of two four-pile groups was therefore conducted to evaluate load transfer among the piles, especially as the groups approach failure, and evaluate potential design implications.

Load Test

The load test was performed in Warrensburg, Missouri, at a test site with a significant volume of published geotechnical test information, including data related to soil strength as well as both axial and lateral load tests of deep foundations. The site has 10 to 15 ft of stiff clay overburden above shale formations with highly variable strength. The test consisted of pulling together two four-pile groups: one constructed with HP10x42 H-piles and the other with 10.75-in. diameter closed-end steel pipe piles backfilled with concrete (CIP piles). Loads were applied 9 ft above the ground surface to simulate the overturning loads experienced by sign foundations. Test piles were instrumented with strain gages and ShapeArrayAccel (SAA) devices to monitor axial loads and bending moments. Displacements and rotations of the sign structures were monitored with LVDTs, dial gages, and wireline devices. Construction of the two pile groups was completed over the course of one week. The load test was performed two weeks later after the concrete had cured sufficiently.

Significant displacements and rotations were achieved during the load test, with the tops of the structures displacing 10 in. on average when the test was terminated. Measured displacements indicate the tension piles in both pile groups failed in geotechnical uplift before the test was terminated, displacing approximately 1.5 in. upward while the compression piles displaced less than 0.5 in downward. The H-pile group moved more laterally than the CIP pile group, most likely because the H-piles were loaded in the direction of their weak axis, which results in a lower moment of inertia and an orientation wherein the flanges of the pile “slice” through the soil. Axial load and bending moment along the piles were interpreted from strain gage data. Bending moment was also interpreted from the SAA measurements.

Interpretation

Axial load-displacement curves were interpreted from the test measurements. Curves determined for the H-pile and CIP pile groups are generally similar. Bending moment-displacement curves were also developed; mobilization of bending moment was generally linear and still increasing at the end of the load test, which suggests that additional bending resistance remained at the end of the test. Several plots were created to track mobilization of axial loads and bending moments as the applied load was increased. The results suggest initial resistance to overturning is provided primarily by the axial force couple that develops in the compression and tension piles. As the axial load in the tension piles approaches the ultimate uplift resistance, the contribution of pile head bending moments become more significant. These trends were examined by modeling the pile groups using Ensoft *GROUP*. The calibrated models confirmed the observed trends and suggest additional overturning resistance, beyond that calculated considering the axial pile resistance alone, can potentially be realized by considering the contribution of pile head bending moments.

Conclusions

The load tests achieved failure of both pile groups by geotechnical uplift of the tension piles. Interpretation of the considerable data set collected during the test suggests overturning load transfer for the four-pile groups typically employed by WisDOT for sign foundations is reasonably predicted from simple consideration of static equilibrium up to loads where the ultimate uplift resistance is approached. Design capacity for overturning of four-pile groups can therefore be calculated using (1) pile loads corresponding to the axial force couple that satisfies bending moment equilibrium of the rigid sign structures and (2) pile

capacities from appropriate design methods for axial and lateral loading of driven piles. Additional load carrying capacity, beyond that attributed to the axial force couple alone, can potentially be mobilized from pile head bending moments that develop as the force couple approaches the tension pile uplift capacity. Some design efficiency could be realized by considering such additional capacity for extreme event loading cases if the structural capacity of the piles is sufficient and if some inelastic deformation can be tolerated. Additional load test data is needed to confirm and quantify the potential contribution from pile head bending resistance.

Table of Contents

Disclaimer i
Technical Report Documentation Page ii
Acknowledgements iii
Executive Summary iv
1. Introduction 1
2. Literature Review 2
2.1 Existing Methods for Design of Pile Groups Subject to Overturning 2
2.2 Other Studies Relevant to Pile Groups Subject to Overturning 3
3. Field Testing Program 5
3.1 Load Test Site 5
3.2 Design of Pile Groups 7
3.3 Construction of Pile Groups 10
3.4 Instrumentation and Data Acquisition 26
3.4.1 H-Pile Strain Gages 26
3.4.2 CIP Pile Strain Gages 29
3.4.3 Shape Array Accelerometer 30
3.4.4 Linear Voltage Displacement Transducers (LVDTs) 31
3.4.5 Dial Gages 33
3.4.6 Wireline Devices 34
3.4.7 Load Measurements 35
3.5 Testing Procedure and Load Test Summary 36
4. Experimental Results 40
4.1 Displacements, Rotations, and Load-Displacement Curves 40
4.2 Displacement Profiles from SAA 43
4.3 Methodology for Interpretation of Axial Force and Bending Moment 44
4.4 Pile Structural Response 46
4.4.1 Axial Force Profiles 46
4.4.2 Bending Moment Profiles from Strain Gage Data 48
4.4.3 Bending Moment Profiles from SAA Data 52
5. Analysis of Experimental Results 55
5.1 Comparison of Applied Test Load to “Typical” Sign Loading 55
5.2 Compiled Results and Static Equilibrium Model 55
5.3 Comparison with Ensoft *GROUP* Model 61
5.3.1 GROUP Model for CIP Pile Structure 62
5.3.2 GROUP Model for H-Pile Structure 64
5.3.3 Predictions at Greater Loads from GROUP Models 67

5.3.4 Summary of Observations from GROUP Models 68
6. Conclusions & Recommendations 70
References 71
Appendix A – Plans and Calculations from WisDOT Sign Structure S-05-168 ..... A-1
Appendix B – Construction Plans B-1
Appendix C – Driven Pile Logs C-1

Table of Figures

Figure 3.1. Location of Warrensburg Load Test Site. (Google Earth, 2011a) 5

Figure 3.2. Location of Warrensburg Load Test Site east of Warrensburg, MO on U.S. Highway 50, near the intersection with State Highway HH. (Google Earth, 2011b) 6

Figure 3.3. Measured values of $\boldsymbol{UCS}$ shown with mean and standard deviation values for Warrensburg Load Test Site. 6

Figure 3.4. Typical pile group plan for WisDOT sign foundation. Primary direction of loading is along the longitudinal axis of the pile cap (i.e. “upward” in the figure). 7

Figure 3.5. Schematic elevation view of loading mechanism. 8

Figure 3.6. Axial load displacement curve for tension piles. 9

Figure 3.7. Bending moment predicted by *GROUP* model for the ultimate applied elevated load of 95 kips. For the *GROUP* model, Pile #1 is compression and Pile #2 is tension. Bending moment profiles are nearly equivalent for compression and tension piles, so the lines shown are indistinguishable. 9

Figure 3.8. Crew places template for piles on level work surface 10

Figure 3.9. Crane and hammer leads used for pile driving. 11

Figure 3.10. Crew monitoring pile driving. 12

Figure 3.11. Hammer stroke was monitored using rings on ram. 13

Figure 3.12. 1-ft intervals marked on piles. 13

Figure 3.13. Crew marked piles every 5 blows once the piles began penetrating shale. Pile driving was terminated when the piles penetrated 2 in. or less in 5 blows. 14

Figure 3.14. Measured final pile penetration after driving. 15

Figure 3.15. Pile penetration for all piles. Last point for each log is extrapolated based on observed penetration for last partial foot of driving. 15

Figure 3.16. Marking pile lengths to be removed. (H-Piles were delivered in various lengths; variation in stickup shown is not an indication of variation in penetration.) 16

Figure 3.17. Placing instrumented pipe into CIP pile. 17

Figure 3.18. Placing concrete in CIP-2. 18

Figure 3.19. Damaged bar for CIP-1 18

Figure 3.20. CIP Pile group after driving, prior to placement of sand. 19

Figure 3.21. H-pile group after driving, prior to placement of sand. 19

Figure 3.22. Crew levels sand prior to placing forms for pile cap. 20

Figure 3.23. Forms and cage in place for H-pile cap prior to placing concrete. 21

Figure 3.24. H-pile cap and stem cages formed together prior to placing concrete for the pile caps. 21

Figure 3.25. Stem cage formed with pile cap cage prior to placement of concrete for pile cap. 22

Figure 3.26. Placing concrete for H-pile cap. 22

Figure 3.27. Performing slump test in accordance with ASTM C143 (2012) on concrete from each pour. 23

Figure 3.28. Finishing concrete for pile cap. 23

Figure 3.29. Finished concrete for pile cap with beveled keyway at joint between cap and stem. 24

Figure 3.30. Forming stems. Pipes for threadbar load application are in place. 24

Figure 3.31. Placing concrete for stems. 25

Figure 3.32. Removing sand from beneath pile cap to create a gap between cap and ground surface. The gap prevents the cap from bearing on the ground surface during the application of overturning loads. 25

Figure 3.33. Completed pile cap-stem structures. 26

Figure 3.34. Welding Geokon 4000 gages to pile head after driving. 27

Figure 3.35. Installed Geokon 4000 gage at pile tip. 27

Figure 3.36. Welding angle section above installed gages. Gage cables were wrapped in aluminum foil to protect from heat. 28

Figure 3.37. DAQ used to read Geokon 4000 gages (Luna, 2014). 28

Figure 3.38. Spot welding Geokon 4150 gage to instrumented pipe. Completed gage with protective cover can be seen on bottom of pipe. 29

Figure 3.39. Geokon datalogger LC-2x16 in lab (left) and field (right). 29

Figure 3.40. SAA joint and segment. 30

Figure 3.41. SAA inserted in HP-2 and CIP-3. 31

Figure 3.42. LVDTs positioned above rear of pile caps to measure uplift. 31

Figure 3.43. LVDTs positioned against front of pile caps to measure lateral deflection. One LVDT was mounted directly above the other to measure rotation. 32

Figure 3.44. Four reference beams used during the test. 32

Figure 3.45. Installation of uplift LVDT. 33

Figure 3.46. Dial gages used to measure uplift at the back of the pile cap. 33

Figure 3.47. Wireline devices on the CIP pile group. Devices were installed in line with compression (left) and tension (right) piles. 34

Figure 3.48. Installing wireline device. 34

Figure 3.49. Hydraulic jack on threadbar applying load to pile structure through a bearing plate. 35

Figure 3.50. Hydraulic pump with pressure gage. 36

Figure 3.51. View of load test with CIP pile group on left and H-pile group on right. Canopy housing computers and DAQs is in background. 36

Figure 3.52. View of load test with H-pile group on left and CIP pile group on right. 37

Figure 3.53. Resetting stroke of the hydraulic jack during the load test. 37

Figure 3.54. Pile structures during final load step. CIP pile cap is at left and H-pile cap is at right. 38

Figure 3.55. Pile structures during final load step. H-pile cap is at left and CIP pile cap is at right. 38

Figure 3.56. H-pile cap during the final load step. 39

Figure 3.57. CIP pile cap during the final load step. 39

Figure 4.1. Load-displacement curves associated with tension piles. Solid symbols are for H-piles and open symbols are for CIP piles. Dashed lines are for wireline devices. 42

Figure 4.2. Load-displacement curves associated with compression piles. Solid symbols are for H-piles and open symbols are for CIP piles. Dashed lines are for wireline devices. 42

Figure 4.3. Load-displacement curves associated with lateral movement of the pile structures. Solid symbols are for the H-pile structure and open symbols are for the CIP pile structure. Dashed lines are for wireline devices. 43

Figure 4.4. Displacement profiles from SAA data for piles (a) HP-2 and (b) CIP-3. 44

Figure 4.5. Bending stiffness curve for CIP piles. 46

Figure 4.6. Axial force for (a) CIP-1, (b) CIP-2, (c) CIP-3, and (d) CIP-4. Compression forces are positive. Weight of cap included per Eq. 4.2. Topmost gages in CIP-1 were damaged during construction (Section 3.4.2). 47

Figure 4.7. Axial force for (a) HP-1, (b) HP-2, (c) HP-3, and (d) HP-4. Compression forces are positive. Weight of cap included per Eq. 4.2. 48

Figure 4.8. Bending moments for (a) CIP-1, (b) CIP-2, (c) CIP-3, and (d) CIP-4. Bending moments from SAA data are included for the final load step for CIP-3 for the sake of comparison. 50

Figure 4.9. Bending moments for (a) HP-1, (b) HP-2, (c) HP-3, and (d) HP-4. Bending moments from SAA data are included for the final load step for HP-2. Large symbols indicate locations of non-functioning strain gages. 51

Figure 4.10. SAA data for CIP-3. 53

Figure 4.11. SAA data for HP-2. 54

Figure 5.1. Axial load-displacement curves. Axial loads are the loads measured in the piles plus 11.7 kips, the weight of the each structure divided by four piles. 56

Figure 5.2. Bending moment-displacement curves. Data are from strain gages unless SAA is indicated in the legend..... 57

Figure 5.3. Axial load progression plots for (a) H-pile group and (b) CIP pile group. Lines are offset from origin because of the weight of the structure. 58

Figure 5.4. Bending moment progression plot. 59

Figure 5.5. Bending moment equilibrium of CIP pile structure, calculated about the center of the base of the structures. Total resisting moment is the sum of the axial force couple and the pile head moments. Dashed lines are used for the ultimate load step to indicate the results from CIP-2 and CIP-3 were doubled since there were no data collected for CIP-1 and CIP-4. 60

Figure 5.6. Axial force equilibrium of the CIP pile structure. Dashed lines are used for the ultimate load step to indicate the results from CIP-2 and CIP-3 were doubled since there were no data collected for CIP-1 and CIP-4. 61

Figure 5.7. Axial load-displacement curve used to calibrate *GROUP* model for CIP pile structure. 62

Figure 5.8. Results of calibrated *GROUP* model for CIP pile structure at maximum test load (99 kip): (a) displacement profile and (b) bending moment profile. 63

Figure 5.9. Static equilibrium from *GROUP* model for CIP pile structure. Solid lines and symbols used for measurements; dashed lines and open symbols used for *GROUP* results. Note the total resisting moment predicted by *GROUP* is perfectly coincident with the applied moment. 63

Figure 5.10. CIP pile head bending moment-displacement curves, including those predicted by *GROUP*. *GROUP* predicts nearly equal bending moments in all four pile heads. 64

Figure 5.11. Axial load-displacement curves used to calibrate *GROUP* models. 65

Figure 5.12. Results of axial match calibrated *GROUP* model for H-pile structure at maximum test load (99 kip): (a) displacement profile and (b) bending moment profile. 66

Figure 5.13. H-pile head bending moment-displacement curves, including those predicted by *GROUP*. *GROUP* predicts nearly equal bending moments in all four pile heads. 66

Figure 5.14. Applied load versus horizontal displacement from *GROUP* models. Solid lines and symbols used for *GROUP* results for actual loads from load test. Dashed lines and open symbols used for *GROUP* predictions beyond loads applied during test. Dotted lines and small symbols used for measured data. . 67

Figure 5.15. Pile head bending moment versus horizontal displacement from *GROUP* models. Solid lines and symbols used for *GROUP* results for actual loads from load test. Dashed lines and open symbols used for *GROUP* predictions beyond loads applied during test. Dotted lines and small symbols used for measured data. 68

Table of Tables

Table 3.1. Parameters used to develop *GROUP* model inputs for soil and rock..... 8

Table 3.2. Results of concrete testing..... 20

Table 4.1. Summary of displacements at end of final (99-kip) load step. For vertical displacements, up is negative..... 40

Table 4.2. Summary of rotations at end of final (99-kip) load step. For pitch values, rotation toward the opposite shaft (i.e. expected direction) is positive. 41

1. Introduction

The Wisconsin Department of Transportation (WisDOT) often employs four-pile foundation groups to support large sign structures, which are subject to a unique loading that is dominated by a large overturning moment. On a national level, design rationale for such loading is lacking. Design methods that predict individual pile loads (e.g. pile group analysis software such as Ensoft's *GROUP*) are available, but the AAHSTO strength limit resistance factors for single piles in uplift are rather low, resulting in piles that are likely overdesigned for the subject loading.

A load test of two sign structures similar to those employed by WisDOT, one with H-piles and the other with cast-in-place (CIP) pipe piles, was conducted to evaluate load transfer among the piles, determine the appropriate geotechnical limit state, and evaluate potential design implications. This report documents the load test and accompanying analyses. Background information related to overturning of pile groups is presented before documenting the experiment, which included design and construction of the pile structures, instrumentation, and the load test, itself. All results from the extensive instrumentation system are presented before analyzing two models of the data, one based on static equilibrium and the other on numerical methods. Finally, the results of the models are interpreted to develop recommendations for design and potential further research.

2. Literature Review

Existing methods for designing pile groups subject to overturning were investigated prior to designing the load test. Other research related to the topic was reviewed as well.

2.1 Existing Methods for Design of Pile Groups Subject to Overturning

The WisDOT Facilities Development Manual (2014) classifies sign structures into two categories, overhead sign supports and sign bridges. Overhead sign supports typically carry smaller signs, and the structures are typically designed by a sign fabricator. Sign bridges carry larger, informational signs, and the structures are designed by WisDOT's Bureau of Structures or a consulting engineer. Chapter 39 of the WisDOT Bridge Manual (2009) provides standard details for sign foundations involving single drilled shafts for overhead sign supports and cantilever sign bridges. Project-specific foundation design is required for full span sign bridges and projects that do not meet the requirements for using the standard details. Typically, the project-specific foundations are also drilled shafts, but driven pile groups are frequently used as well for sites that are not suited for drilled shafts or spread footings.

Regarding the design of pile group foundations, Chapter 11 of the WisDOT Bridge Manual (2012) states the pile group capacity may be less than the sum of individual pile capacities for foundations in clay. The WisDOT Bridge Manual requires an equivalent pier analysis, the procedure for which is outlined in the AASHTO LRFD Bridge Design Specifications (2014), Sec. 10.7.3.9. The procedure involves computing two values for pile group capacity and using the lesser as the nominal capacity for pile groups in compression:

- The sum of the individual pile capacities, multiplied by an efficiency factor varying from 0.65 to 1 depending on pile spacing, the contact between the pile cap and ground surface, and the stiffness of the soil at the ground surface.
- The capacity of an "equivalent pier" bounded by the piles in the group and including the block of soil within the piles. The capacity of the equivalent pier is derived from the full shear strength on the sides of the pile group and tip resistance for the total base area below the piles.

Both the WisDOT and AASHTO manuals state that pile group capacity in sand is always controlled by the sum of the individual pile capacities.

Similarly, the AASHTO LRFD Bridge Design Specifications procedure for computing the uplift capacity of driven pile groups involves comparing the sum of the uplift capacities of the individual piles with the uplift capacity of an equivalent pier. For pile groups in sand, the uplift capacity of the equivalent pier is computed from the weight of soil assuming a load distribution of 1:4 (horizontal:vertical) from the base of the piles. For pile groups in clay, the uplift capacity of the equivalent pier is computed from shear strength along the sides of the pile group and the weight of the block (without load distribution).

The AASHTO equivalent pier analyses are rational for pile groups in either compression or uplift, but not both at the same time, as is the case for pile groups subject predominantly to overturning moments. A more rational approach for pile groups with large overturning moments is to determine the compression or tension load on each pile and then design the piles accordingly. The pile loads can be predicted from the applied loading and pile group configuration using stiffness-based methods implemented with computer software such as Ensoft *GROUP*. An example of such an approach is presented in Appendix A for WisDOT sign structure S-05-168. The design engineer used *Pile Group Analysis*, a computer program developed by Digital Canal, to predict axial forces in a four-pile group and an eight-pile group before proceeding with structural design of the pile caps.

Methods that predict individual pile loads for each pile in the group result in designs that are controlled geotechnically by uplift capacity. Uplift capacity of an individual pile is less than compression capacity, and for most cases of wind loading (i.e. those in which the wind direction is not prescribed), the designer must assume any of the piles in the group could be subject to either uplift or compression. In addition, the strength limit resistance factors for piles subject to uplift are less than those for compression as listed in Sec. 10.5.5 of the Bridge Manual (AASHTO, 2014). Without a load test, the resistance factors for single

piles in uplift range from 0.2 to 0.4. Application of such low values to the design of pile groups subject to overturning may be inappropriate since the failure of such groups is ductile. This is discussed further in Chapter 6.

Lastly, the AASHTO Standard Specifications for Structural Supports for Highway Signs, Luminaires and Traffic Signals (2001) was consulted. Section 13 of the Specifications addresses foundation design. The Specifications reference the AASHTO Bridge Specifications (e.g. AASHTO, 2014) as the primary basis for foundation design. For drilled shafts, the Specifications' commentary presents design information based on Broms' methods for laterally loaded deep foundations, but there is no design information related to pile groups other than a brief paragraph regarding the use of piles for otherwise unacceptable soil conditions and another reference to the AASHTO Bridge Manual for design purposes.

An LRFD version of the AASHTO Specifications for Highway Signs is forthcoming. The reliability study conducted to develop the load and resistance factors for the new document is described in NCHRP Report 796 (2014). The updated document is not anticipated to provide any new geotechnical design guidance for pile groups used to support sign foundations. However, the document is anticipated to provide more clarity on appropriate resistance factors for wind loading, likely indicating the 3-second, 90 mph wind loading can be considered an "extreme event" associated with greater resistance factors than those discussed above (0.2 to 0.4).

2.2 Other Studies Relevant to Pile Groups Subject to Overturning

Most of the previous research that resulted from the literature search was relevant only peripherally; none specifically addressed pile groups subjected primarily to overturning. Nevertheless, some significant findings pertinent to this project were encountered:

- In NCHRP Report 461 (2001), Brown et al. investigated lateral loading of pile groups with load tests and numerical models. The authors confirmed the *p-y* model is appropriate for pile groups and summarized observed *p*-multipliers from their load test program and others. The small number of piles (4) and large spacing (7 pile diameters) for this project (Chapter 3) make it likely that group/spacing effects for lateral load response (i.e. *p-y* curves) are negligible. The authors found that pile cap rotation was sensitive to the axial pile response (i.e. *t-z*), especially for fixed head conditions. The authors also reported that strain gage pairs worked well for measuring pile structural response, though they experienced some difficulty for steel pipe piles. The ShapeArrayAccel devices used for this project (Chapter 3) were intended to overcome some of these difficulties.

- Lehane et al. (2014) conducted centrifuge testing and finite element modeling of large overturning loads on single piles and on single piles embedded in a footing. The piles embedded in a footing had greater rotational stiffness and moment capacity than the individual piles with no footing. The footing reduced moments applied to the individual piles, and the authors report the structural capacity of the piles would control "typical configurations." The authors discuss the significant contribution of footing bearing pressures. Bearing of the pile caps for this project would only confound the interpretation of load transfer among the piles in the pile groups, so the pile cap structures will be constructed with a small gap between the bottom of the caps and the ground surface. This is discussed further in Chapter 3.

- Rollins et al. (2003) performed full-scale lateral load tests of pile groups and developed design curves that assign *p*-multipliers for pile rows as a function of spacing. For the first and second rows of piles, there is no reduction (i.e. *p*-multiplier is 1.0) for pile spacing greater than 7 diameters. The same study also included cyclic lateral load tests of single piles. The tests were deflection-controlled, with loads maintained for approximately 3 minutes on the first cycle and 10 to 20 minutes on subsequent cycles (up to 15). The authors report an approximately 15 percent reduction in peak lateral resistance as determined by the pile head load-displacement curve, with most of the reduction occurring in the first three cycles. The 15 percent reduction in peak lateral resistance is likely tolerable, but the authors also reported a significant loss of stiffness for subsequent cycles, which is explained by the gap left after unloading a previous load cycle.

- In a study of pile cap connections, Rollins and Stenlund (2010) measured deflections and rotations of 12.75-in. diameter steel pipe piles embedded in pile caps subjected to lateral loading. The pile heads were best modeled as fixed (rather than pinned), even when the piles were only embedded 6 in. The authors recommended assuming similar pile to pile cap connections are fixed and suggested truly pinned connections are difficult to create.

3. Field Testing Program

As documented in the previous chapter, literature regarding overturning of pile groups is limited. The project therefore focused on performing a full-scale lateral load test of pile groups similar to those frequently used by WisDOT. The primary focus of the load test was to measure the response of pile groups to static overturning applied via an elevated lateral load. Two four-pile groups were tested, one with 10-in. diameter cast-in-place (CIP) piles and the other with 10x42 H-piles. The CIP piles are constructed by driving closed-ended pipe piles before filling the pipes with concrete. This chapter presents details of the load test site, design and construction of the pile groups, instrumentation, and testing procedure.

3.1 Load Test Site

The load test site is located near the city of Warrensburg, in west-central Missouri approximately 60 miles east of Kansas City as shown in Figure 3.1. The site was selected because previous research at the site for the Missouri Department of Transportation (MoDOT) involved extensive lab testing of soil and rock as well as axial and lateral load tests of drilled shafts, so the site is rather well characterized (Pierce et al. 2014; Boeckmann et al., 2014a). The test pile groups were constructed in the right-of-way for U.S. Highway 50, near the intersection of Missouri Highway 13 and State Highway HH, as shown in Figure 3.2.

Figure 3.1. Location of Warrensburg Load Test Site. (Google Earth, 2011a)

Figure 3.2. Location of Warrensburg Load Test Site east of Warrensburg, MO on U.S. Highway 50, near the intersection with State Highway HH. (Google Earth, 2011b)

The site is composed of approximately 15 ft of silty clay overburden soil overlying shale formations with highly variable strength along with sporadic sandstone. The bedrock consists of the Pennsylvanian Croweburg and Fleming formations containing sandstone, siltstone, limestone, and coal beds. The Croweburg formation had a UCS ranging from 3 to 80 ksf while UCS for the Fleming formation ranged from 5 to 240 ksf. The Croweburg formation had equivalent Standard Penetration Test (SPT) N-values ranging from 93 to 122 blows/ft while equivalent N-values for the Fleming formation ranged from 122 to 304 blows/ft. Figure 3.3 presents UCS measurements from the site along with the mean and standard deviation of UCS for each layer.

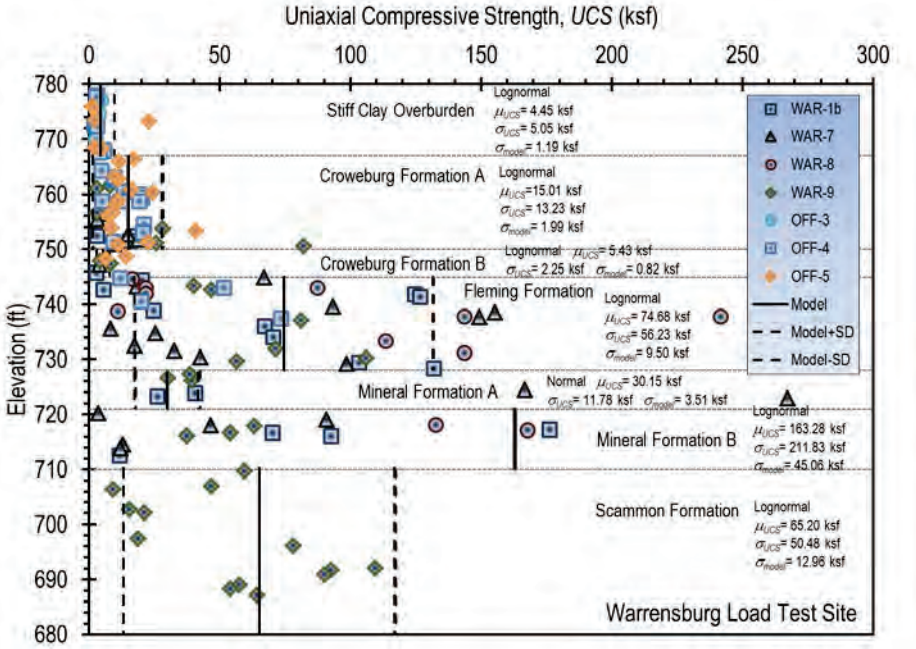

Figure 3.3. Measured values of UCS shown with mean and standard deviation values for Warrensburg Load Test Site.

3.2 Design of Pile Groups

The pile group design involved selecting pile lengths using analyses with Ensoft *GROUP* and considering the objectives and constraints of the test program. The objective of the load test was to load the pile groups to geotechnical failure by applying an elevated lateral load so that the primary loading was an overturning moment like those applied to sign foundations. The layout of the four-pile groups was given by WisDOT as the typical configuration shown in Figure 3.4. The research team decided to use a stem structure atop pile caps as shown schematically in Figure 3.5. The design resembles typical sign structures used by WisDOT. The stem was "truncated" at 10 ft (whereas a typical sign structure might be closer to 30 ft) to reduce construction costs and to limit the height of load application to a practical level. One constraint on the objective geotechnical failure was that the piles should display fixity at depth, i.e. the piles should be long enough to prevent their rigid body rotation.

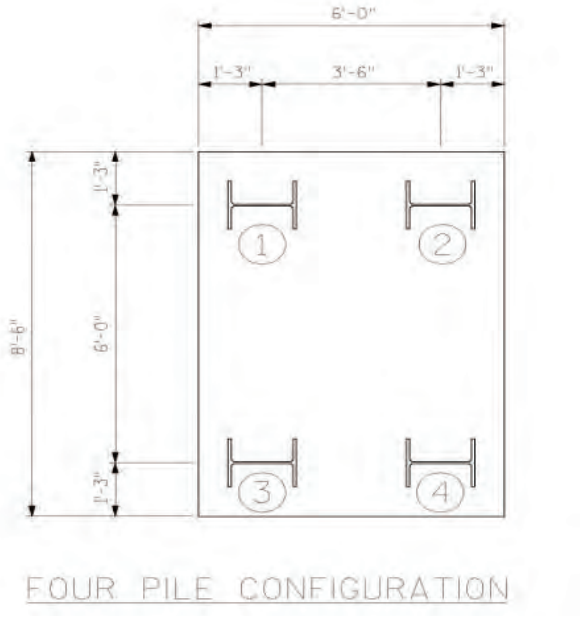

Figure 3.4. Typical pile group plan for WisDOT sign foundation. Primary direction of loading is along the longitudinal axis of the pile cap (i.e. "upward" in the figure).

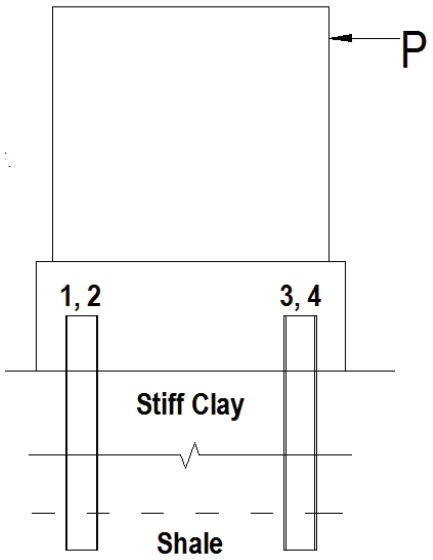

Figure 3.5. Schematic elevation view of loading mechanism.

After the preliminary details of the pile group structures were established, Ensoft *GROUP* v8.0 (Reese et al., 2010) was used to analyze different pile lengths and depths to shale. The analyses were evaluated to determine how well different configurations met the load test objectives (i.e. intended geotechnical failure mechanism) and the magnitude of the required load to achieve failure. Soil and rock inputs for the *GROUP* model were derived from previous load tests of drilled shafts at the load test site as summarized in Table 3.1. The axial load – displacement curves for the pile head were calculated using the alpha method with α = 0.5 for soil, the results of axial load tests at the site for shale (Vu, 2013), and assuming the hyperbolic load-displacement curve function reported by Vu (2013). The *p-y* curves for lateral load analyses were those reported by Boeckmann et al. (2014a).

Table 3.1. Parameters used to develop *GROUP* model inputs for soil and rock.

			Lateral Load Parameters $p = p_{ult}\left(1 - \exp\left(-\frac{k_{py}}{p_{ult}} * y\right)\right)$		
Layer	UCS ksf	f_{s-ult} kips/ft^2	z ft	p_{ult} kips/in.	k_{py} kips/in.^{2}
Silty Clay	4.45	1.1 (from α = 0.5)	2	2.68	1.69
			5	2.88	2.54
			10	2.87	5.91
			12	2.67	9.69
Sandy Shale	15	4.7 (average from Vu (2013) for shale with UCS = 15 ksf)	16	2.61	331
			20	2.76	576
			22	2.49	800
			25	1.70	2913

For all preliminary models, the geotechnical failure predicted using *GROUP* involved failing the tension piles, labeled 3 and 4 in Figure 3.5, in uplift. Uplift of the piles is characterized by the axial load displacement curves for the tension piles, which result directly from the parameters described above and which are shown in the *GROUP* output of Figure 3.6. The uplift capacity for H-piles and CIP piles driven

equivalently were predicted to be approximately equal since they have similar surface and cross-sectional areas. The research team decided to drive piles 1 ft into shale, which is sufficient to establish fixity as shown in the bending moment profile of Figure 3.7 but not so deep as to substantially risk an inability to fail the pile groups during the load test. Depth of shale at the load test site is variable but is generally between 10 and 15 ft. The *GROUP* model predicted failure of the pile groups at about 95 kips of load applied 9 ft above the ground surface.

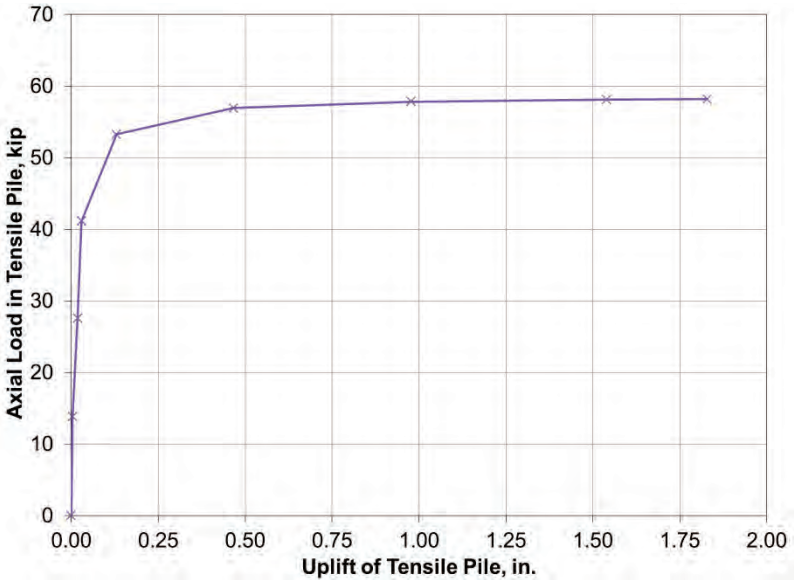

Figure 3.6. Axial load displacement curve for tension piles.

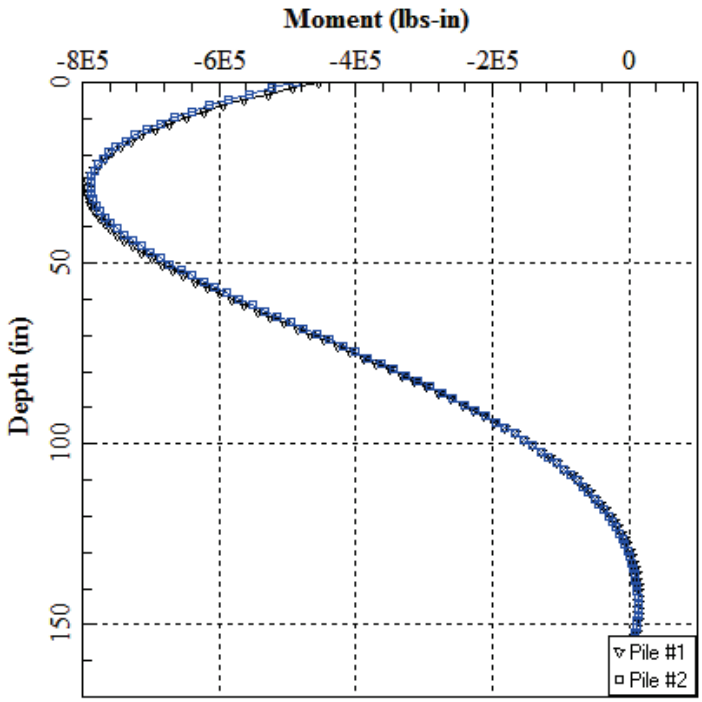

Figure 3.7. Bending moment predicted by *GROUP* model for the ultimate applied elevated load of 95 kips. For the *GROUP* model, Pile #1 is compression and Pile #2 is tension. Bending moment profiles are nearly equivalent for compression and tension piles, so the lines shown are indistinguishable.

The resulting design was laid out in the construction plans included as Appendix B. Structural details of the pile caps and stems were designed after determining the pile lengths and loading configuration. Plans for previous WisDOT sign projects were consulted and structural calculations were performed. The structural design was conservative by typical project standards in order to prevent failure of structural components prior to geotechnical failure of the piles.

3.3 Construction of Pile Groups

Boone Construction Co. of Columbia, Missouri completed construction of the pile groups June 2 through 6, 2014. The crew spent one day installing the CIP piles, one day driving H-piles, and one day each on the concrete caps and stems. Work was rained out Thursday, June 5. Pile driving logs are included as Appendix C, and photographs and descriptions of construction are included in this section.

The first task undertaken by the construction crew was to clear grass and level the work surface. The level work surface was particularly important since the two caps would be pulled together through a common bar. Once grading was completed, the pile locations were laid out using a wood template (Figure 3.8). A crane-supported ICE-32S hammer with a rated energy of 26,000 ft-lbs was used to drive the piles (Figure 3.9). The stroke of the hammer's 3,000-lb ram was monitored by observing rings on the ram (Figure 3.11). Penetration during pile driving was monitored by counting hammer blows per 1-ft segment of driving (Figure 3.10), observed with marks on piles (Figure 3.12). When the piles began to penetrate shale, indicated by increased hammer stroke and reduced penetration, the crew marked pile penetration every 5 blows (e.g. Figure 3.13, Figure 3.14) and terminated driving when the penetration in 5 blows was 2 in. or less. The final logs of pile driving are included as Appendix C. A plot of penetration versus depth for all piles is shown in Figure 3.15. The final penetration of all piles was between 14 and 15.5 ft. Pile driving was similar for all piles, though the penetration into shale was slightly more abrupt for the H-piles than the CIP piles. Pile capacities (in compression) predicted by the ENR formula were generally around 40 to 50 tons.

Figure 3.8. Crew places template for piles on level work surface.

Figure 3.9. Crane and hammer leads used for pile driving.

Figure 3.10. Crew monitoring pile driving.

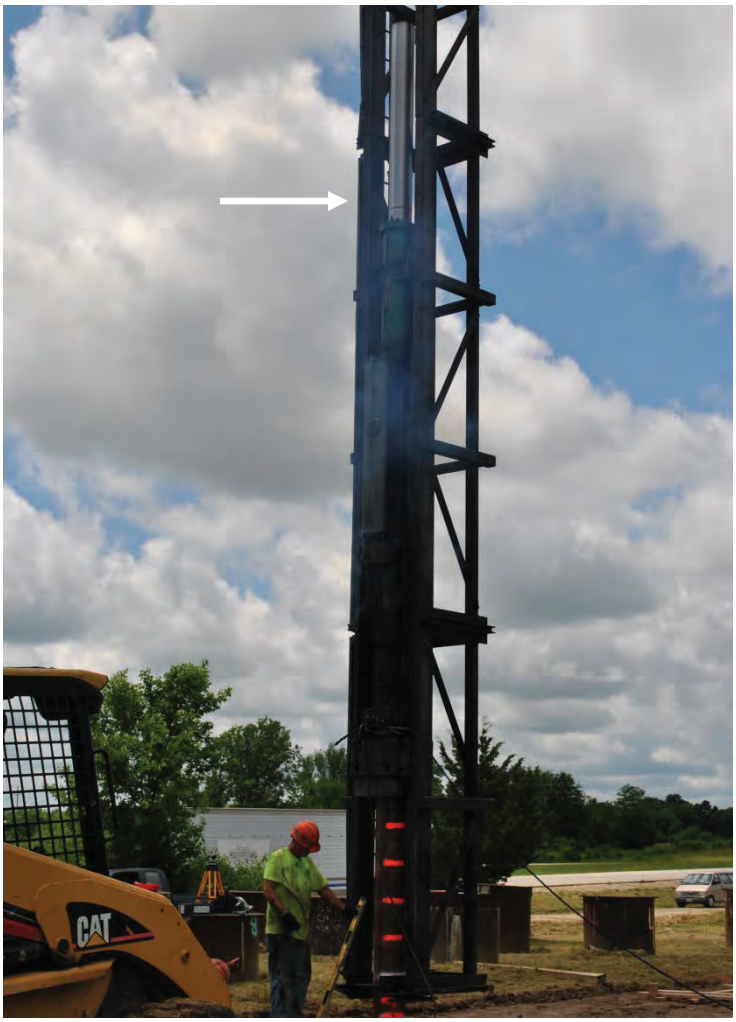

Figure 3.11. Hammer stroke was monitored using rings on ram.

Figure 3.12. 1-ft intervals marked on piles.

Figure 3.13. Crew marked piles every 5 blows once the piles began penetrating shale. Pile driving was terminated when the piles penetrated 2 in. or less in 5 blows.

Figure 3.14. Measured final pile penetration after driving.

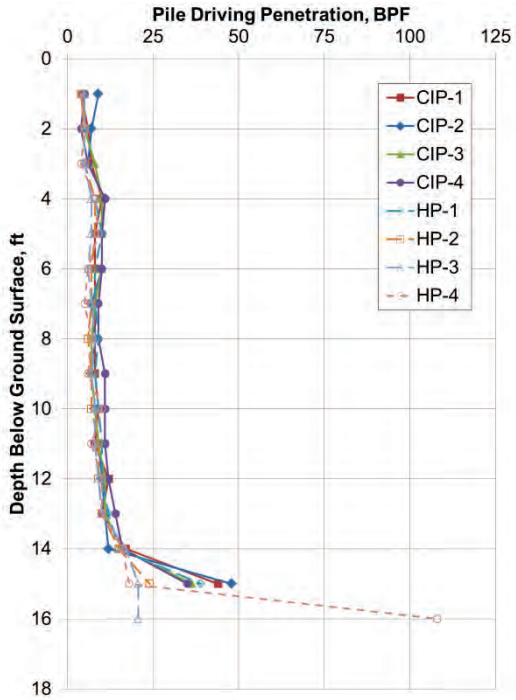

Figure 3.15. Pile penetration for all piles. Last point for each log is extrapolated based on observed penetration for last partial foot of driving.

After driving, extra pile lengths beyond that needed for embedment in the pile cap were removed by torching (Figure 3.16). After removing extra length from the CIP piles, a 1-in. diameter instrumented pipe was placed in the center of the pipe pile (Figure 3.17) before filling the CIP with concrete (Figure 3.18). As discussed in a subsequent section, the small pipes were instrumented with strain gages to measure the structural response of the CIP piles, and the small pipe also served as housing for the ShapeArrayAccel (SAA) devices during the test. Centralizers donated by C&M Manufacturing Co. were used to keep the instrumented bars in the center of the CIP pipes. The concrete truck's chute struck the top of the instrumented bar for CIP-1 (Figure 3.19), so the top two gages for that pile were not operational during the load test. The last step of the pile driving process prior to forming the caps was to place approximately 4 in. of sand at the ground surface as the base for the pile caps. The sand was removed after construction of caps, leaving a gap between the ground surface and the bottom of the pile caps. The gap was intended to remove the effect of the pile cap bearing on the ground surface during overturning, which would be difficult to quantify and would therefore confound interpretation of the axial loads that developed in the piles. Photographs of the pile groups prior to placing sand and forming caps are shown in Figure 3.20 (CIP piles) and Figure 3.21 (H-piles).

Figure 3.16. Marking pile lengths to be removed. (H-Piles were delivered in various lengths; variation in stickup shown is not an indication of variation in penetration.)

Figure 3.17. Placing instrumented pipe into CIP pile.

Figure 3.18. Placing concrete in CIP-2.

Figure 3.19. Damaged bar for CIP-1.

Figure 3.20. CIP Pile group after driving, prior to placement of sand.

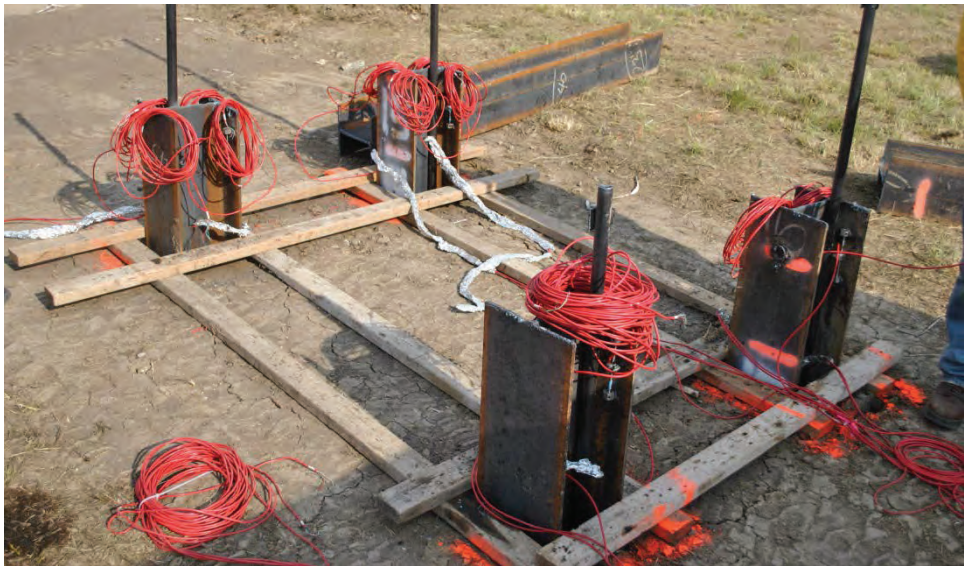

Figure 3.21. H-pile group after driving, prior to placement of sand.

After two days of pile driving and instrumentation work, the remainder of the construction week involved concrete work. Results of concrete slump (ASTM C143, 2012) and concrete compression strength tests (ASTM C39, 2014) are presented in Table 3.2. The sand was leveled (Figure 3.22) prior to placing the forms for the pile caps, which were assembled away from the caps and lifted into place. Steel rebar for the caps was tied in place in accordance with the construction plans after the forms were in place (Figure 3.23), and steel rebar for the stem structures was tied into the cap steel (Figure 3.24, Figure 3.25) prior to placing concrete for the pile caps. Concrete for both pile caps was placed in one day (Figure 3.26). Meanwhile, the university research team performed concrete slump tests in accordance with ASTM C143 (2012) (Figure 3.27). The construction crew finished concrete on the cap (Figure 3.28), including the beveled keyway at the joint with the stem structure (Figure 3.29), before the cap concrete was allowed to

set for two days. Rain delayed progress the first day, but the stems were formed (Figure 3.30) and concrete placed (Figure 3.31) on the second day. Completed cap structures after blowing out sand to create the gap between pile cap and ground surface (Figure 3.32) are shown in the photograph of Figure 3.33. As described previously in this section, the gap between the bottom of the pile caps and the ground surface was intended to prevent the caps from bearing on the ground surface during loading. Load transfer by bearing would have been difficult to quantify and would have made test results difficult to interpret.

Table 3.2. Results of concrete testing.

Structural Component	Placement Date	Slump, in.	Date of Test	Age, days	Compressive Strength, psi	Comments
CIP-4 (Pile)	6/2/2014	9.5	6/13/2014	11	1237	High slump mix used for constructability in instrumented piles.
CIP-2 (Pile)	6/2/2014	9.5	6/16/2014	14	1505	
H-Pile Cap	6/4/2014	6.0	6/13/2014	9	4083	
H-Pile Cap	6/4/2014	6.0	6/16/2014	12	4643	
CIP Cap	6/4/2014	5.5	6/16/2014	12	4163	
HP Stem	6/6/2014	6.5	6/16/2014	10	3487	
CIP Stem	6/6/2014	7.0	6/13/2014	7	3057	
CIP Stem	6/6/2014	7.0	6/16/2014	10	3845	

Figure 3.22. Crew levels sand prior to placing forms for pile cap.

Figure 3.23. Forms and cage in place for H-pile cap prior to placing concrete.

Figure 3.24. H-pile cap and stem cages formed together prior to placing concrete for the pile caps.

Figure 3.25. Stem cage formed with pile cap cage prior to placement of concrete for pile cap.

Figure 3.26. Placing concrete for H-pile cap.

Figure 3.27. Performing slump test in accordance with ASTM C143 (2012) on concrete from each pour.

Figure 3.28. Finishing concrete for pile cap.

Figure 3.29. Finished concrete for pile cap with beveled keyway at joint between cap and stem.

Figure 3.30. Forming stems. Pipes for threadbar load application are in place.

Figure 3.31. Placing concrete for stems.

Figure 3.32. Removing sand from beneath pile cap to create a gap between cap and ground surface. The gap prevents the cap from bearing on the ground surface during the application of overturning loads.

Figure 3.33. Completed pile cap-stem structures.

3.4 Instrumentation and Data Acquisition

All 8 piles were instrumented with vibrating wire strain gages to measure strain at discrete elevations. One pile per group was instrumented with a ShapeAccelArray (SAA) to measure deflection along the pile length. Movements of the pile caps were monitored using linear voltage displacement transducers (LVDTs), dial gages, and wireline devices. In addition, the load applied to the shafts was measured by monitoring the hydraulic pressure supplied to the jacks. Each instrument and the associated data acquisition (DAQ) system are described in more detail in the sections that follow.

3.4.1 H-Pile Strain Gages

Eight Geokon Model 4000 arc-weldable vibrating wire strain gages (Geokon, 2013a) were applied to each H-pile (32 total). As shown in Figure 3.34, four gages were welded on the inside flanges 6 in. below the top of the each pile to define the axial load and bending moment at the pile head. Prior to driving, the other four gages per pile were placed in pairs on opposite sides of the pile web, with one pair 3 ft below the estimated ground surface and the other 1 ft above the pile tip. The pair at 3-ft was intended to capture the maximum bending moment (Figure 3.7). The tip gages were intended to measure the load transferred to the bottom of the pile. An installed tip gage is shown in Figure 3.35, and angle iron welded to protect the gages during driving is shown in Figure 3.36. Despite the angle iron protection, several of the below ground gages were out of range during testing, likely because the gages were not properly adjusted to mid-range prior to driving.

Because 32 vibrating wire strain gages were applied to CIP piles as well (Section 3.4.2), it was required to record measurements from 64 vibrating wire devices among the other instrumentation/DAQ needs. To help with the high DAQ demand, the vibrating wire DAQ developed by Luna (2014) for the Missouri Department of Transportation shown in Figure 3.37 was borrowed. It was capable of reading and recording 16 gages at one time, so half of the H-pile gages were read at one time before switching to the other half of the gages for each load step during testing. Further details of the H-pile strain gage DAQ are provided in Luna (2014). (A different DAQ was used for the CIP pile gages.) The testing procedure is described in Section 3.5.

Figure 3.34. Welding Geokon 4000 gages to pile head after driving.

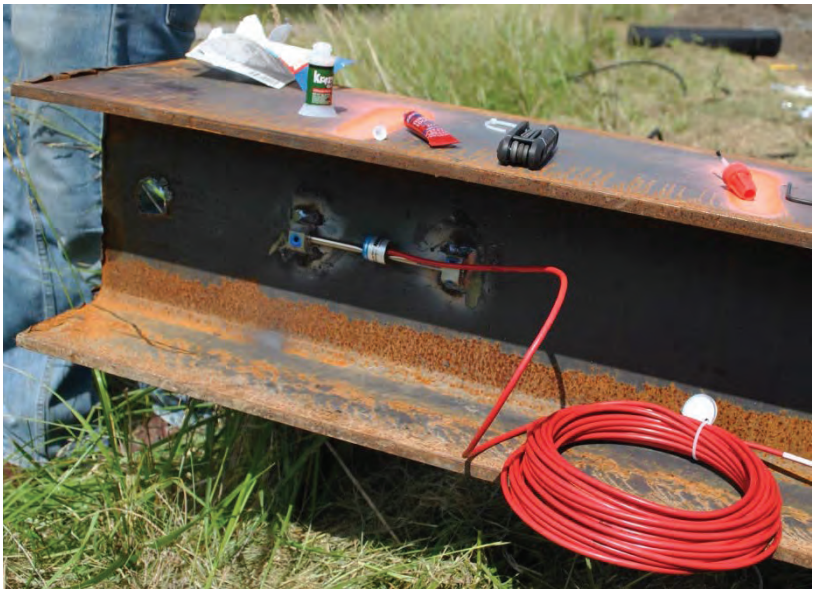

Figure 3.35. Installed Geokon 4000 gage at pile tip.

Figure 3.36. Welding angle section above installed gages. Gage cables were wrapped in aluminum foil to protect from heat.

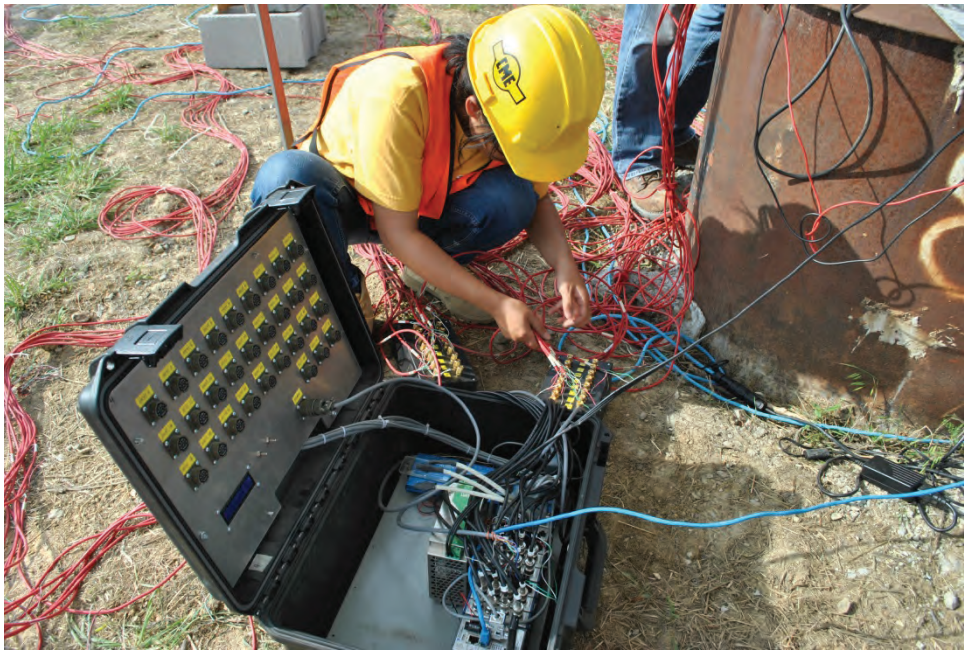

Figure 3.37. DAQ used to read Geokon 4000 gages (Luna, 2014).

3.4.2 CIP Pile Strain Gages

As described in Section 3.3, strain gages for the CIP piles were attached to 1-in. diameter steel pipes that were inserted in the CIP piles between driving and filling with concrete (Figure 3.17). Eight Geokon spot-weldable vibrating wire strain gages (Model 4150) (Geokon, 2013b) were applied to each instrumented pipe (32 total). The gages were installed in pairs along the length of the pipes so that axial load and bending moment profiles along the length of the CIP pile could be measured. Each of the four pipes consisted of two segments, the lengths of which were adjusted in the field after driving to position the gage depths appropriately. The gages were installed according to manufacturer instructions in a laboratory as shown in Figure 3.38 prior to transporting the pipes to the field for installation. Similar to the H-pile gages, DAQ presented a challenge because of the large number of gages. A Geokon datalogger Model LC-2x16 capable of recording 16 gages was used during the test, so one half of the gages were recorded at one time before switching over to the other half for each load step (see Section 3.5for testing details). Photographs of the datalogger are shown in Figure 3.39.

Figure 3.38. Spot welding Geokon 4150 gage to instrumented pipe. Completed gage with protective cover can be seen on bottom of pipe.

Figure 3.39. Geokon datalogger LC-2x16 in lab (left) and field (right).

3.4.3 Shape Array Accelerometer

ShapeAccelArray (SAA) devices were used to measure shaft deflection profiles in lieu of conventional inclinometers. The SAA is a chain of rigid segments with sensors that use MEMS (microelectromechanical systems) technology to measure the tilt of each segment/joint (Measurand, 2012). The sensorized segment and joint are shown in Figure 3.40. The measuring principle of the SAA is similar to that of traditional inclinometers, and both provide excellent precision and accuracy, but the SAA provides a continuous record of shaft deflection throughout testing. This presents safety, reliability, and time advantages compared with taking manual readings with the conventional inclinometers at the end of each load step.

The university owns two SAA devices. As shown in Figure 3.41, one SAA was used for HP-2, a compression pile, and one was used for CIP-3, a tension pile. The SAA were placed in 1-in. Schedule 40 metal pipe. For the H-pile, the pipe were welded to the inside corner of the pile section prior to driving. For the CIP pile, the pipe was inserted in the center of the pile using centralizers prior to placing concrete. (As described previously, the CIP inner pipe was also instrumented with strain gages.) SAA data were recorded continuously using the SAA software program, which ran on a laptop computer to which the SAA were connected.

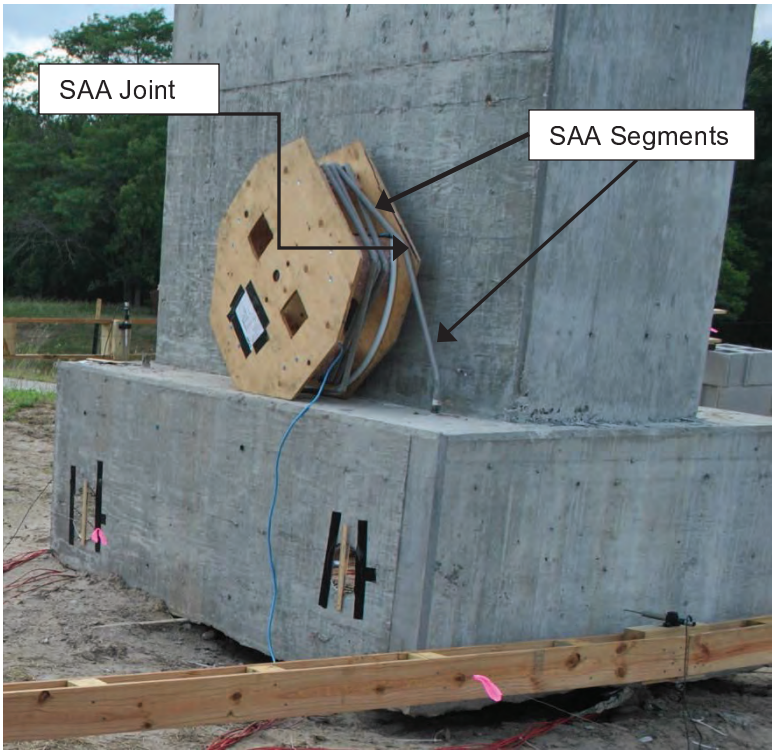

Figure 3.40. SAA joint and segment.

Figure 3.41. SAA inserted in HP-2 and CIP-3.

3.4.4 Linear Voltage Displacement Transducers (LVDTs)

LVDTs supplied by Bridge Diagnostics, Inc. were used to measure displacement of the pile cap. Eight were used: two above the top rear corners of each cap to measure pile cap uplift and two in front of each pile cap to measure the lateral deflection of the caps. The uplift LVDTs are shown in Figure 3.42, and the lateral LVDTs are shown in Figure 3.43. The lateral LVDTs were mounted with one above the other on each cap to allow for interpretation of pile cap rotation. Reference beams can also be seen in the photographs and in Figure 3.44. The reference beams were fabricated from timber 4x4 segments and mounted on cinder block towers approximately 10 ft from the pile caps. Care was taken during installation of the LVDTs to ensure verticality (Figure 3.45). A 10-V power supply was used to operate the LVDTs, which were read with a digital multimeter and recorded manually.

Figure 3.42. LVDTs positioned above rear of pile caps to measure uplift.

Figure 3.43. LVDTs positioned against front of pile caps to measure lateral deflection. One LVDT was mounted directly above the other to measure rotation.

Figure 3.44. Four reference beams used during the test.

Figure 3.45. Installation of uplift LVDT.

3.4.5 Dial Gages

One dial gage was mounted above the center of the back of each pile cap as shown in Figure 3.46 (two total). The dial gages provided a degree of redundancy for the uplift LVDTs. Dial gage measurements were recorded manually during testing.

Figure 3.46. Dial gages used to measure uplift at the back of the pile cap.

3.4.6 Wireline Devices

Eight wireline devices were installed to measure the vertical movement of the pile cap at each pile location. In addition, four wireline devices were installed to measure lateral movement of the back (tension edge) of the pile caps. Wireline devices are shown in Figure 3.47. The device consists of a mirror and ruler attached to the pile cap with a tensioned wire (fashioned from rebar tie wire) in front of the mirror/rulers. The wire is tensioned between two posts driven away from the pile caps. The devices were read by lining up the wire and mirror such that the wire and its reflected image coincided, ensuring consistent readings. The mirror/rulers were installed to ensure verticality as shown in Figure 3.48.

Figure 3.47. Wireline devices on the CIP pile group. Devices were installed in line with compression (left) and tension (right) piles.

Figure 3.48. Installing wireline device.

3.4.7 Load Measurements

The load applied to the pile structures was measured from the hydraulic pressure applied to the jack (Figure 3.49) by the pump (Figure 3.50). This pressure can be converted to a force via a simple calibration provided for the jack (0.037 kip/psi). Pressure readings were recorded manually for each load step. The pressure gage was marked in 100 psi increments.

Figure 3.49. Hydraulic jack on threadbar applying load to pile structure through a bearing plate.

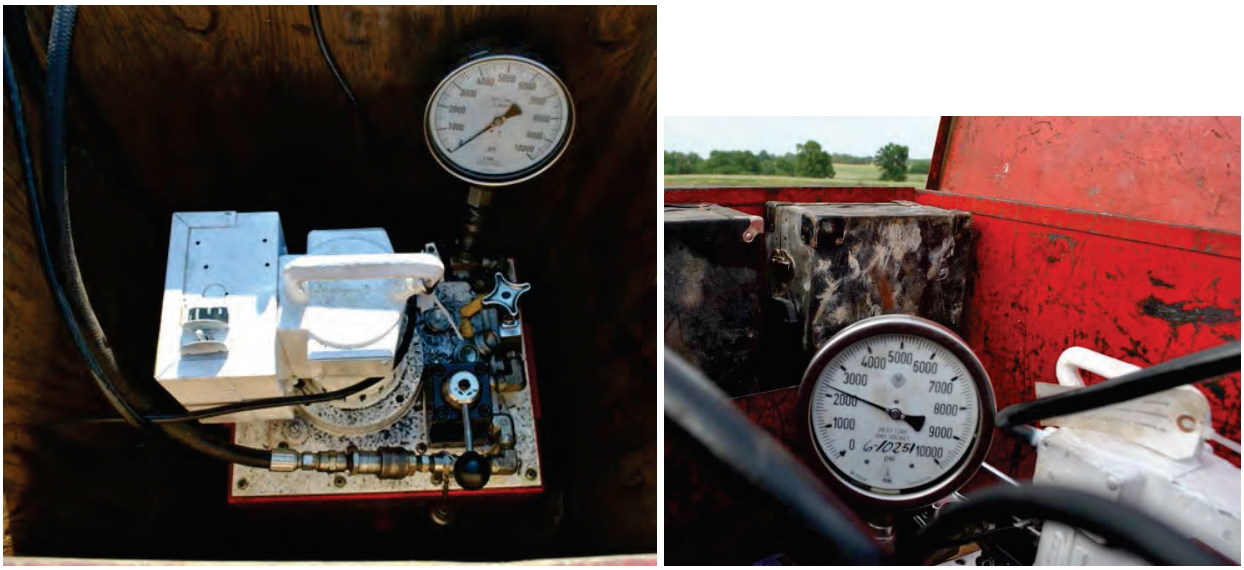

Figure 3.50. Hydraulic pump with pressure gage.

3.5 Testing Procedure and Load Test Summary

The test was performed by pulling the two pile groups together so that both were loaded and monitored simultaneously, producing two sets of test results for one individual lateral load test. The load test setup is shown in Figure 3.51 and Figure 3.52. The center-hole jack (110 MP series 01) was provided by Dywidag-Systems International (DSI) and were used to tension Grade 150 steel THREADBAR®, also supplied by DSI. The bar was installed through 6-in. diameter steel pipes that were cast into each stem as shown in Figure 3.30. Application of pressure to the jacks tensioned the bar, thereby pulling together the pile structures.

Figure 3.51. View of load test with CIP pile group on left and H-pile group on right. Canopy housing computers and DAQs is in background.

Figure 3.52. View of load test with H-pile group on left and CIP pile group on right.

The lateral load test was performed similar to the procedure outlined in ASTM D3966 (2007), which was written for single foundation elements rather than groups. The load sequence generally followed Procedure B for Static Excess Loading. Loads were applied using the hydraulic system provided by DSI following the provided operating instructions including preparation, bleeding the jack, and stressing. As shown in Figure 3.53, the jack was reset several times during the test when its stroke had been consumed by displacement of the structures and elongation of the bar. During resetting of the jacks, the load was locked into the loading frame by tightening locking nuts housed within the neck of the centerhole jacks against the bearing plates. During each load step, a near constant pressure was maintained until several consecutive dial gage readings, taken in one-minute increments, were unchanged. At that point, the strain gage cables were switched and several readings were taken with the second set of strain gages (see Section 3.4.1 and 3.4.2) before proceeding to the next load increment. Longer load increments were required for higher loads, during which the pump was operated frequently to maintain a constant pressure as the pile structures displaced.

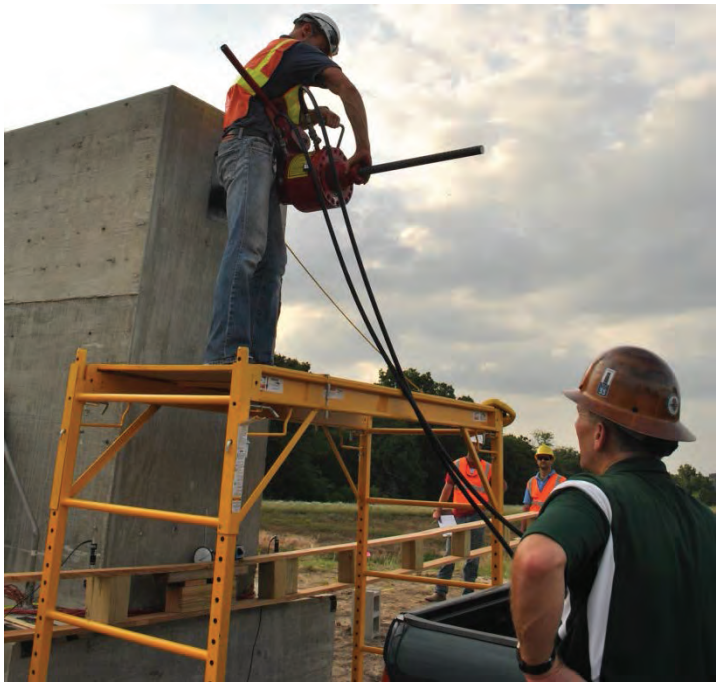

Figure 3.53. Resetting stroke of the hydraulic jack during the load test.

Initial base readings for all of the instrumentation were recorded prior to loading. Readings from the dial gages and wireline devices were recorded manually and frequently throughout each load step to inform loading decisions. The LVDTs were also recorded manually, but only at the end of each load step. The SAA data were recorded continuously. Readings for all instruments were also recorded during unloading at the end of the test. The LVDTs, wireline devices, and dial gages were monitored to ensure they did not run out of stroke during loading. Due to the amount of displacement, this required resetting several reference beams during loading.

The test was terminated when the load on the structures was 99 kips. Pictures of the pile structures near the end of the test are shown in Figure 3.54 through Figure 3.57. The final load was rather difficult to maintain as the movement of the structures was considerable, with uplift at the tension piles between 1 and 2 in. and displacement of the top of the structures of approximately 10 in. on average (as measured using a tape stretched atop the structures). The load was released as darkness set in, but it was apparent from the persistent rotation of the structures the final load was ultimate or nearly ultimate. The gap between pile caps and ground surface was maintained throughout the test, as shown in the pictures.

Figure 3.54. Pile structures during final load step. CIP pile cap is at left and H-pile cap is at right.

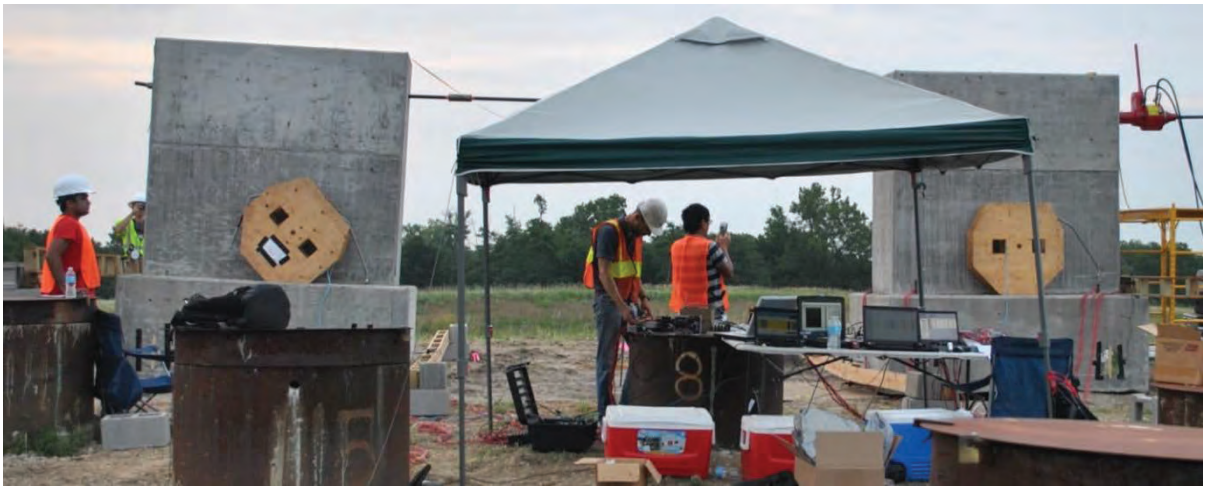

Figure 3.55. Pile structures during final load step. H-pile cap is at left and CIP pile cap is at right.

Figure 3.56. H-pile cap during the final load step.

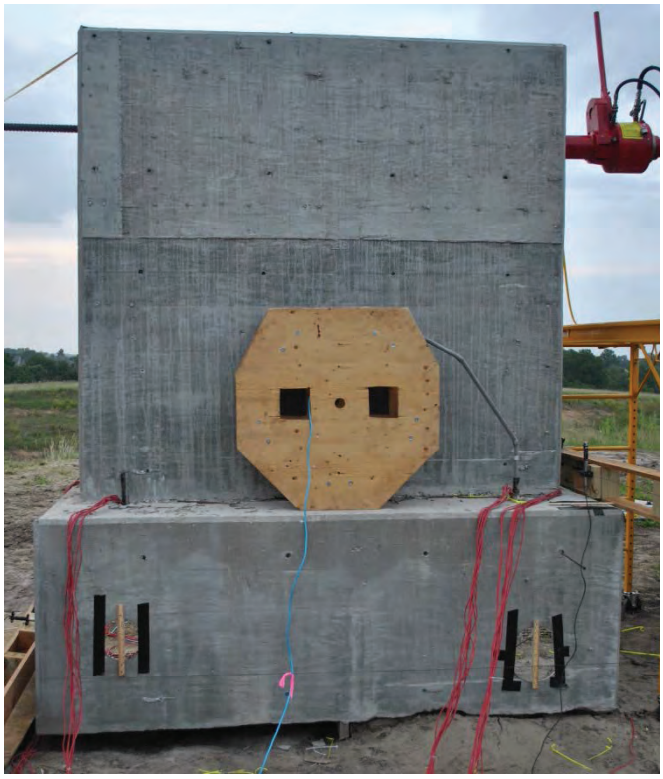

Figure 3.57. CIP pile cap during the final load step.

4. Experimental Results

After the test was completed, pile responses were calculated from the load test measurements. The pile response is characterized by the final displacements and rotations, load-displacement behavior, and the bending moment and axial force along the length of the pile. This chapter presents applied load-displacement curves as measured by LVDTs, dial gages, wireline devices, and the SAA segment at the top of the shaft and pile displacement profiles derived from SAA measurements. A summary of the methodology for interpreting bending moments from strain gage and SAA data is also presented along with bending moments and axial forces derived from strain gage measurements and bending moments derived from SAA data.

4.1 Displacements, Rotations, and Load-Displacement Curves

As described in Sections 3.4.4 through 3.4.6, twenty two instruments were used to measure displacements of the pile structures. Ten instruments were used to measure upward displacement of the tension piles (HP-3, HP-4, CIP-3, CIP-4): two LVDTs and one dial gage on the back (tension side) of the caps, and one wireline device per tension pile (placed on the outside of the cap in line with the respective pile head). To measure downward displacement of the compression piles (HP-1, HP-2, CIP-1, CIP-2), four wireline devices (one per compression pile) were installed on the outside of the cap in line with the respective pile head. Eight instruments were used to measure lateral displacement of the pile caps: two LVDTs in the front of each pile cap and two wireline devices on the top of each pile cap at the tension edge of the caps. The movement of the top segment of the SAA provides an additional measure of lateral displacement for each cap.

A summary of displacements at the end of the maximum (99-kip) load step from each instrument is included in Table 4.1. The measured displacements indicate the H-pile structure generally moved more at the end of the test than the CIP pile structure, but both structures moved significantly. A potential explanation for the greater displacement of the H-pile group is because the H-piles are oriented along their weak axis (consistent with typical WisDOT plans for sign structures). The weak axis orientation not only results in a primary bending moment of inertia less than that for the CIP piles, but it also means the flanges of the H-piles were essentially "slicing" through the soil as the piles deflected laterally. For both pile groups, upward displacement of the tension piles was several times greater than downward displacement of the compression piles. Lateral displacements were greater than vertical displacements for both caps. Lateral displacement was greater at the back (tension side) of the caps than at the front (compression face) of the caps, which is consistent with observed rotation of the structures.

Table 4.1. Summary of displacements at end of final (99-kip) load step. For vertical displacements, up is negative.

Instrument	Final Displacement, in.	
	H-Pile	CIP Pile
Tension LVDT, Piles 1-4	−1.64	−1.40
Tension LVDT, Piles 2-3	−1.38	−1.39
Tension Dial Gage	−1.49	−1.62
Tension Wireline, Pile 3	−2.07	−1.14
Tension Wireline, Pile 4	−1.97	−1.14
Compression Wireline, Pile 1	0.39	0.30
Compression Wireline, Pile 2	0.10	0.28
Lateral LVDT, Top	2.13	1.06
Lateral LVDT, Bottom	1.83	0.86
Lateral Wireline, Piles 1-4	3.05	1.75
Lateral Wireline, Piles 2-3	3.25	1.71

Various rotations were calculated using the displacements from Table 4.1. The resulting rotations at the end of the final load step are included in Table 4.2. The calculated pitch rotations are the expected

rotation of the structures in response to the applied overturning moment. The two values for the rotation of the back half of the H-pile cap (−3.2 and −1.6) are erroneous since the rotation of the H-pile cap was clearly in the positive direction. The negative calculated values result from the wireline devices recording greater upward displacement than the LVDTs on the back (tension) side of the H-pile caps. This is likely a result of reference beam adjustment during the final load step. The other values for rotation are generally consistent for each structure, indicating rotation of 1 to 3 degrees with slightly greater rotation of the H-pile caps. The first two measures of rotation listed in the table (yaw and roll) represent rotation in directions not anticipated based on the loading. The small values calculated confirm the structures were not twisting significantly and provide a degree of confirmation in the precision of displacement measurements. In general, the rotation values indicate reliable displacement measurements, especially considering the sensitivity of rotation calculations of such small magnitude.

Table 4.2. Summary of rotations at end of final (99-kip) load step. For pitch values, rotation toward the opposite shaft (i.e. expected direction) is positive.

Rotation Description	Final Rotation, deg.		Instruments used in Calculation (numbers refer to pile designation)
	H-Pile	CIP Pile	
Twist about vertical axis (yaw)	-0.16	0.03	Lateral Wireline Devices
Twist about longitudinal axis (roll)	0.35	0.01	Tension LVDTs
Rotation of Pile 1-Pile 2 face (pitch)	1.8	1.3	Top LVDT to Bottom LVDT
Rotation of Pile 1-Pile 4 face (pitch)	1.9	1.1	Wireline 4 to Wireline 1
Rotation of Pile 3-Pile 2 face (pitch)	1.7	1.1	Wireline 3 to Wireline 2
Rotation of Pile 1-Pile 4 face (pitch)	1.4	1.2	Tension LVDT to Wireline 1
Rotation of Pile 3-Pile 2 face (pitch)	1.0	1.1	Tension LVDT to Wireline 2
Rotation of Pile 3-Pile 2 face, back half only (pitch)	−3.2	1.2	Tension LVDT to Wireline 3
Rotation of Pile 1-Pile 4 face, back half only (pitch)	−1.6	1.2	Tension LVDT to Wireline 4
Average rotation of cap (pitch)	2.4	1.5	Average Lateral Wireline to Top LVDT
Average rotation of cap (pitch)	2.2	1.5	Average Lateral Wireline to Bottom

Load-displacement curves were determined from the measurements of each displacement instrument. Curves from the devices associated with tension piles (LVDTs and dial gages on the back of the pile caps; wireline devices associated with HP-3, HP-4, CIP-3, and CIP-4) are shown in Figure 4.1. The load-displacement curves for tension piles are similar, with the exception of curves derived from the dial gage on the CIP pile cap, the initial readings of which were affected by wind. All of the load-displacement curves are rather stiff initially, with more significant displacements occurring after the applied load exceeded approximately 50 kips. Beyond about 85 kips applied load, it appears the capacity of the tension piles had been reached. It is also noteworthy that in the final load step, it appears the H-pile cap's tension piles continued to pull out while the CIP pile cap's tension piles experienced an apparent stiffening. This is perhaps the result of not reaching static equilibrium during the final load step (i.e. the piles were still moving and the applied load was not maintained consistently at 99 kips).

Displacement devices associated with compression piles (HP-1, HP-2, CIP-1, CIP-2) were limited to wireline devices. Load-displacement curves from these devices are shown in Figure 4.2. The scale of the displacement axis compared to that for the tension piles in Figure 4.1 is consistent with the observation that upward movement of the tension piles was several times greater than downward movement of the compression piles. The curves display noise and some variability, neither of which is surprising considering the difficulty of measuring small displacements and the precision of the wireline devices. The general shape of the curves is similar to that for the tension piles in displaying high initial stiffness and then greater displacement after about 60 kips applied load.

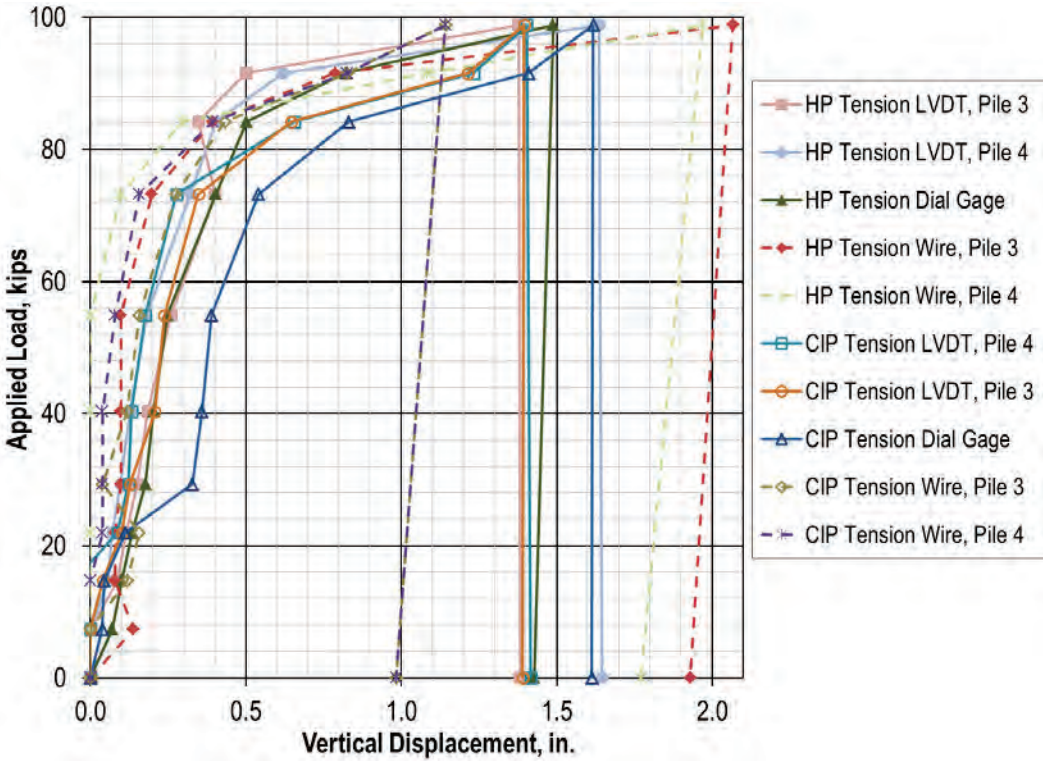

Figure 4.1. Load-displacement curves associated with tension piles. Solid symbols are for H-piles and open symbols are for CIP piles. Dashed lines are for wireline devices.

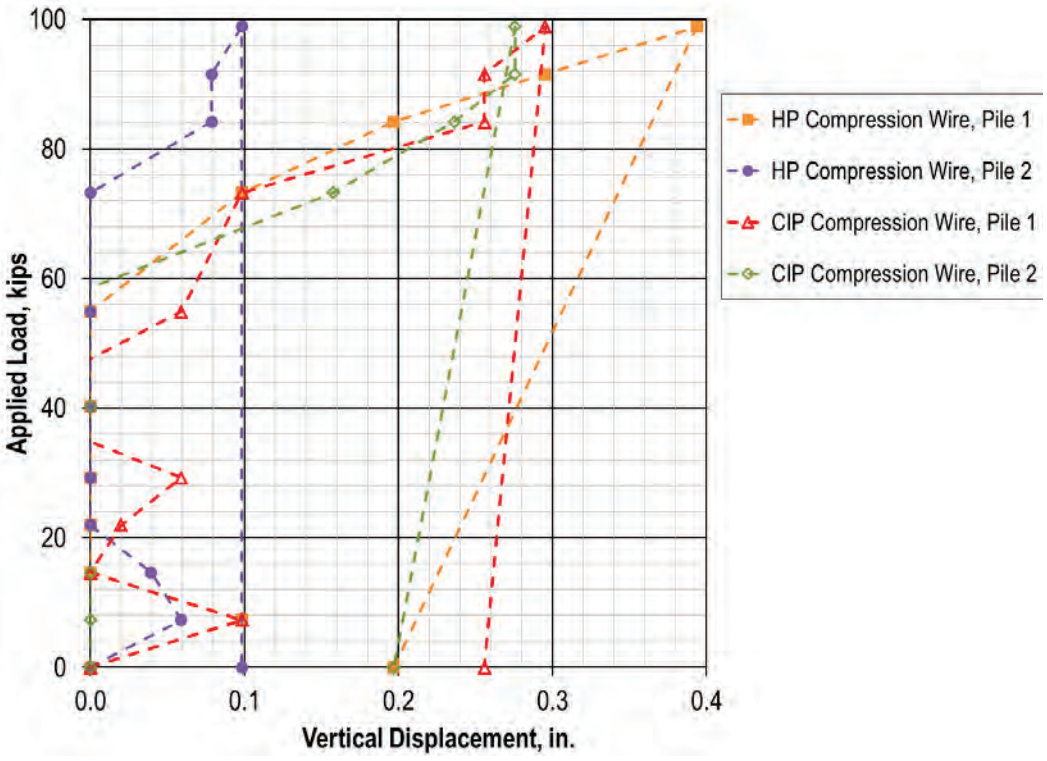

Figure 4.2. Load-displacement curves associated with compression piles. Solid symbols are for H-piles and open symbols are for CIP piles. Dashed lines are for wireline devices.

Load-displacement curves associated with lateral movement of the pile structures are included in Figure 4.3. Included are one curve from the top segment of the SAA for each pile cap. Several observations from the graph are consistent with those discussed regarding Table 4.1 and Table 4.2: the H-pile structure experienced greater displacement than the CIP-pile cap, and the back (tension) side of each cap displaced more laterally than the front (compression) side, which is consistent with the observed rotation of the structures. The lateral load-displacement curves are consistent. This is consistent with the observed response of drilled shafts in Boeckmann et al. (2014a), which cited the "averaging" nature of laterally loading deep foundations. Finally, it appears the H-pile cap's piles continued to displace laterally while the CIP pile cap's tension piles experienced an apparent stiffening in the final load step. This is similar to the observed load-displacement behavior for the tension piles and is also likely the result of not reaching static equilibrium during the final load step.

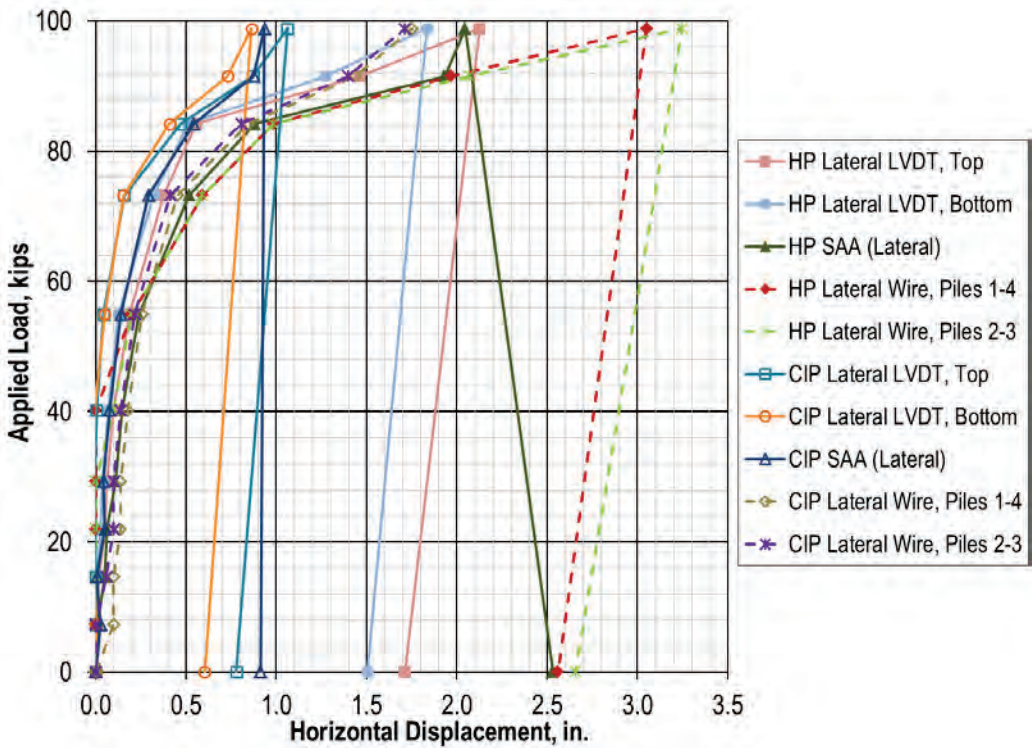

Figure 4.3. Load-displacement curves associated with lateral movement of the pile structures. Solid symbols are for the H-pile structure and open symbols are for the CIP pile structure. Dashed lines are for wireline devices.

4.2 Displacement Profiles from SAA

The SAAs used in piles HP-2 and CIP-3 consist of a chain of 30 segments, each 500 mm (19.7 in.) in length. Position data for each segment were recorded in three dimensions, with the cross section of the pile defining the horizontal x and y axes and the vertical z axis. Lateral displacement values at the end of each load increment were calculated from the differential movement in the x and y directions:

$$\delta_i = \sqrt{(x_i - x_{i0})^2 + (y_i - y_{i0})^2} \qquad \text{(consistent units of length)} \qquad \textbf{Eq. 4.1}$$

where δ_i = total lateral displacement of the i^{th} segment of the SAA
x_i = position of the i^{th} segment along the x-axis
x_{i0} = initial (zero load) position of the i^{th} segment along the x-axis
y_i = position of the i^{th} segment along the y-axis
y_{i0} = initial (zero load) position of the i^{th} segment along the y-axis

This calculation is necessary since the direction in which the piles were pulled was aligned somewhere between the x and y axes. Presumably, the total displacement occurred toward the opposing test structure. Profiles of displacement with depth for each load step were calculated according to Eq. 4.1 for both instrumented piles. The results are included in Figure 4.4, with all profiles for one pile contained in the same plot and with plots from the two pile groups presented side-by-side.

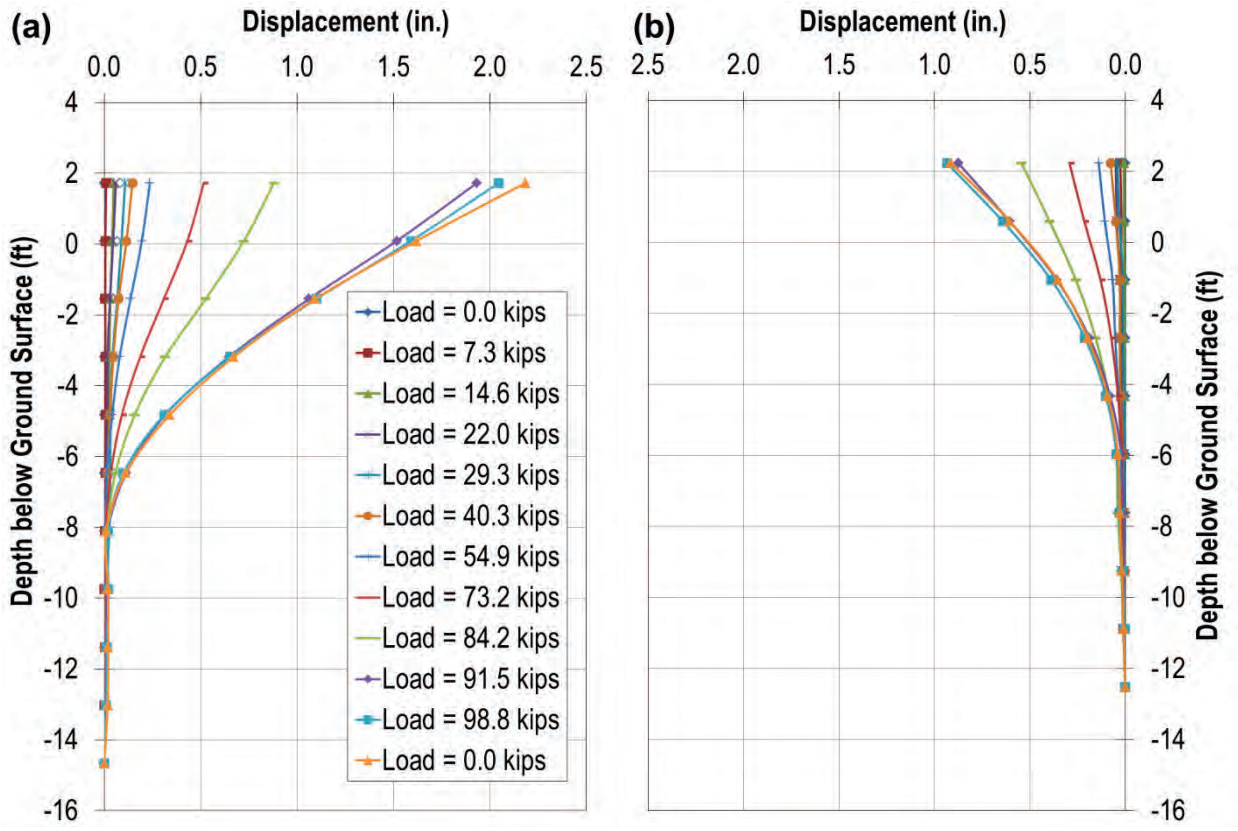

Figure 4.4. Displacement profiles from SAA data for piles (a) HP-2 and (b) CIP-3.

The magnitudes of the deflection profiles of Figure 4.4 are consistent with observations in Section 4.1, primarily in that the H-pile cap deflected considerably more than the CIP pile cap, and the difference was especially pronounced for the final two load steps. The shapes of the deflection profiles are reasonable and are generally consistent from one load step to the next for both piles. The shapes also indicate the test objective of maintaining fixity above the pile tip was achieved for both piles. Neither pile displayed much (if any) rebound after unloading, which is unlike typical single-pile behavior. It is possible the considerable weight of the pile structures (47 kips each) prevented significant rebound.

4.3 Methodology for Interpretation of Axial Force and Bending Moment

Determining pile structural response from strain gage and SAA data requires interpretation using geometry and structural mechanics of varying complexity depending on the response (axial force or bending moment) and pile type. The SAA devices do not measure elongation, so they provide no axial data. Calculations for axial force from strain gages are relatively simple for both types of piles, since the axial strain is assumed to be the average strain measured along the cross-section for any depth. The axial force calculations included the dead load from the weight of the structures, which was assumed to be distributed equally among the four piles. The dead load from the weight of the structures had to be added because the initial strain measurements were recorded after concrete for the structures had been placed and sand beneath the pile caps had been removed.

$$P_j = \varepsilon_{j-axial} \cdot EA_j + 11.7 \text{ kips} \quad \text{(consistent units)} \quad \textbf{Eq. 4.2}$$

where P_j = axial force at the level of the j^{th} strain gage
$\varepsilon_{j-axial}$ = average strain measured by the j^{th} level strain gages, compression positive
EA_j = pile axial stiffness at the j^{th} strain gage
11.7 kip = weight of structure divided by four piles

Calculating bending moments (Eq. 4.3) requires data related to bending curvature, which varies by instrument, and bending stiffness, which varies by pile type. Two profiles of bending moment were calculated along the length of piles HP-2 and CIP-3: one from the SAA data and the other from strain gage data. For the other piles, only strain gage data were available.

$$M = \phi \cdot EI \quad \text{(consistent units)} \quad \textbf{Eq. 4.3}$$

where M = bending moment
ϕ = bending curvature, radians per unit length
EI = shaft bending stiffness

Bending curvature from SAA data was obtained by differentiating the displacement profiles described in Section 4.2 twice, first to obtain cross-sectional rotation of the pile (Eq. 4.4), which is then differentiated to obtain bending curvature (Eq. 4.5):

$$\theta_i = \frac{d\delta}{dz} \approx \tan^{-1}\left(\frac{\delta_i - \delta_{i-1}}{L}\right) \quad \textbf{Eq. 4.4}$$

where θ_i = cross-sectional rotation of the i^{th} segment of the SAA, radians
L = SAA segment length (500 mm = 19.7 in.)

$$\phi_i = \frac{1}{\rho_i} = \frac{d^2\delta}{dz^2} = \frac{d\theta}{dz} \approx \frac{\theta_i - \theta_{i-1}}{L} \quad \textbf{Eq. 4.5}$$

where ϕ_i = bending curvature of the i^{th} segment of the SAA, radians per unit length
ρ_i = radius of curvature of the i^{th} segment of the SAA, consistent units of length
L = SAA segment length (500 mm = 19.7 in.)

Bending curvature is equivalent to the slope of the strain across the cross-section. Calculating bending curvature from strain gage data therefore depends on the pile geometry. For the CIP strain gages, which were installed on opposite sides of the instrumented 1-in. pipe, and the H-pile strain gages below ground, which were installed on opposite sides of the web, the bending curvature is simply the difference between strain readings divided by the distance between gages. For the gage layout employed at the head of H-piles, the difference between average flange strain readings was divided by the distance between these gages.

Bending stiffness for the H-piles was assumed to be constant and was calculated from the weak-axis moment of inertia and the elastic modulus of steel. Determining the bending stiffness of the CIP piles is a nontrivial exercise, primarily because the stiffness is nonlinear and greatly influenced by concrete cracking, which is difficult to predict. The procedure used here was to predict values of bending stiffness along the length of the shaft as a function of the bending curvature. Values for bending stiffness as a function of curvature were computed using Ensoft L-Pile v2012. The routine employed by L-Pile is documented in the program's technical manual (Isenhower & Wang, 2011). In summary, L-Pile iterates on the location of the neutral axis until force equilibrium is satisfied, accounting for concrete cracking. Cracking of the concrete is predicted as a function of the compressive strength of the concrete, which was estimated from Table 3.2. The resulting pile bending stiffness predicted by L-Pile is shown in Figure 4.5. The bending stiffness decreases abruptly at small values of curvature, which corresponds to initial

cracking of the concrete. After the concrete cracks, the decrease in stiffness is more gradual as the steel yields.

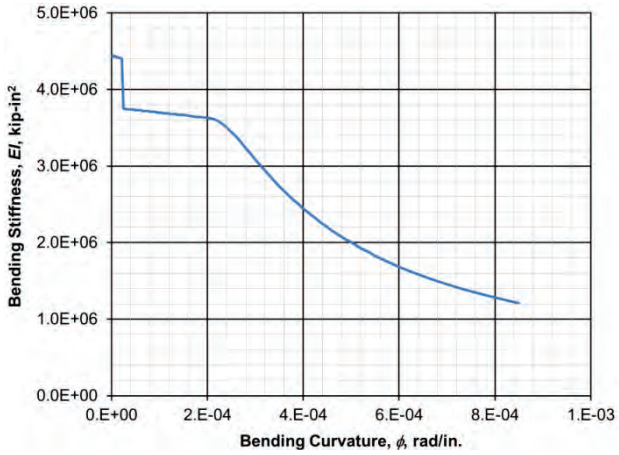

Figure 4.5. Bending stiffness curve for CIP piles.

For all calculations, the bending stiffness at a particular depth was limited to its minimum historic value if the L-Pile analysis indicated concrete cracking had ever occurred at that depth. For example, if the curvature at a depth of 5 ft was great enough to initiate concrete cracking for an applied lateral load of 50 kips, the bending stiffness used to calculate the bending moment for subsequent loads would be limited to a maximum value of the stiffness calculated for the 50-kip load, even if the bending curvature at a subsequent load was less than it had been at the 50-kip load.

4.4 Pile Structural Response

The methodology and equations presented in Section 4.3 were used to create profiles of axial force and bending moment with depth. Each of the profiles was calculated for each load step and each pile, and results are presented and discussed in the sections below. Additional discussion and interpretation of the results is presented in Chapter 5. As discussed previously, the two piles per structure that were anticipated to be in compression (HP-1 and HP-2, CIP-1 and CIP-2) are referred to as "compression piles" and the two piles per cap anticipated to be in tension (HP-3 and HP-4, CIP-3 and CIP-4) are referred to as "tension piles."

4.4.1 Axial Force Profiles

Strain gage data were analyzed to produce plots of axial force with depth for all CIP piles (Figure 4.6) and H-piles (Figure 4.7). The calculations were performed according to Eq. 4.2, so the results include the weight of the cap structure, which is assumed to be distributed equally among the piles. Only gages for one compression pile and one tension pile from each cap (HP-2, HP-3, CIP-2 and CIP-3) were recorded for the final load step (99 kips) and after unloading because maintaining the applied load was deemed more important than reading all gages considering the time required for switching cable sets. One limitation of the axial force data analysis was encountered for the gages installed at the pile head, where it is very difficult to estimate the axial stiffness. The axial stiffness of the pile was used, but this ignores the likely significant stiffness contribution from the pile cap, which results in axial load magnitudes that are too low.

The shape of the axial load profiles for CIP piles (Figure 4.6) is generally consistent, with similar axial loads measured in the two middle levels of gages within the soil and less load measured near the tip, which was installed in the shale. This suggests load transfer within the soil zone was small and that the piles developed most of their resistance in the shale. Further, it suggests the loads at the pile head, where cap stiffness confounds interpretation, are likely not much greater than those calculated around 2 ft below the ground surface. The axial load during the ultimate load step was around 50 kips, with CIP-4 being slightly less than the others.

The axial force data for the H-piles is less informative due to installation issues encountered during construction (Section 3.4.1). For several depths, one gage of the pair was not functional and the axial strain was assumed to be equal to the strain in the lone operational gage. This ignores the effect of bending and will thus tend to either overreport or underreport the actual axial force value. Nevertheless, several meaningful observations can be derived from Figure 4.7. First, the calculated axial loads nearly all follow the expected sign, i.e. compression was calculated for compression piles and tension was calculated for tension piles. The axial force magnitudes generally decrease with depth, consistent with load shedding to the soil. The magnitudes generally vary from very small (HP-1 and HP-4 though there were no ultimate readings for those piles) to nearly 100 kips. The unexpected (compression) axial loads observed at the end of the test for HP-3 could be a result of increased bending (making the axial force more difficult to interpret with nonfunctioning gages) or of previously operational gages ceasing to function upon greater stress and strain.

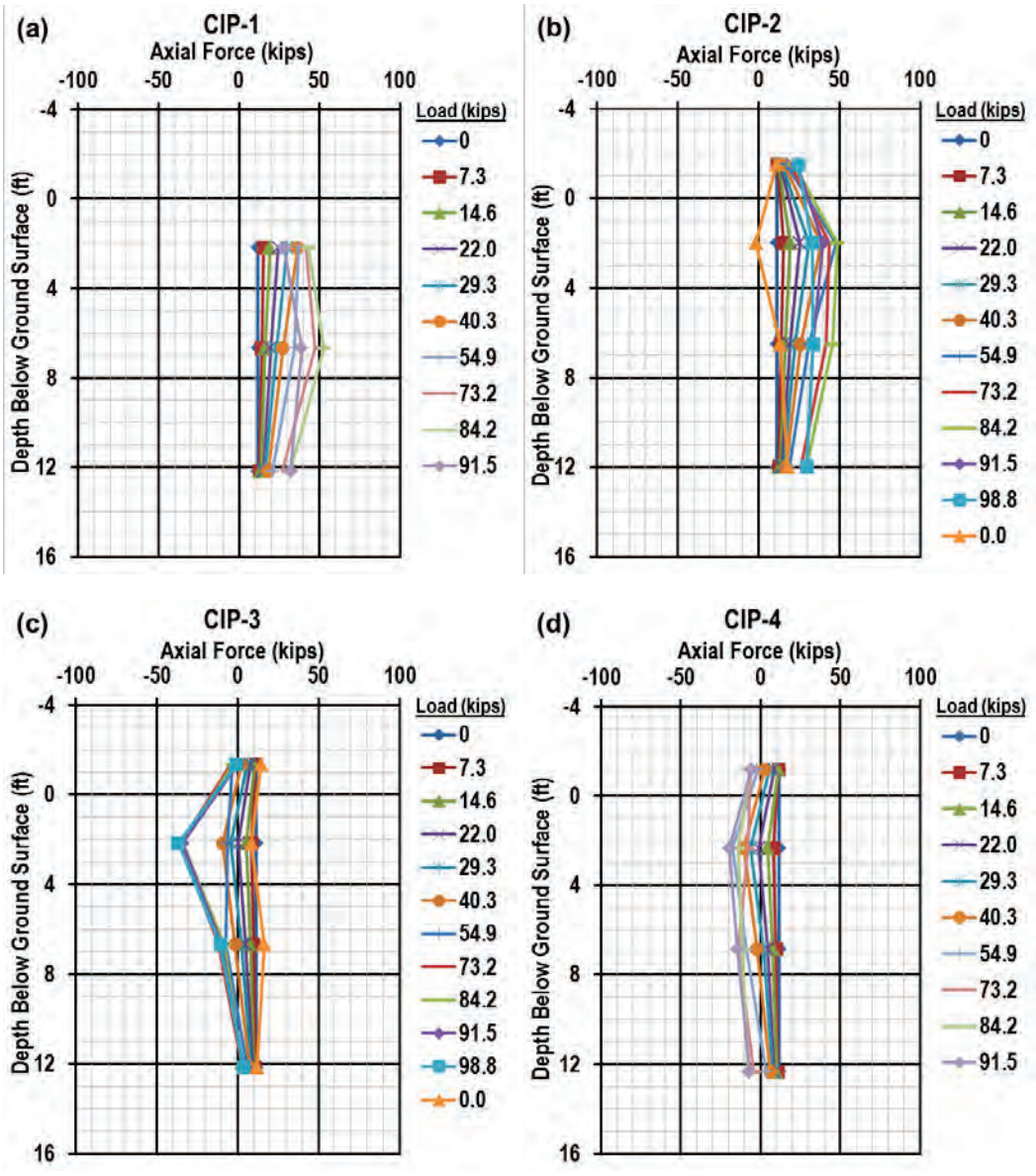

Figure 4.6. Axial force for (a) CIP-1, (b) CIP-2, (c) CIP-3, and (d) CIP-4. Compression forces are positive. Weight of cap included per Eq. 4.2. Topmost gages in CIP-1 were damaged during construction (Section 3.4.2).

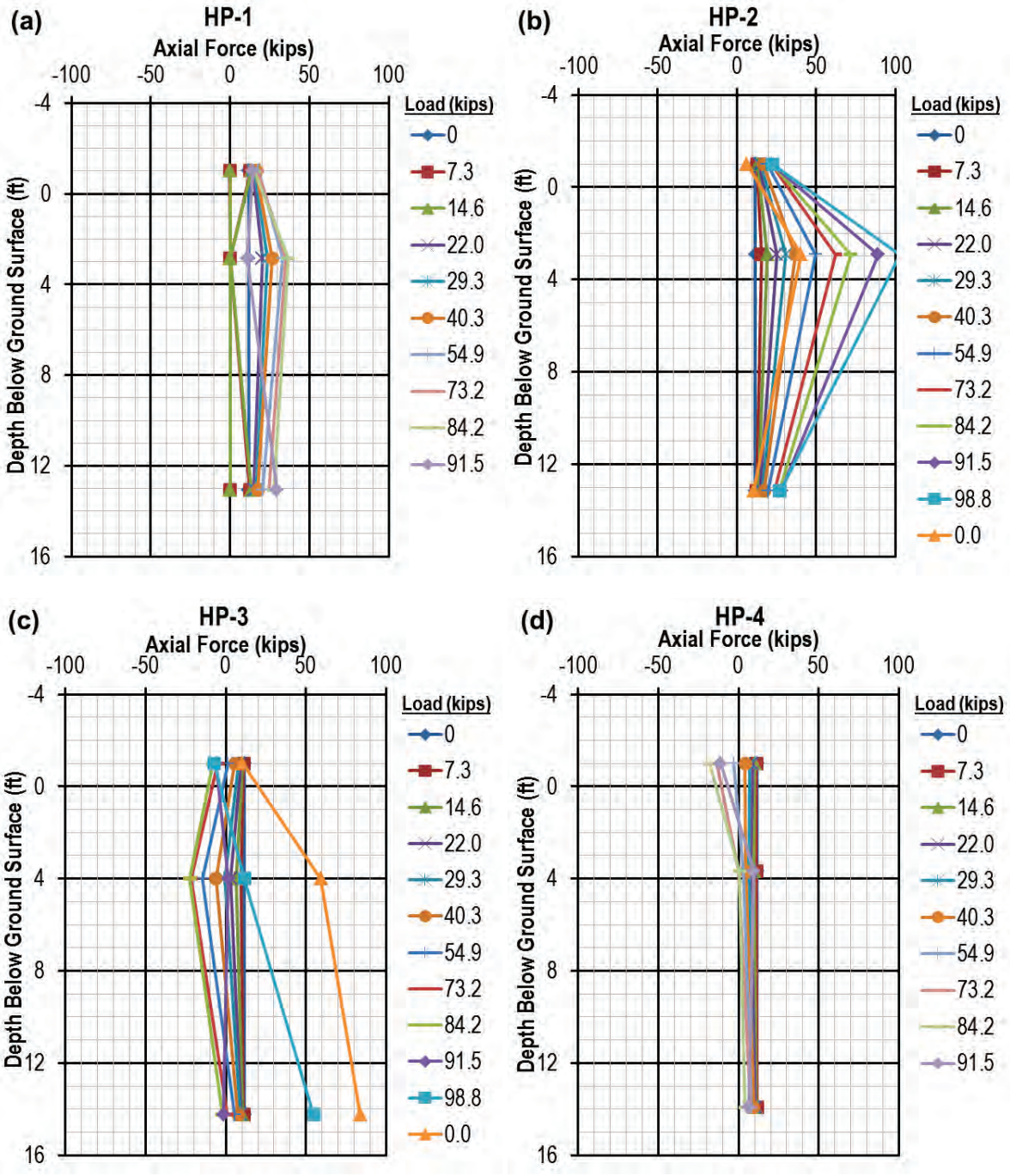

Figure 4.7. Axial force for (a) HP-1, (b) HP-2, (c) HP-3, and (d) HP-4. Compression forces are positive. Weight of cap included per Eq. 4.2.

4.4.2 Bending Moment Profiles from Strain Gage Data

Bending moment profiles from strain gages for the CIP piles are shown in Figure 4.8. The bending moment profiles for CIP-1, CIP-2, and CIP-3 are similar, irrespective of axial loading. All three indicate single curvature with maximum bending moments around 50 kip-ft. The bending moment data for CIP-4 are suspect; the data are inconsistent with the other three piles and, as for the axial forces from CIP-4, the magnitudes are small. The data indicate there was some bending moment at the pile heads, which

indicates the pile heads were restrained rotationally, probably to the point of fixity. Fixed pile heads are consistent with the observations by Rollins and Stenlund (2010).

Also included in Figure 4.8 is the bending moment profile for CIP-3 from SAA data during the final load step. The SAA bending moment profile is consistent with the respective profile from strain gage data, lining up atop one another at the mid-pile strain gage levels and showing similar shapes and magnitudes otherwise. The SAA profile has more data points, capturing a greater maximum value just below the ground surface as well as a slightly different shape near the bottom of the pile. Similar agreement between bending moments interpreted from SAA measurements and bending moments interpreted from strain gage measurements was reported in a paper by Boeckmann et al. (2014b) on the topic.

Bending moment profiles for H-piles are shown in Figure 4.9. The bending moment profile from the SAA data is included for HP-2. Most of the calculated bending moments from strain gage measurements were near zero. The issues that made interpreting axial force data for the H-piles difficult are even more problematic for calculations of bending moment, which require two readings of strain.

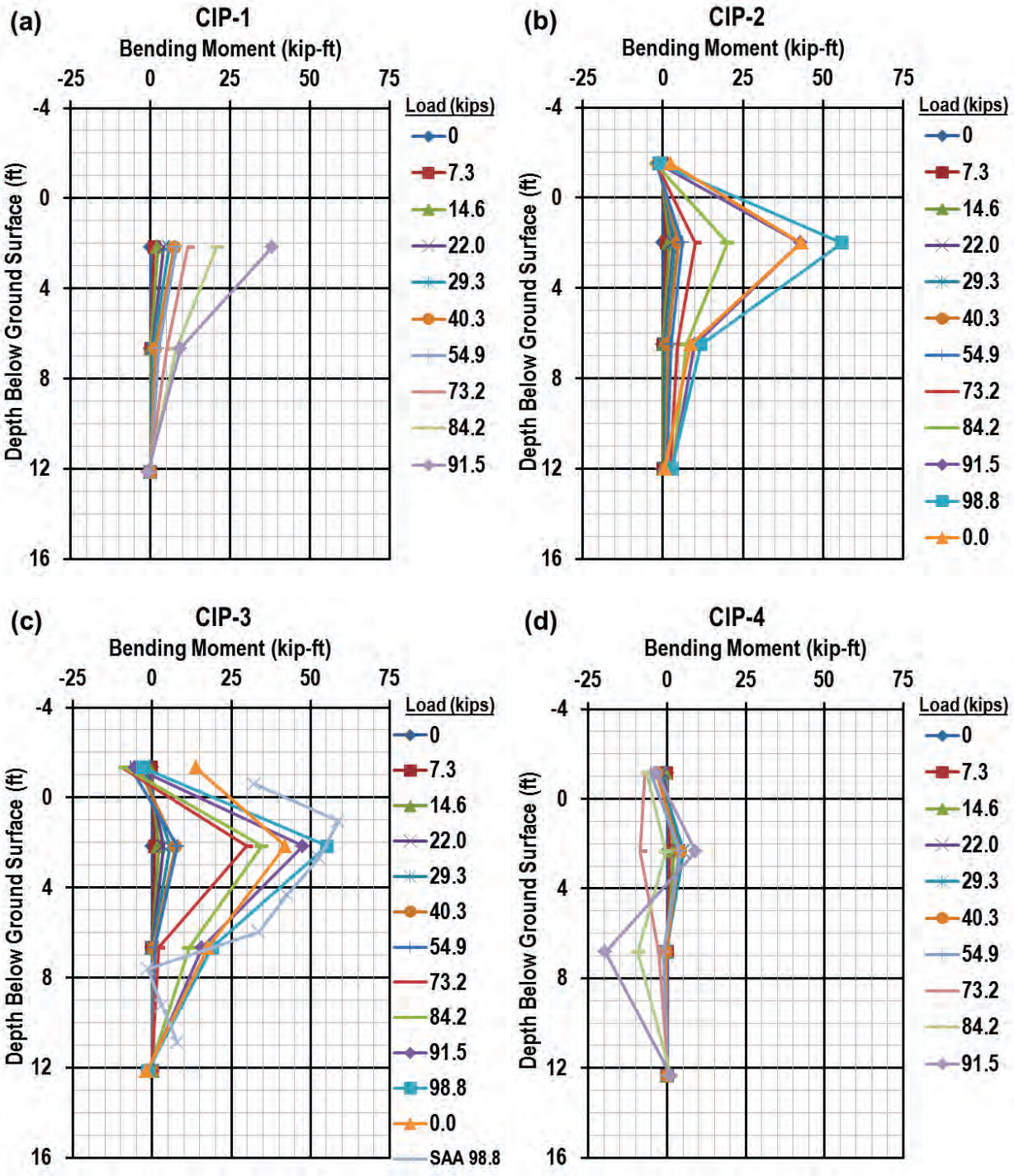

Figure 4.8. Bending moments for (a) CIP-1, (b) CIP-2, (c) CIP-3, and (d) CIP-4. Bending moments from SAA data are included for the final load step for CIP-3 for the sake of comparison.

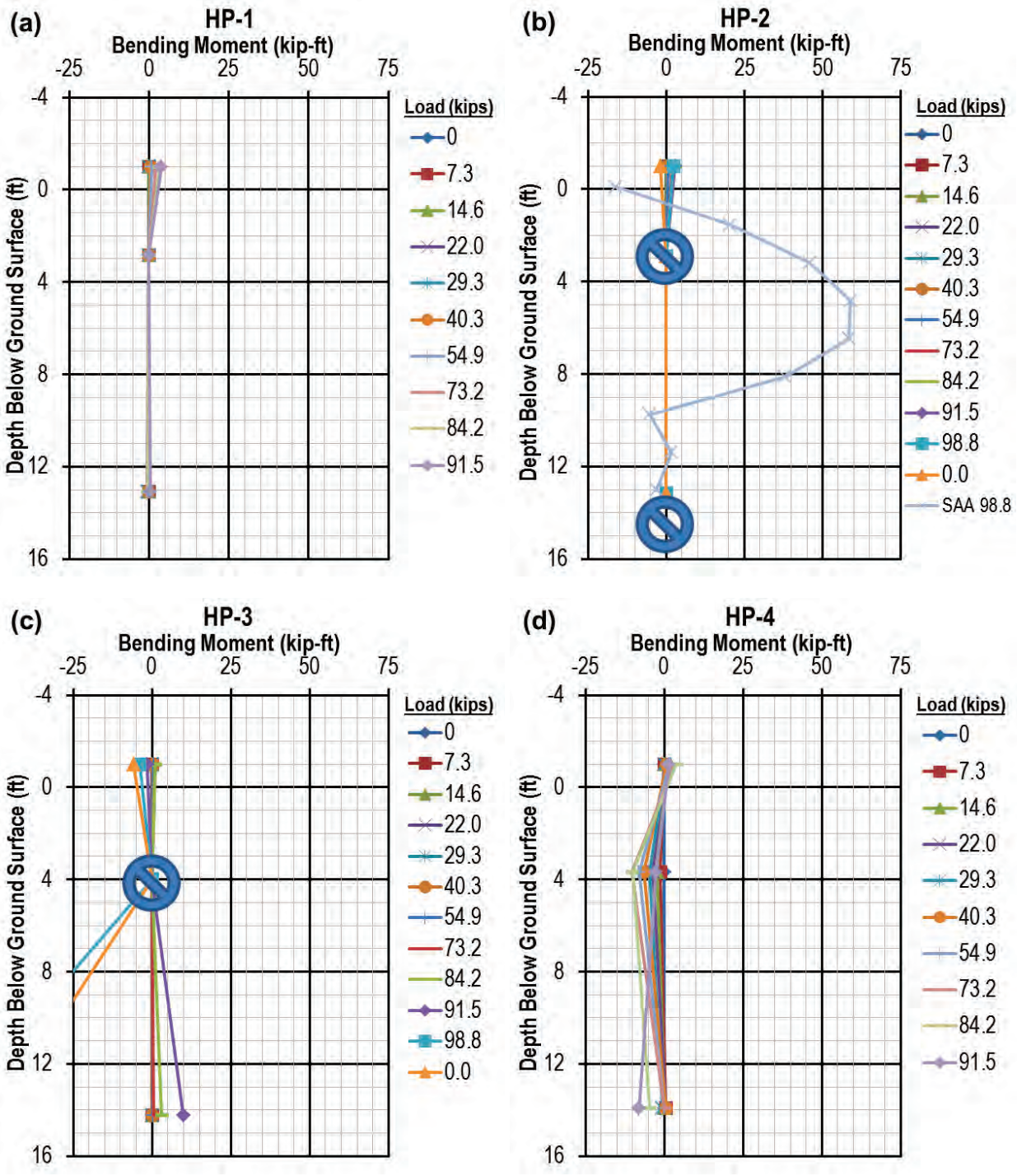

Figure 4.9. Bending moments for (a) HP-1, (b) HP-2, (c) HP-3, and (d) HP-4. Bending moments from SAA data are included for the final load step for HP-2. Large symbols indicate locations of non-functioning strain gages.

4.4.3 Bending Moment Profiles from SAA Data

SAA displacement profiles were presented in Section 4.2, and bending moments derived from SAA data for the final load step were discussed in Section 4.4.2. Additional interpretations from SAA data are included in Figure 4.10 (CIP piles) and Figure 4.11 (H-piles). These figures include the displacement data (same as Figure 4.4), cross-sectional rotation, bending moment, shear force, and unit lateral pressure. The interpretation technique described in Section 4.3 was extended to calculate the shear force and unit lateral pressure as the first and second derivatives, respectively, of bending moment.

The bending moment profiles are similar in shape and magnitude for both piles, with single-curvature shapes and maximum observed bending moments slightly greater than 50 kip-ft. As was observed for bending moments derived from strain gage measurements, the SAA bending moments calculated at the pile head are too low because of the unaccounted for stiffness contribution of the pile cap.

The shear force and unit lateral pressure profiles for both piles are noisy to the point of not being useful. This is consistent with the observation of some noise in the SAA bending moment profiles; the bending moment noise was exacerbated upon further differentiation. Measurement limitations make it very difficult to produce meaningful results for third and higher-order derivative quantities. The limitations of numerical differentiation, which also apply to strain gage data, provide a large motivation for using computer models such as those documented in Chapter 5 to further interpret the test results.

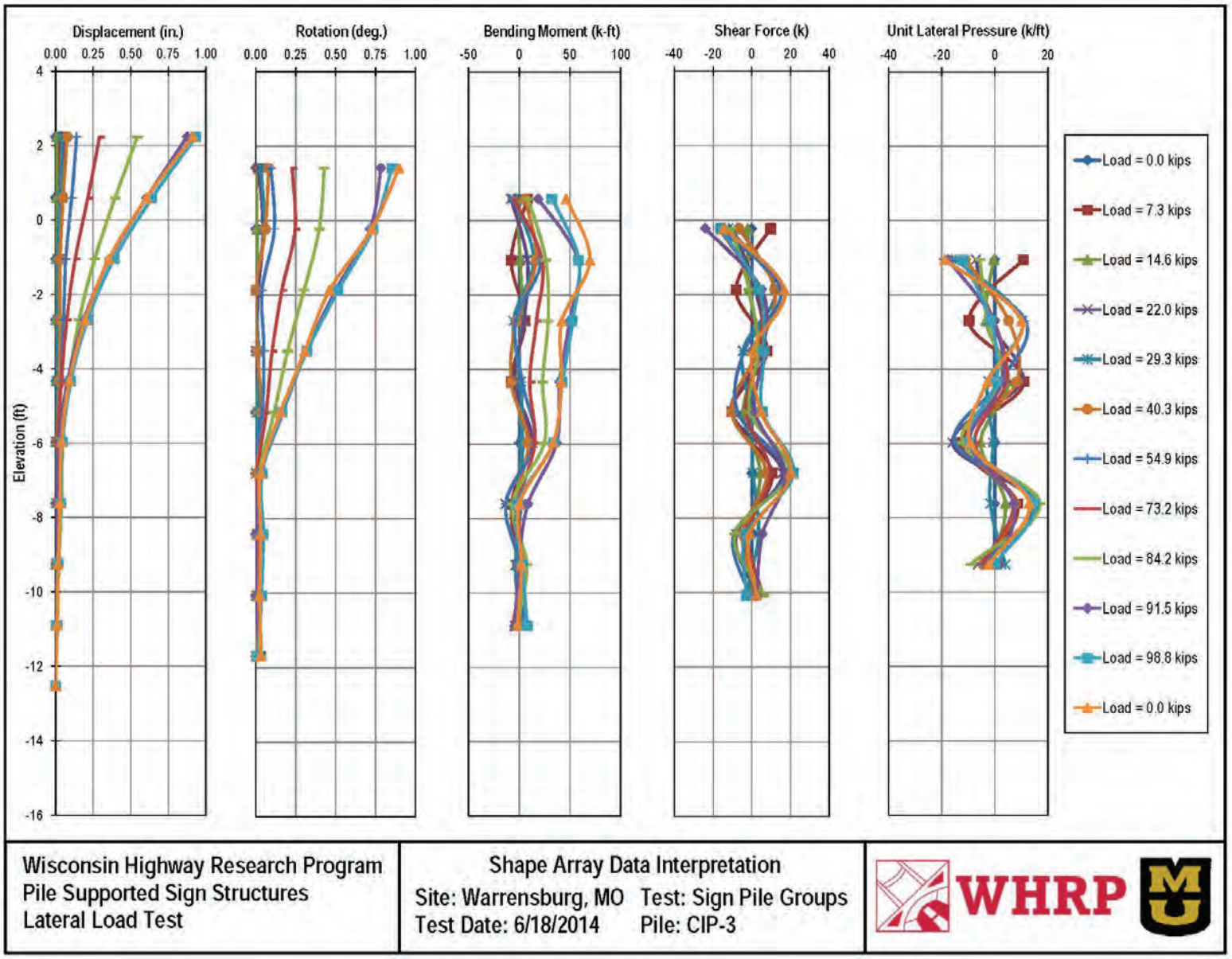

Figure 4.10. SAA data for CIP-3.

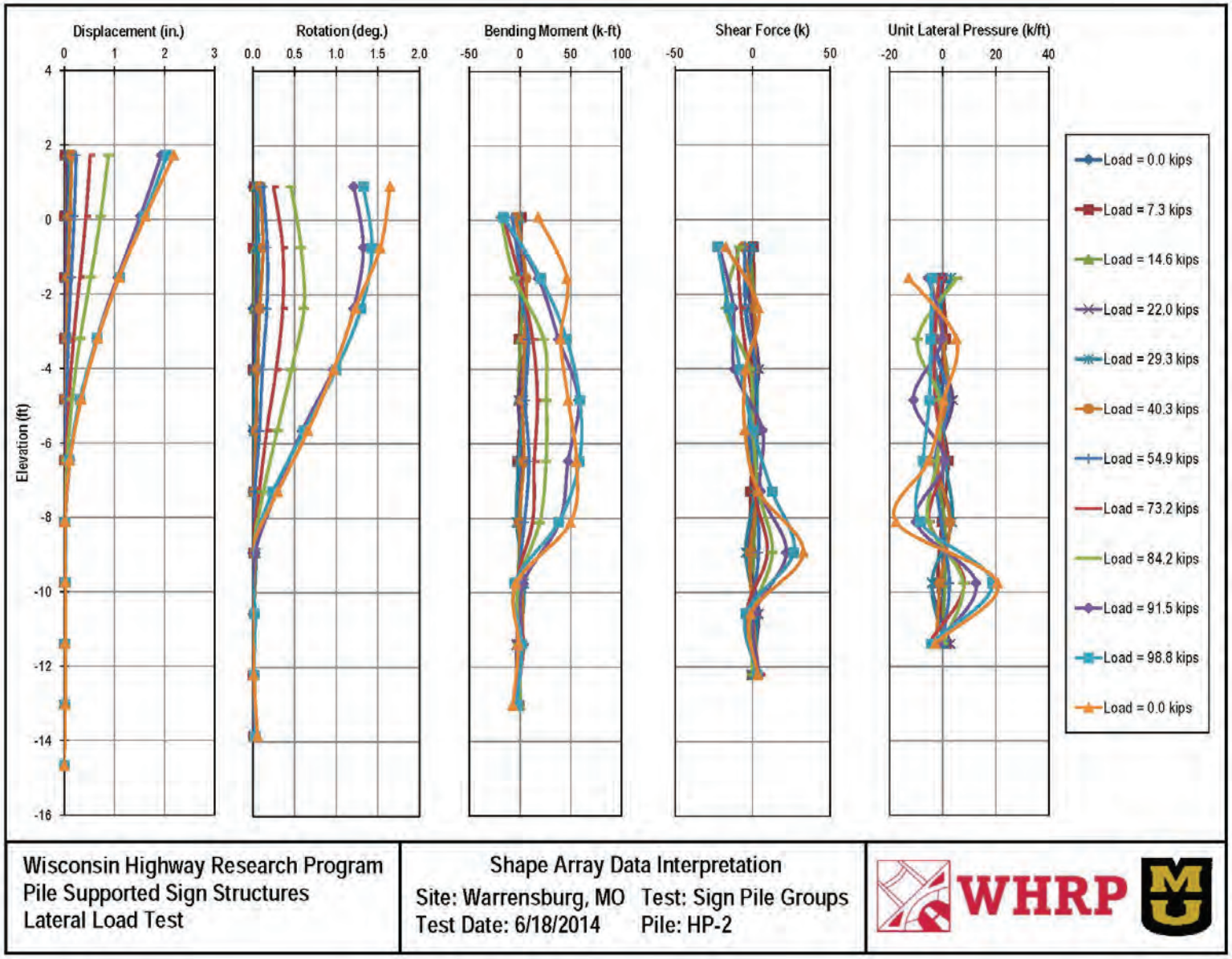

Figure 4.11. SAA data for HP-2.

5. Analysis of Experimental Results

Further analysis of the data presented in Chapter 4 was performed to model the results. Load-displacement curves for axial and lateral loading are presented before interpreting the data in the context of design based on static equilibrium. Further analysis was then pursued using numerical methods.

5.1 Comparison of Applied Test Load to "Typical" Sign Loading

At the end of the load test, the applied load was approximately 100 kips, which corresponds to an applied overturning moment of 900 kip-ft. These values are similar to the loads considered in the design example documented in Appendix A, which includes two relatively long spans and relatively large sign faces. The calculations for that large sign were performed in accordance with AASHTO's 17th Edition bridge specifications (AASHTO, 2002), which is based on allowable stress design. The calculations consider two load cases for the sign's four-pile group: (1) 90-kip horizontal load and 777-kip-ft overturning load, and (2) 96-kip horizontal load and 400-kip-ft overturning load. These are the dominant loads for each case; other, smaller loads are included transverse to the cap. The magnitude of the loads applied to the test structures for this project were therefore similar to those predicted for a relatively large sign structure.

While the magnitude of the applied loading was similar to that for a "typical" sign structure, the nature of the test loading was differs from actual loading on sign structures in some ways. The load test involved one cycle of static loading. Design sign foundation overturning loading is primarily from wind gusts of short duration, and the loading could be cyclic if the structure is assumed to experience the design load multiple times over its life. The short duration of the wind loading would presumably result in more favorable performance (i.e. less deformation) compared to the static loading applied during the load test, but cyclic loading would likely result in reduced lateral resistance and stiffness as reported by Rollins et al. (2003) and summarized in Chapter 2.

5.2 Compiled Results and Static Equilibrium Model

To begin to characterize the pile and pile group behavior observed during the load test, several graphs summarizing the data presented in Chapter 4 were created. The first, Figure 5.1, contains the axial load-displacement curves for all 8 piles. The axial loads include the measured load from strain gages just below the ground surface as well as 11.7 kips per pile to account for the weight of the cap. As explained in Chapter 4, the gages at the pile heads were difficult to interpret due to the contribution of pile cap stiffness, and there likely was little load shed to the top 2 ft of soil. The displacements are from the wireline devices since they were installed in line with the pile heads. The wireline devices are not as precise as the other displacement instruments, which explains why the initial portions of the curves are not very well defined and the plots are not particularly smooth.

Nevertheless, the axial load-displacement curves are informative. Foremost, the data indicate the piles reached an ultimate state since the axial loads in nearly every pile reached a maximum value after which the axial load either decreased or was maintained with significant additional displacement. This is discussed further in subsequent analyses described below. The magnitude of the ultimate uplift load ranged from 20 to 30 kips. (Data for HP-4 is around zero, but data for this pile is suspect as discussed throughout Chapter 4.) The final loads on the compression piles were greater, around 35 to 50 kips with HP-2 having much greater values, likely due to strain gage difficulties discussed previously. These compression loads are likely not ultimate values; the compression loads are only as great as required for vertical force equilibrium, and tip resistance should result in greater geotechnical capacity for compression piles than uplift piles. (Compression loads were higher than uplift loads because of the weight of the structures.) The compression loads appear to have decreased unexpectedly before the applied load was removed. This is perhaps a result of the difficulties interpreting axial loads from strain gage data when the piles are subject to large bending moments. The initial portions of all axial load-displacement curves are not well defined, but they are clearly rather steep.

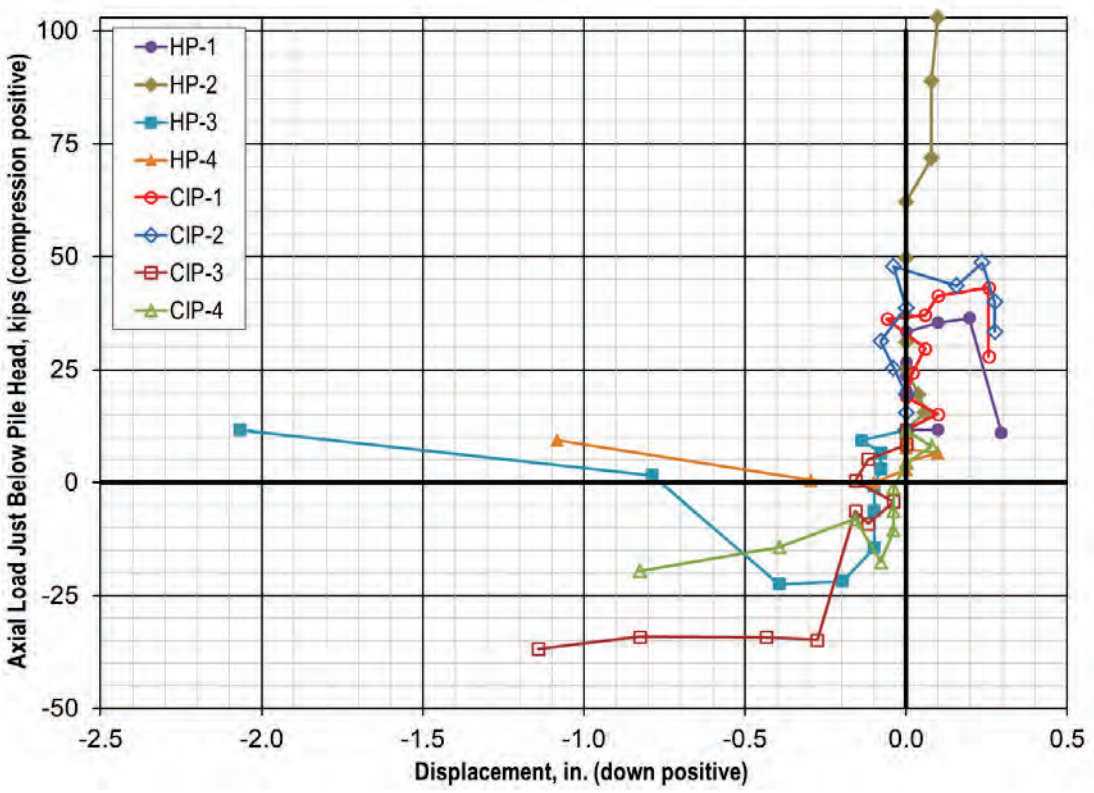

Figure 5.1. Axial load-displacement curves. Axial loads are the loads measured in the piles plus 11.7 kips, the weight of the each structure divided by four piles.

Bending moment-displacement curves were also plotted as shown in Figure 5.2. Bending moments from H-pile strain gages were not included due to the issues described in Section 4.4. The curves plot maximum bending moment, which was just below the ground surface for CIP strain gage and SAA data and about 5 ft below ground for HP-2 SAA data, versus displacement from the bottom LVDT on the front (compression) side of the caps since there were no instruments to measure the specific lateral displacement of each pile head. The curves are all rather similar except for CIP-4, the data for which is suspect based on discussion in Section 4.4.2. Otherwise, the bending moment-displacement data are rather linear with no breaks in the curves, suggesting the piles did not reach an ultimate state with respect to lateral loading.

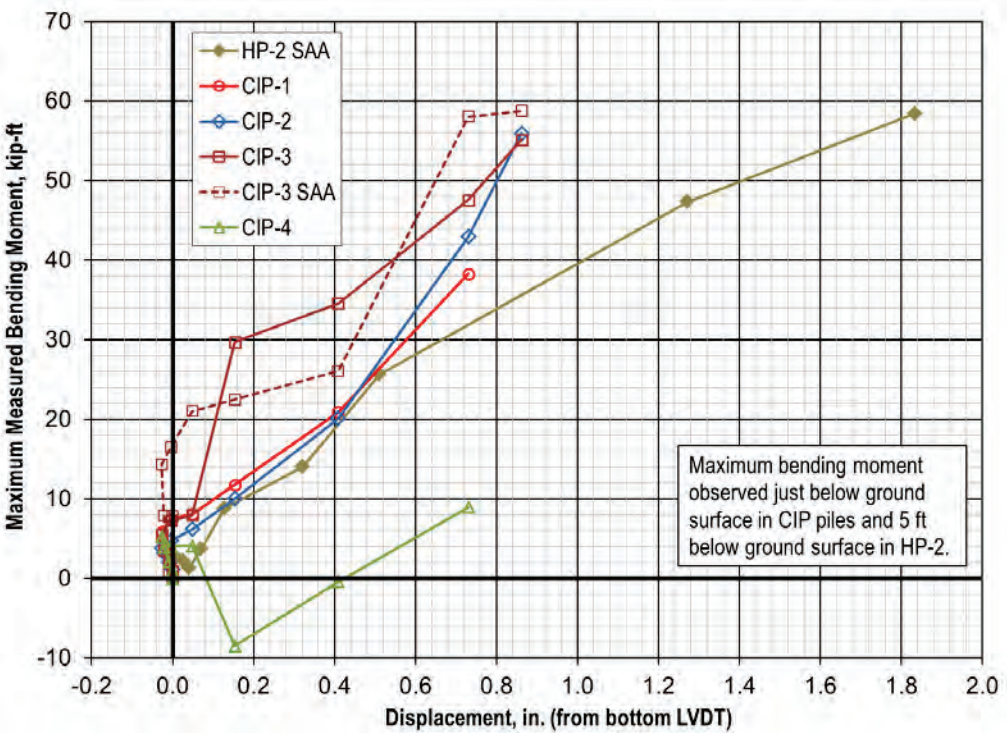

Figure 5.2. Bending moment-displacement curves. Data are from strain gages unless SAA is indicated in the legend.

Taken together, the data from Figure 5.1 and Figure 5.2 suggest the piles had reached their axial geotechnical capacities, at least for uplift, but had additional lateral capacity remaining at the end of the test. Two additional sets of graphs were created to confirm these observations. The first, Figure 5.3, plots the measured axial loads just below the pile head versus the applied load to track the development of axial loads throughout the test. Included on the plots are dashed lines indicating the axial load couple that would need to be developed to counteract the applied overturning moment. These were calculated according to Eq. 5.1, which is based on static equilibrium of bending moments about the center of the cap at the ground surface, assuming a rigid structure and neglecting moments that would develop at the pile heads. The calculations also satisfy vertical force equilibrium, i.e. the sum of all axial loads at the pile head equals the weight of the structure (47 kips).

$$F_{applied} \cdot Height = 2 \cdot P_{head:comp} \cdot \frac{d}{2} + 2 \cdot P_{head:ten} \cdot \frac{d}{2} \qquad \textbf{Eq. 5.1}$$

where $F_{applied}$ = load applied to the pile structure
$Height$ = height of load application = 9 ft
$P_{head:comp}$ = axial load developed at compression pile head (two piles)
d = distance between tension and compression piles = 6 ft
$P_{head:ten}$ = axial load developed at tension pile head (two piles)

For small loads, the data indicate axial loads just less than those required to counteract the applied moment. As the applied load was increased beyond 40 kips, the departure from the counteracting axial force couple became more significant as the measured axial loads leveled off, presumably because they had reached their geotechnical capacity. These trends are more clear for the CIP pile data than the H-pile data due to the instrumentation and interpretation difficulties described in Chapters 3 and 4.

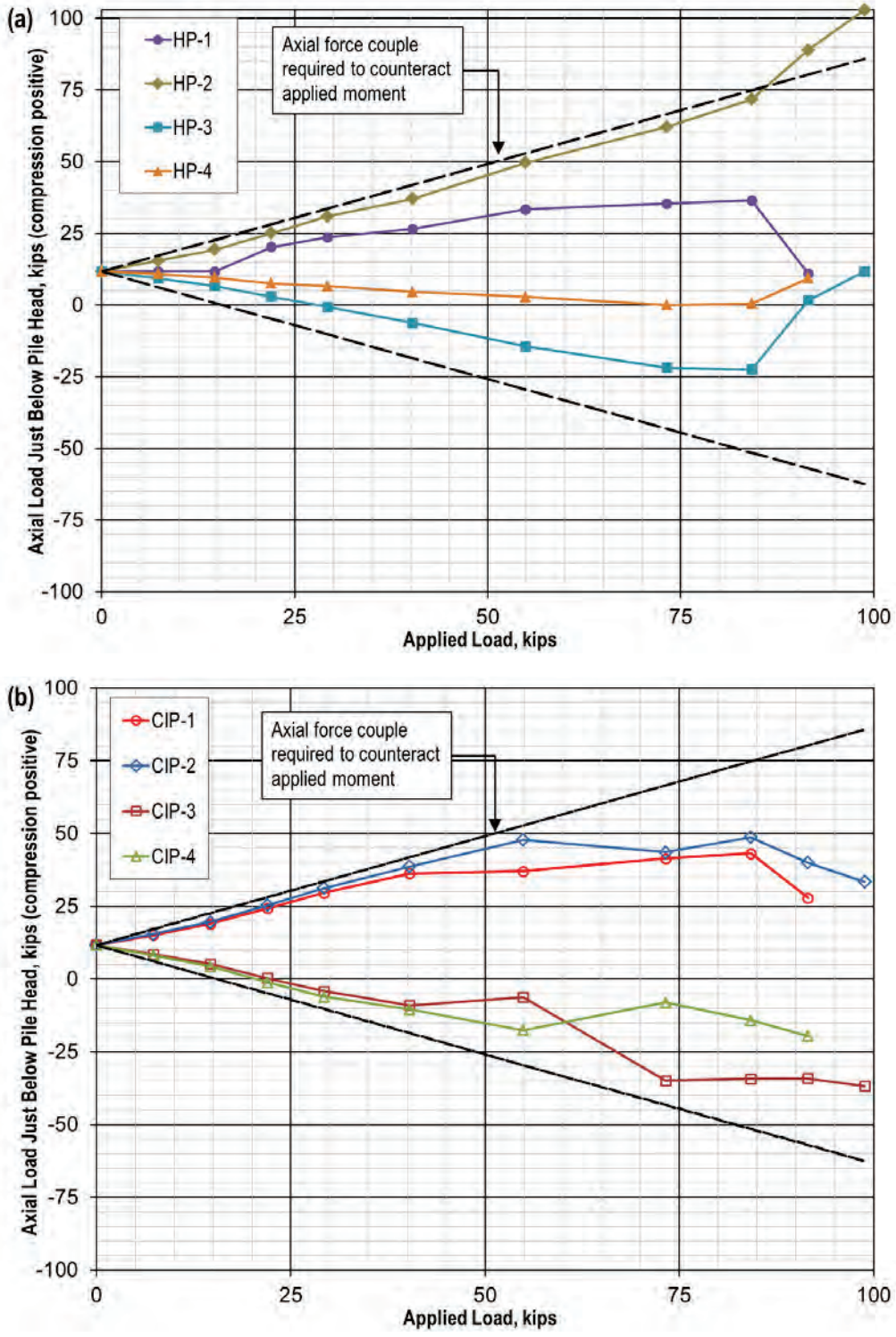

Figure 5.3. Axial load progression plots for (a) H-pile group and (b) CIP pile group. Lines are offset from origin because of the weight of the structure.

Similar plots were prepared to track the development of bending moments during the test. The graph of Figure 5.4 shows maximum pile bending moments versus the load applied to the structure. As for the bending moment-displacement curves, strain gage data for the H-pile cap was neglected, so only SAA

bending moments are available for the H-pile group. The curves indicate modest increases in bending moment with applied load until the applied load was about 55 kips, at which point the increases in bending moment were more substantial. It is interesting and slightly misleading to note that if the axes had been reversed, the curve shapes would resemble "typical" load-displacement curves. This should not lead to the erroneous conclusion the piles had reached their lateral capacity, since Figure 5.2 suggests the bending moments never peaked or leveled off, even at the ultimate test load. Instead, the shape of the curves in Figure 5.4 suggests the bending resistance of the piles was not mobilized significantly until the applied overturning load began to fully mobilize the axial geotechnical capacity of the piles. The curve for CIP-4 is inconsistent with the other CIP pile data, as discussed in Section 4.4.2.

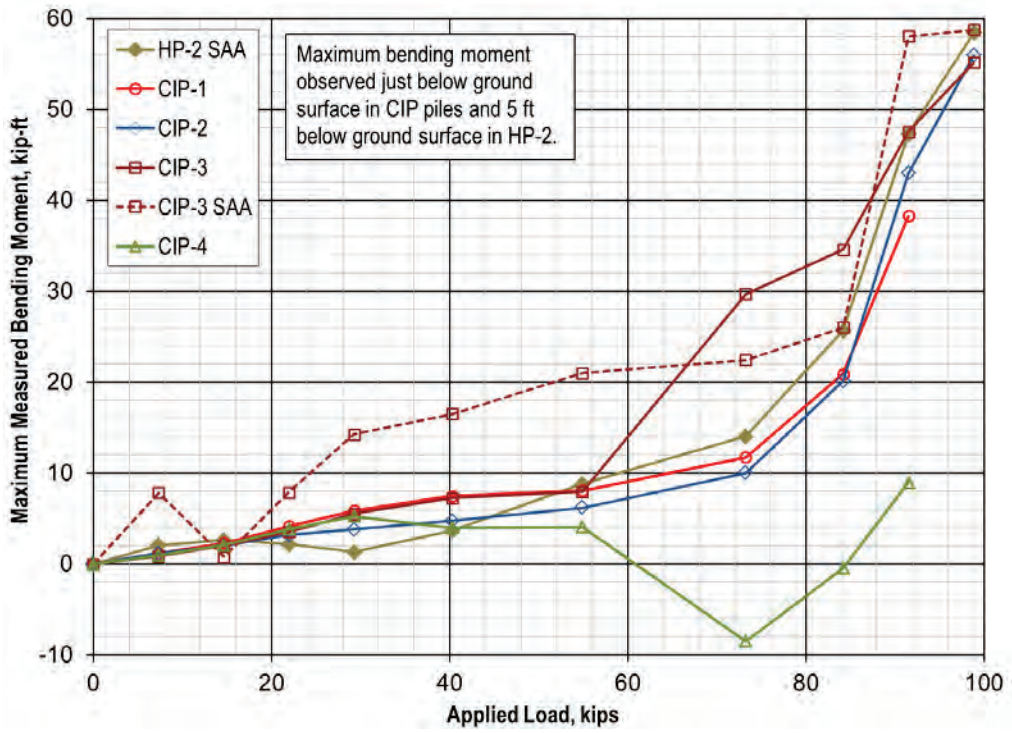

Figure 5.4. Bending moment progression plot.

A more rigorous exploration of the trends observed in Figure 5.3 and Figure 5.4 was pursued with calculations related to static equilibrium of the CIP structure. As discussed in Section 3.3, the gap between pile caps and ground surface was maintained throughout the test, so bearing forces were not included. The results of static equilibrium analysis of the CIP pile cap are presented in Figure 5.5 (bending moment equilibrium) and Figure 5.6 (axial force equilibrium). A similar analysis was pursued for the H-pile cap but limitations of the strain gage data produced interpretations of no additional value to the discussions above.

The bending moment equilibrium calculations (Figure 5.5) confirm a primary observation from the previous interpretations: axial forces increased proportionally with the applied overturning load for small loads, but when the applied load reached about 50 kips, the axial forces ceased to keep pace with the increasing applied load, likely because the piles had reached ultimate geotechnical capacity in uplift. At this point, significant bending moments began to develop at the pile heads, where bending previously was minor, especially in comparison to the axial force couple. The data of Figure 5.2 suggest the piles had not reached their ultimate lateral resistance, so it's possible and perhaps likely the pile structures could have resisted some additional loading albeit with substantial lateral deformation.

In general, the measurements support this static equilibrium analysis, with the measured resistance (axial force couple and bending moments at pile head) 10 to 40 percent less than the applied overturning moment. The difference is not surprising considering the difficulties measuring and interpreting strain

gages and the tendency to underreport stiffness. Further, the loads used in the calculations were measured slightly below ground, not at the pile head, so their values would be expected to be less than at the pile heads. The greatest differences were observed at the end of the test, when significant bending makes strain gage interpretation more difficult and when the applied load was perhaps not as great as reported since the structures may not have reached equilibrium during loading. Greater differences calculated for small loads are likely just a result of the sensitivity of the calculations for small numbers.

The weight of the cap has been factored out of the axial force equilibrium calculations presented in Figure 5.6 to make comparisons simpler and more meaningful. As a result of neglecting cap weight, the axial forces presented are just those developed in response to the applied loading. The axial force equilibrium calculations presented in Figure 5.6 are less informative than those for moment equilibrium, but they offer useful perspective on the precision of the strain gage data and its analysis. The differences between compression and tension loads were by far greatest at the end of the test, when data were recorded only CIP-2 and CIP-3.

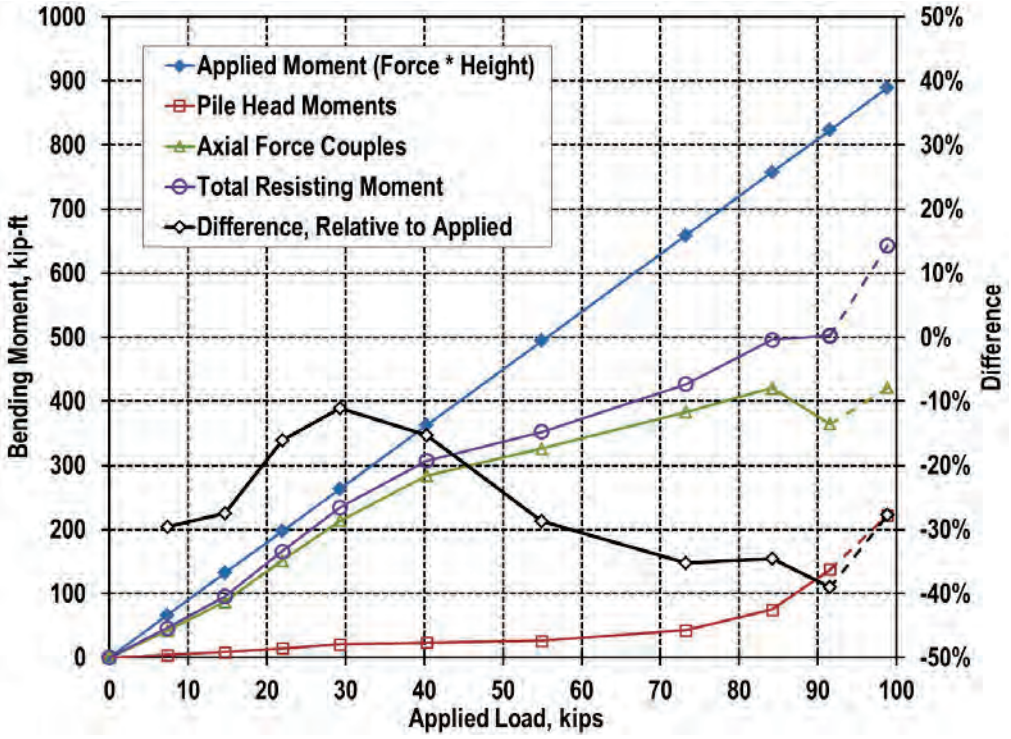

Figure 5.5. Bending moment equilibrium of CIP pile structure, calculated about the center of the base of the structures. Total resisting moment is the sum of the axial force couple and the pile head moments. Dashed lines are used for the ultimate load step to indicate the results from CIP-2 and CIP-3 were doubled since there were no data collected for CIP-1 and CIP-4.

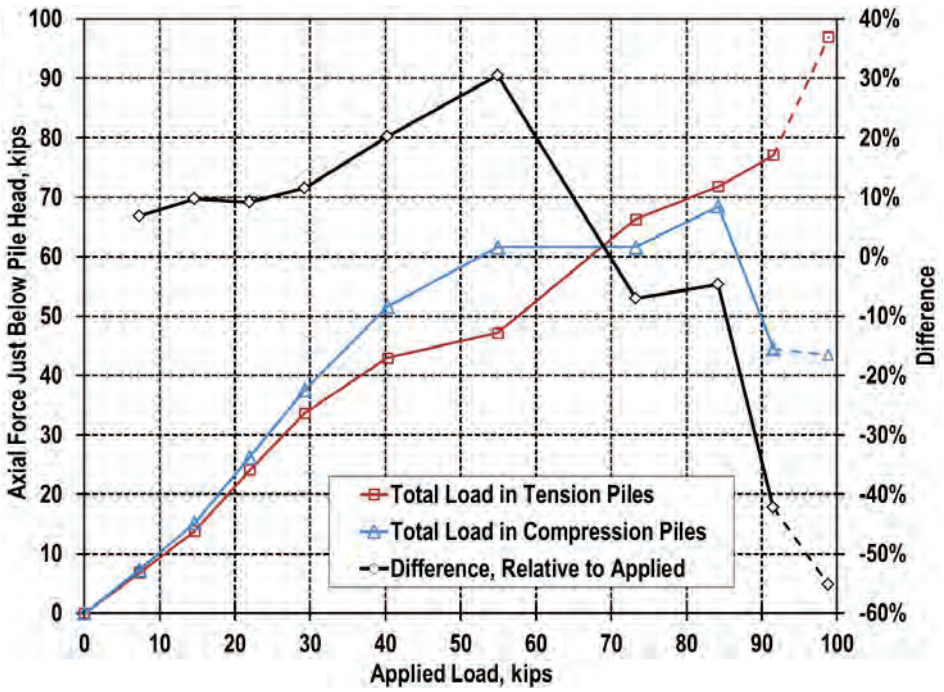

Figure 5.6. Axial force equilibrium of the CIP pile structure. Dashed lines are used for the ultimate load step to indicate the results from CIP-2 and CIP-3 were doubled since there were no data collected for CIP-1 and CIP-4.

5.3 Comparison with Ensoft *GROUP* Model

The static equilibrium calculations discussed above and captured in Figure 5.5 provide a useful explanation of the observed behavior of four-pile groups subjected primarily to overturning loads. The load test was modeled with Ensoft *GROUP* 2014 (Reese et al., 2014) to further evaluate the load test data, with three objectives:

(1) Confirm the program would predict similar behavior, which was expected since *GROUP* assumes a rigid cap and static equilibrium;

(2) Calibrate axial load-displacement and lateral *p-y* parameters for the load test data, acknowledging that there is no unique solution for one load test;

(3) Predict behavior of the pile caps for greater loads, i.e. explore the possibility of applying greater loads to fully mobilize additional bending capacity of the piles.

As described in Section 3.2, a *GROUP* model was created to aid in the design of the experiment. During the course of preparing for and performing the load test, *GROUP* 2014 was released. The original model was updated to the new version. In addition, a second model was created to model the H-Pile group since the original model was only for CIP piles. Both calibrated models are discussed in the sections below. All pile head to cap connections were assumed to be fixed, which is consistent with the data (Sections 4.4.2 and 4.4.3) and recommendations from Rollins and Stenlund (2010) discussed in Chapter 2.

The strategy adopted for calibration of the models was to develop axial load-displacement curves for the pile heads that resemble the ones plotted in Figure 5.1 and then adjust model parameters to produce reasonably accurate predictions of observed displacement profiles, bending moment profiles, and load-displacement curves. There are numerous model parameters that could be adjusted, but the analysis focused on the magnitude and initial stiffness of the axial load-displacement curves and *p-y* parameters since these were deemed most uncertain and significant. After calibrating the models, they were used to predict response for greater loads than those applied during the load test.

5.3.1 GROUP Model for CIP Pile Structure

The CIP pile group was modeled first since its data set is more complete. The axial load-displacement curve used for CIP piles is shown in Figure 5.7. The calibrated curve is plotted alongside the measured data (same as Figure 5.1). The curve is based on *t-z* analysis with ultimate unit side resistance of 1.25 ksf in the stiff clay and 4 ksf in the shale and ultimate unit tip resistance of 50 ksf in the shale. The calibrated curve represents a reasonable model of the measured response.

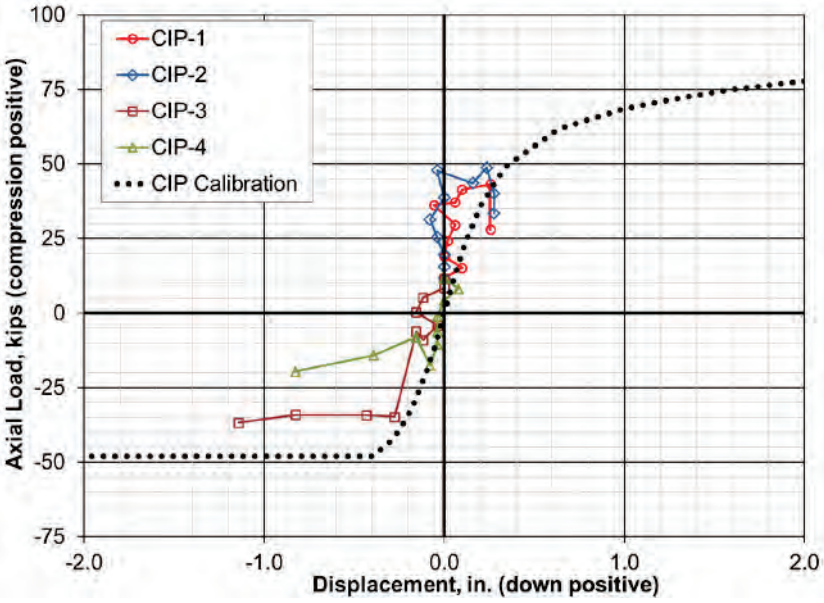

Figure 5.7. Axial load-displacement curve used to calibrate *GROUP* model for CIP pile structure.

To match the observed bending behavior, the calibrated *GROUP* model used the same *p-y* curves from the design model, which were based on results of for load tests of drilled shafts at the same site (Boeckmann et al. 2014), but the calibrated model applied a *p*-multiplier of 2.5. The resulting lateral deflection and bending moment profiles for the final load step are shown in Figure 5.8. The results shown in Figure 5.8 are in good agreement, with the model overpredicting moments to a reasonable degree but matching both profile shapes reasonably well, although the predicted deflections are small for much of the shaft's length. The *p*-multiplier of 2.5 effectively increases the lateral resistance by a factor of 2.5. This is reasonable considering the original curves were from 36- and 42-in. diameter drilled shafts, and greater resistance per unit width is expected from smaller diameter piles. The *p*-multiplier of 2.5 is a calibration tool to achieve the match shown in Figure 5.8; it is not an indication of lateral response of all similar four-pile groups, and it is not recommended for use beyond this research.

A summary of the results predicted by the *GROUP* model is presented in Figure 5.9, which contains similar information related to static equilibrium as Figure 5.5. As expected, the *GROUP* model results comply with static equilibrium, with the total resisting moment from axial force couple and pile head moments equaling the total moment applied for each load step. As discussed in the previous section, the measured forces and moments sum to total resisting moments that are 10 to 40 percent less than applied moments. The *GROUP* model predicts slightly greater values for axial force couples and pile head moments in order to satisfy static equilibrium. The shapes of the measured and *GROUP*-predicted curves are similar; most notably, both predict an increase in pile head moments at about the same load (55 kips), which corresponds to the tension piles approaching their uplift capacity. Interestingly, the *GROUP* model predicts mobilization of pile head bending moments at smaller loads than observed, though the values are the same by the end of the load test. This is explored further in the bending moment-displacement curve from *GROUP* shown in Figure 5.10, which also includes the measured data originally shown in Figure 5.2. The predicted data are consistent with the measured data although the predicted displacements are slightly less than those observed.

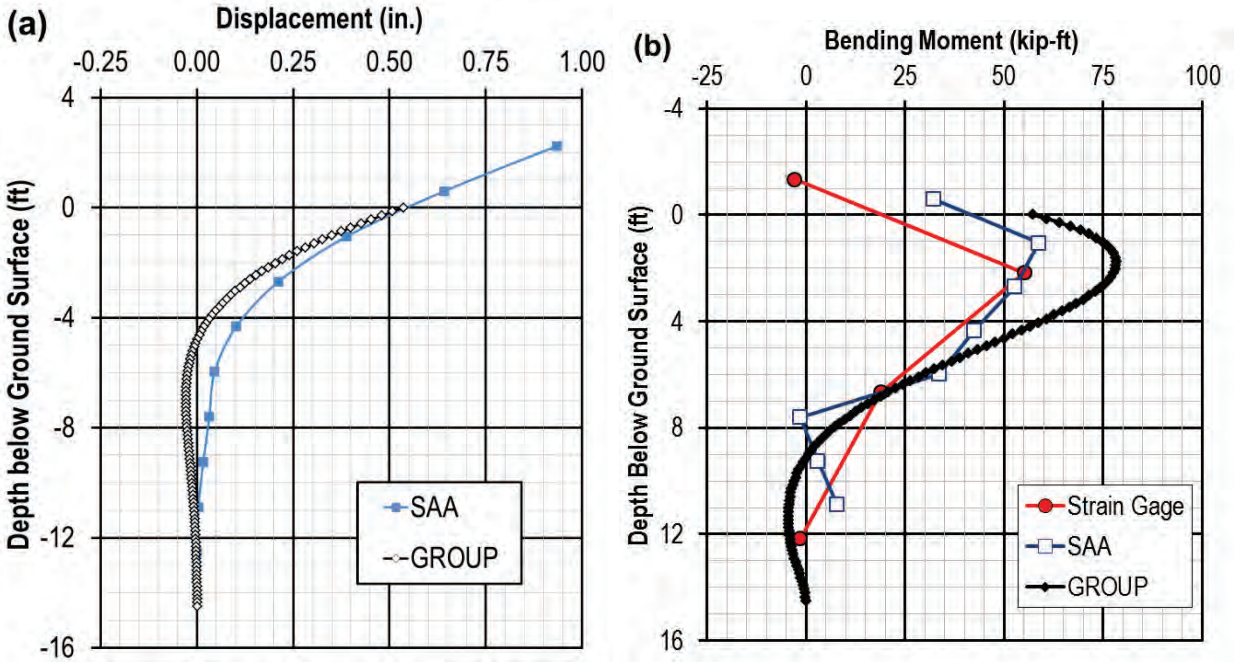

Figure 5.8. Results of calibrated *GROUP* model for CIP pile structure at maximum test load (99 kip): (a) displacement profile and (b) bending moment profile.

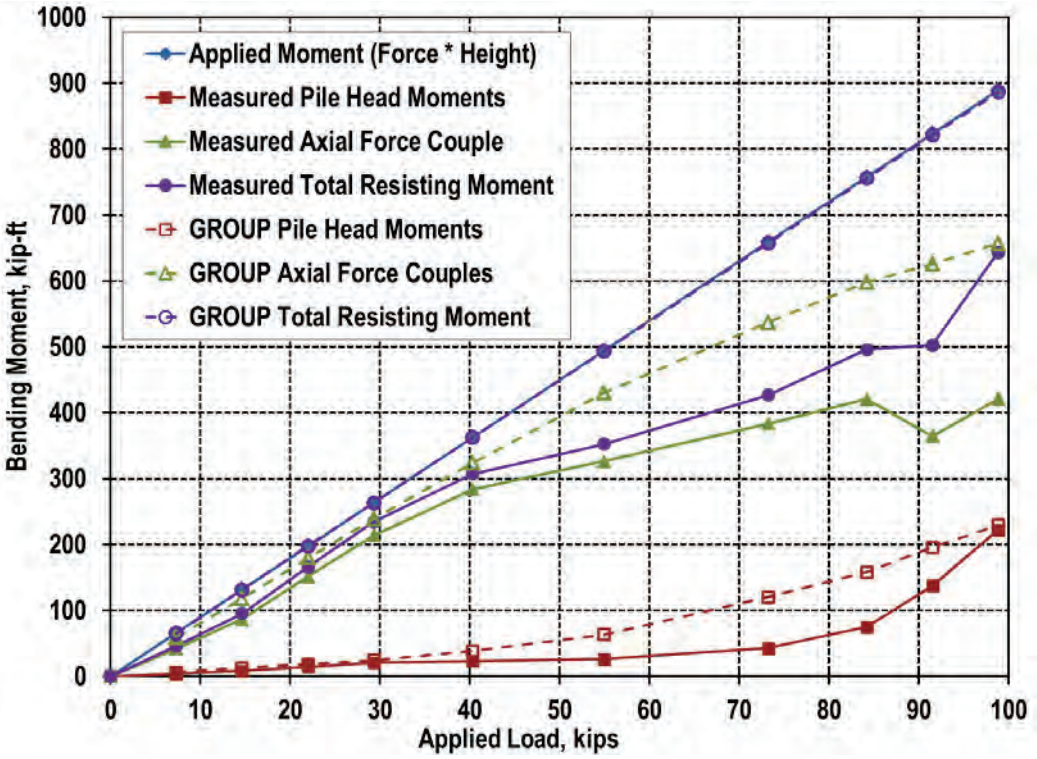

Figure 5.9. Static equilibrium from *GROUP* model for CIP pile structure. Solid lines and symbols used for measurements; dashed lines and open symbols used for *GROUP* results. Note the total resisting moment predicted by *GROUP* is perfectly coincident with the applied moment.

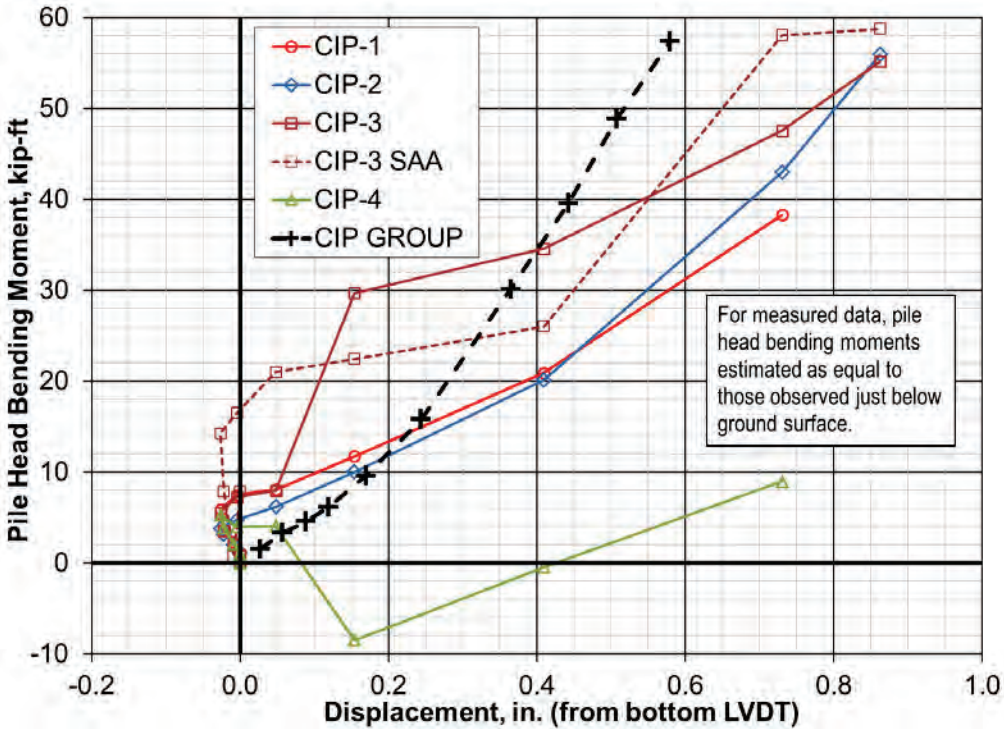

Figure 5.10. CIP pile head bending moment-displacement curves, including those predicted by *GROUP*. *GROUP* predicts nearly equal bending moments in all four pile heads.

5.3.2 GROUP *Model for H-Pile Structure*

Modeling the H-pile structure in *GROUP* was more difficult since its data set was less robust, particularly for axial loads. The axial load-displacement curve used to calibrate the model is shown in Figure 5.11. The calibrated curve is plotted alongside the measured data as well as the curve for the calibrated CIP model (same as Figure 5.7). The curve for the calibrated model is based on *t-z* analysis with ultimate unit side resistance of 1.25 ksf in the stiff clay and 4 ksf in the shale and ultimate unit tip resistance of 50 ksf in the shale. These are the same parameters used to develop the CIP model curve, but the H-pile axial load-displacement curve has greater axial load capacities because the side and tip areas of the H-piles are greater, assuming the piles were plugged. The axial load-displacement curve for the calibrated model is perhaps slightly greater than the measured data, but not to an unreasonable degree considering the quality and variability of the H-pile axial load data and the response from HP-2. Also, the axial load-displacement curve for the calibrated model has a greater initial stiffness value than was used for the CIP model. Greater stiffness values were used to provide a better match to the overall set of test data, not because the measured axial load-displacement data necessarily suggest such a difference.

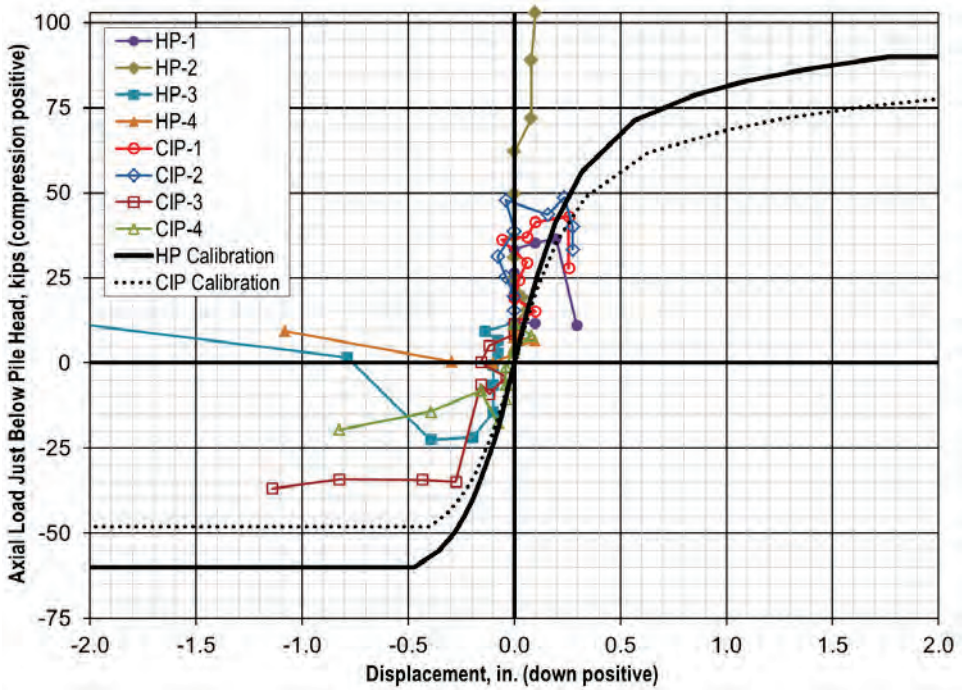

Figure 5.11. Axial load-displacement curves used to calibrate *GROUP* models.

The H-pile *GROUP* models also used the *p-y* curves from Boeckmann et al. (2014) for load tests of drilled shafts at the same site. A *p*-multiplier of 0.4 was used. The resulting lateral deflection and bending moment profiles for the final load step are shown in Figure 5.12. The *p*-multiplier of 0.4 effectively decrease the lateral resistance by a factor of 2.5. This is reasonable considering the H-piles were pulled along their weak bending axes, so the flanges were essentially cutting through the soil as the caps deflected. The effective diameter for lateral loading, then, was much less than the 10-in. pile width used in the *GROUP* calculations. As for CIP pile group calibration, the *p*-multiplier for H-pile groups was essentially a calibration tool and is not recommended for specific use beyond this project. Nevertheless, some reduction in lateral resistance should likely be considered for H-piles loaded along their weak axis.

The results shown in Figure 5.12 indicate a rather good match to the deflection data as well as the bending moment data. Significantly, though, the predicted bending moment at the pile head is opposite in sign the moment from SAA data, which has substantial consequences for the overall stability of the structure (the negative interpreted bending moment from SAA data is detrimental to stability; the *GROUP* bending moment adds resistance). It is likely the interpreted SAA bending moments at the pile head are mistaken due to difficulties associated with pile cap stiffness and interpreting rotation data at the pile head. (These issues were likely avoided to some degree for the CIP data because of how the SAA joints lined up with the cap.) Because of these difficulties, the interpreted SAA bending moment at the ground surface and 2 ft below the ground surface were plotted against displacement in Figure 5.13 alongside the *GROUP* prediction. (The interpreted SAA data are different from those in Figure 5.2, which were maximum values from 5 ft below ground.)

The *GROUP* prediction of bending moments at the pile head is between the two values plotted from SAA data, starting negative and finishing positive near the end of the test. The interpretation is consistent with the observation noted throughout this chapter: pile head bending moments are mobilized and play a significant role in stabilizing the pile group structure once the load in the tension piles approaches the geotechnical uplift capacity. The results for the SAA data are an especially obvious case of this behavior, as the initial pile head bending moments are detrimental to stability, becoming stabilizing only when the uplift capacity of the tension piles has been almost fully utilized. Finally, it's worth noting *GROUP* analyses do not predict negative pile head bending moments when the *p*-multiplier is 1.0 and the H-piles are oriented in the strong direction.

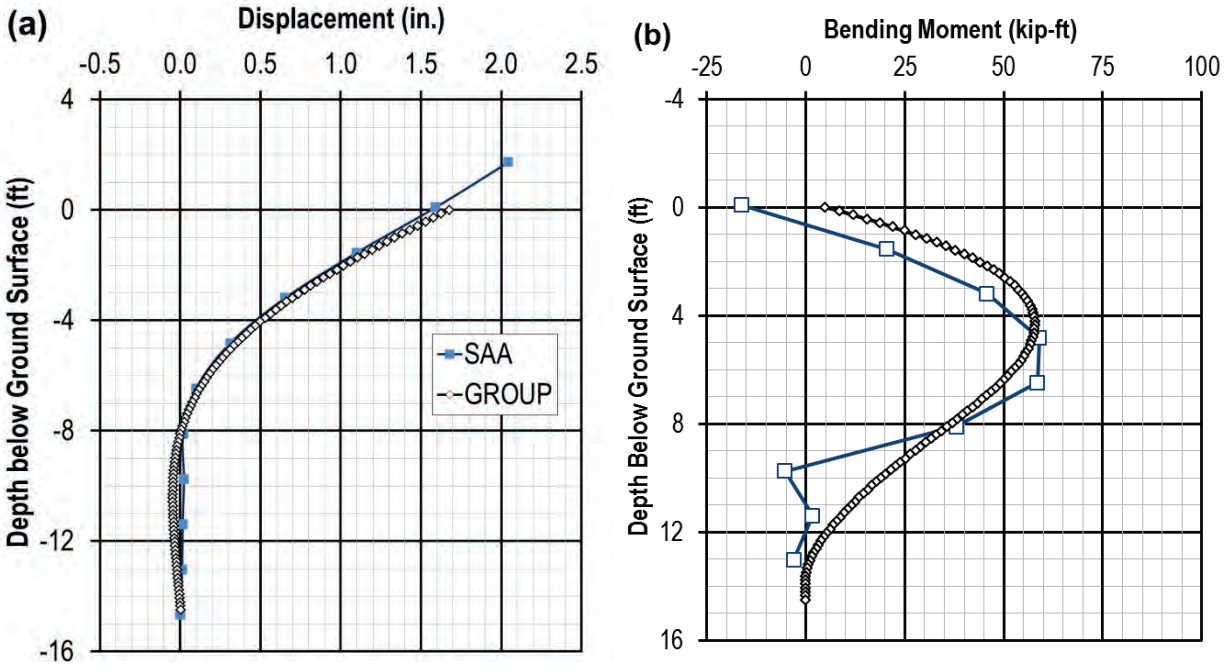

Figure 5.12. Results of axial match calibrated *GROUP* model for H-pile structure at maximum test load (99 kip): (a) displacement profile and (b) bending moment profile.

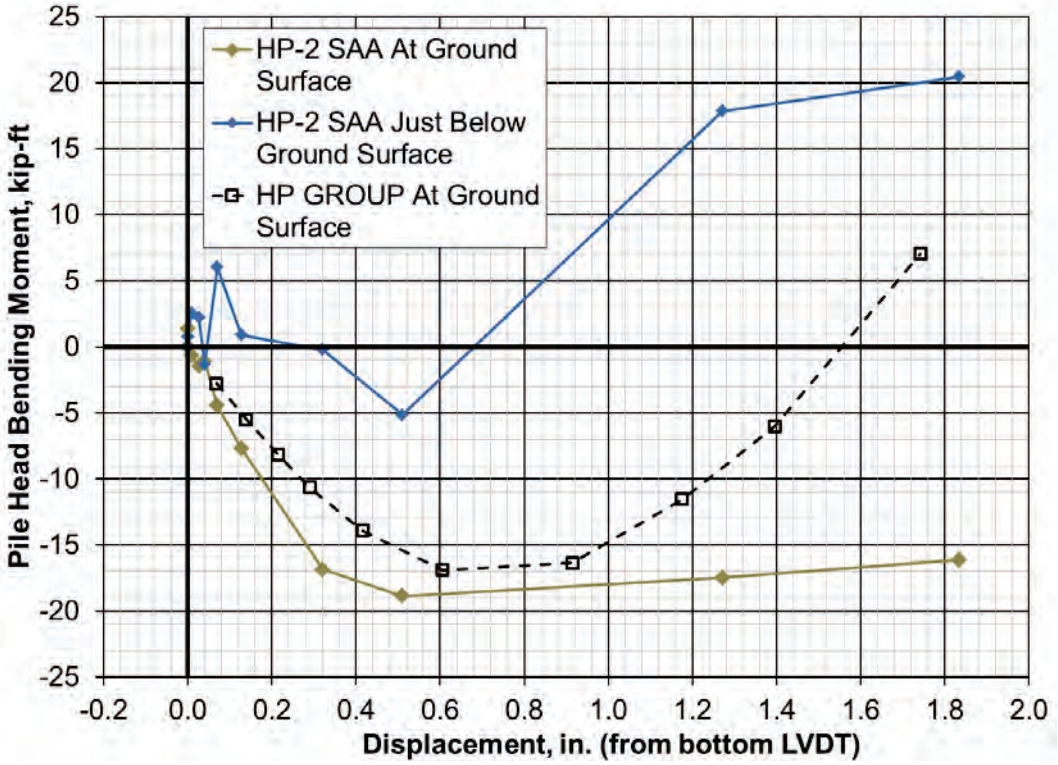

Figure 5.13. H-pile head bending moment-displacement curves, including those predicted by *GROUP*. *GROUP* predicts nearly equal bending moments in all four pile heads.

5.3.3 Predictions at Greater Loads from GROUP *Models*

As described in Section 3.5, both pile structures were deflecting considerably and it was difficult to apply additional load when the load test was terminated. However, darkness was also a consideration in terminating the test, so it is possible the pile structures could have supported additional load had more time been allowed. To investigate this possibility, the calibrated *GROUP* models were used to predict behavior at loads beyond those reached during the load test. The results are shown in Figure 5.14 and Figure 5.15. For the CIP model, the applied load at which *GROUP* predicted failure was 110 kips, just above the actual applied load at failure of 100 kips. However, the *GROUP* model failure was related to moment capacity of the CIP pile, so an additional model was created using a CIP pile with elastic EI similar to that for the nonlinear CIP model. The resulting model reached failure at 240 kips, with pile head bending moments 7 times greater than those observed during the load test resulting in a group capacity nearly 2.5 times the ultimate applied load from the load test. The H-pile *GROUP* model was calibrated with a linear EI. The model predicted failure at 120 kips, beyond which the model would not converge. Predicted pile head moments and overall group overturning capacity for the H pile group were likely limited by the orientation of the piles, which was speculated in Section 5.3.2 as the cause for model calibrations requiring a *p*-multiplier of 0.4.

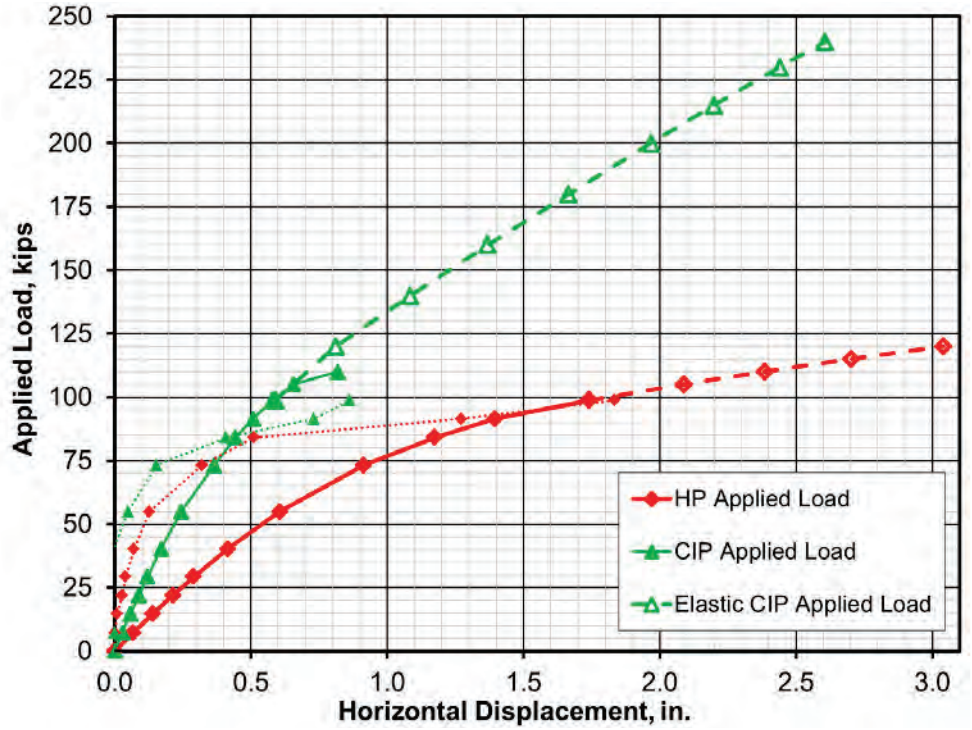

Figure 5.14. Applied load versus horizontal displacement from *GROUP* models. Solid lines and symbols used for *GROUP* results for actual loads from load test. Dashed lines and open symbols used for *GROUP* predictions beyond loads applied during test. Dotted lines and small symbols used for measured data.

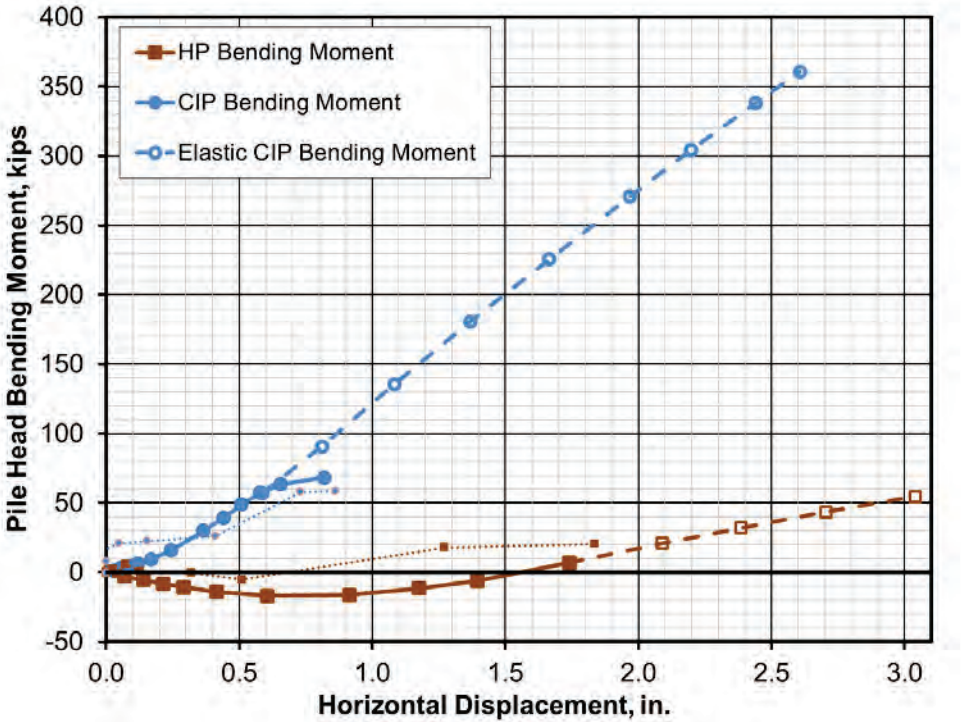

Figure 5.15. Pile head bending moment versus horizontal displacement from *GROUP* models. Solid lines and symbols used for *GROUP* results for actual loads from load test. Dashed lines and open symbols used for *GROUP* predictions beyond loads applied during test. Dotted lines and small symbols used for measured data.

5.3.4 *Summary of Observations from* GROUP *Models*

The *GROUP* models are very useful for expanding upon the findings from the summary plots and static equilibrium analyses presented in Section 5.1. In summary:

- The models were largely successful in predicting performance of the pile groups. Displacements and bending moment magnitudes agreed rather well. The shape of bending moment profiles were generally similar. The overall test performance (i.e. load-displacement curves such as Figure 5.10 and test summary plots such as Figure 5.9 and Figure 5.14) also showed good agreement.
- The quality of the agreement between models and test data is qualified by noting there is likely no unique set of parameters to match the observed performance considering there was only one load test per pile group, the variability of observed responses, and the number of parameters needed to specify an axial load-displacement curve and *p-y* curves, among other model inputs.
- The axial load displacement curves were specified from *t-z* analyses to approximately match the observed responses. The matches were reasonable, but the measured axial loads were rather variable. The results of the *GROUP* models were sensitive to axial load-displacement curves at the pile head. The initial stiffness of the curves seemed to be of particular importance. This is similar to the observations in NCHRP Report 461 (2001), as reported in Chapter 2.
- The *GROUP* model results offer additional evidence that bending moments that develop at the pile heads can offer significant additional resistance to overturning loads, especially once the geotechnical uplift capacity of the tension pile heads has been exceeded. With additional study, this trend could potentially have benefits for design as discussed further in Chapter 6.
- Calibration of lateral response was achieved via *p*-multipliers. The specific values used (2.5 for CIP piles and 0.4 for H-piles) are not recommended for use beyond this project, but the H-pile multiplier being less than 1.0 is an indication some reduction in lateral resistance should be considered when H-piles are loaded along their weak axis.

- The pile head connections were best modeled as fixed, which is consistent with the recommendation from Rollins and Stenlund (2010), as reported in Chapter 2.
- CIP piles appear to have developed bending moments at the pile head that were beneficial to overturning stability throughout the test, whereas bending moments at the head of the H-piles were initially detrimental until greater loads were applied. This could be related to the orientation of the H-piles, which results in lower bending stiffness and the pile flanges "slicing" through the soil. Additional parametric study and load tests would be necessary to quantify this trend and others observed from the test results.

6. Conclusions & Recommendations

The load test was successful, resulting in axial geotechnical failure of the tension piles while maintaining fixity toward the bottom of the piles. The resulting data set is considerable and useful. Displacement data were collected at 11 points on each pile structure. The displacement data offer confirmation of three main observations from the pile load test: the tension piles had reached their uplift capacity when the test was terminated, the H-pile structure experienced more significant displacement and rotation than the CIP pile structure, and both pile caps rotated rigidly. The strain gage and SAA data were useful for characterizing the axial and bending moment behavior of the piles. Driving damage perhaps related to installation issues hampered the usefulness of the strain gage data for H-piles, but the SAA data redundancy was helpful for characterizing lateral response. Pile head connections appeared to be fixed, which is consistent with literature as reported in Chapter 2.

Interpretation of the measured loads and displacements suggests overturning load transfer for the four-pile groups typically employed by WisDOT for sign foundations is reasonably predicted from simple consideration of static equilibrium up to loads where the uplift capacity of the tension piles is approached. Design capacity for overturning of four-pile groups can therefore be calculated using (1) pile loads corresponding to the axial force couple that satisfies moment equilibrium of the rigid sign structures and (2) pile capacities from appropriate design methods for axial and lateral loading of driven piles.

Additional load carrying capacity, beyond that attributed to the axial force couple alone, can potentially be mobilized from pile head bending moments that develop as the force couple approaches the tension pile uplift capacity. The test measurements support the potential for mobilizing this additional resistance, and numerical modeling with Ensoft *GROUP* lends confirmation as well. Contributions from pile bending resistance would be accompanied by significant inelastic displacement. However, some design efficiency could be realized by considering such additional capacity for extreme event loading cases if the structural capacity of the piles is sufficient. Additional load tests are needed to confirm and quantify potential contributions from pile head bending moments.

Results of the load test indicate the strength limit state resistance factors for single piles in uplift discussed in Chapter 2 (ranging from 0.2 to 0.4) are likely to be inappropriately low for pile groups subjected to overturning loads. The observed failure was ductile and the structures likely could have withstood greater loads had the test continued. A more appropriate resistance factor for the four-pile groups could be established based on probabilistic analysis of the groups. Such a study could also consider and quantify the additional resistance offered by pile head moments.

References

AASHTO (2001), *Standard Specifications for Structural Supports for Highway Signs, Luminaires, and Traffic Signals*, American Association of State Highway and Transportation Officials, 4th Edition with 2006 Interim Revisions.

AASHTO (2002), *Standard Specifications for Highway Bridges*, American Association of State Highway and Transportation Officials, 17th Edition.

AASHTO (2014), *AASHTO LRFD Bridge Design Specification: Customary U.S. Units*, American Association of State Highway and Transportation Officials, 7th Edition.

ASTM Standard C39 (2014), "Standard Test Method for Compressive Strength of Cylindrical Concrete Specimens," ASTM International, West Conshohocken, PA, 2012, DOI: 10.1520/C0039_C0039M-14A, www.astm.org.

ASTM Standard C143 (2012), "Standard Test Method for Slump of Hydraulic-Cement Concrete," ASTM International, West Conshohocken, PA, 2012, DOI: 10.1520/C0143_C0143M-12, www.astm.org.

ASTM Standard D3966 (2007), "Standard Test Methods for Deep Foundations Under Lateral Load," ASTM International, West Conshohocken, PA, 2007, DOI: 10.1520/D3966-07, www.astm.org.

Boeckmann, A.Z., S. Myers, M. Uong, and J.E. Loehr (2014a), *Load and Resistance Factor Design of Drilled Shafts in Shale for Lateral Loading*, Report to Missouri Department of Transportation.

Boeckmann, A., S. Myers, M. Uong, and J.E. Loehr (2014b), "Comparison of Drilled Shaft Structural Response from Strain Gage and ShapeAccelArray (SAA) Data," *Proceedings of the 39th Annual Conference on Deep Foundations*, Atlanta, Georgia, October 21-24, 2014, Deep Foundations Institute.

Bridge Diagnostics, Inc., Technical Specification for LVDT Displacement Transducer, accessed online http://bridgetest.com/products/lvdt-displacement-sensor/.

Geokon (2013a), *Model 4000 (and 4050) Series Vibrating Wire Strain Gages Instruction Manual*, Document Rev. X.

Geokon (2013b), *Model 4100/4150 Vibrating Wire Strain Gages Instruction Manual*, Document Rev. U.

Geokon (2013c), *Model LC-2x16 16 Channel Vibrating Wire Datalogger Instruction Manual*, Document Rev. O.

Google Earth (2011a), 38º 56' 08.74" N and -92º 22' 17.03" E. Google Earth. May 3, 2010, August 13, 2011.

Google Earth (2011b), 38º 46' 12.76" N and -93º 42' 48.50" E. Google Earth. June 15, 2009, August 13, 2011.

Lehane, B.M., B. Pedram, J.A. Doherty, and W. Powrie (2014), "Improved Performance of Monopiles When Combined with Footings for Tower Foundations in Sand," *ASCE Journal of Geotechnical and Geoenvironmental Engineering*, Vol. 140, No. 7, 8 pp.

Luna, R. (2014), *Evaluation of Pile Load Tests for Use in Missouri LRFD Guidelines*, Report to Missouri Department of Transportation, Report cmr14-015.

Measurand Inc. (2013), *ShapeAccelArray Manual*, Rev. 0.

NCHRP (2001), *NCHRP Report 461 – Static and Lateral Loading of Pile Groups*, Transportation Research Board, 57 pp.

NCHRP (2014), *NCHRP Report 796 – Development and Calibration of AASHTO LRFD Specifications for Structural Supports for Highway Signs, Luminaires, and Traffic Signals*, Transportation Research Board, 37 pp.

Pierce, M.D., J.E. Loehr, B.L. Rosenblad (2014), *Load and Resistance Factor Design of Drilled Shafts in Shale Using SPT and TCP Measurements*, Report to Missouri Department of Transportation.

Reese, L.C., S-T Wang, J.A. Arrellaga, J. Hendrix, and L. Vasquez (2010), *Computer Program GROUP Version 8.0: Program for the Analysis of a Group of Piles Subjected to Vertical and Lateral Loading (User's Manual)*, for Ensoft Inc. GROUP 8.0.2.

Reese, L.C., S-T Wang, and L. Vasquez (2014), *Computer Program GROUP Version 2014: A Program for the Analysis of a Group of Piles Subjected to Vertical and Lateral Loading (Technical Manual)*, for Ensoft Inc.

Rollins, K., R. Olsen, J. Egbert, K. Olsen, D. Jensen, and B. Garrett (2003), *Response, Analysis, and Design Of Pile Groups Subjected to Static and Dynamic Lateral Loads*, Report to Utah Department of Transportation UT-03.03.

Rollins, K.M. and T.E. Stenlund (2010), *Laterally Loaded Pile Cap Connections*, Report to Utah Department of Transportation UT-10.16.

Vu, T. (2013), *Load and Resistance Factor Design for Drilled Shafts at Service Limit State*, Dissertation Presented to the Faculty of the Graduate School of the University of Missouri.

Wisconsin Department of Transportation (2009), *Bridge Manual*, Chapter 39: Sign Structures, Rev. July 2009, 12 pp.

Wisconsin Department of Transportation (2012), *Bridge Manual*, Chapter 11: Foundation Support, Rev. July 2012, 60 pp.

Wisconsin Department of Transportation (2014), *Facilities Development Manual*, Sec. 11-55-20: Overhead Sign Supports, Rev. Sept. 19, 2014.

Appendix A – Plans and Calculations from WisDOT Sign Structure S-05-168

STATE PROJECT NUMBER

1133-09-71

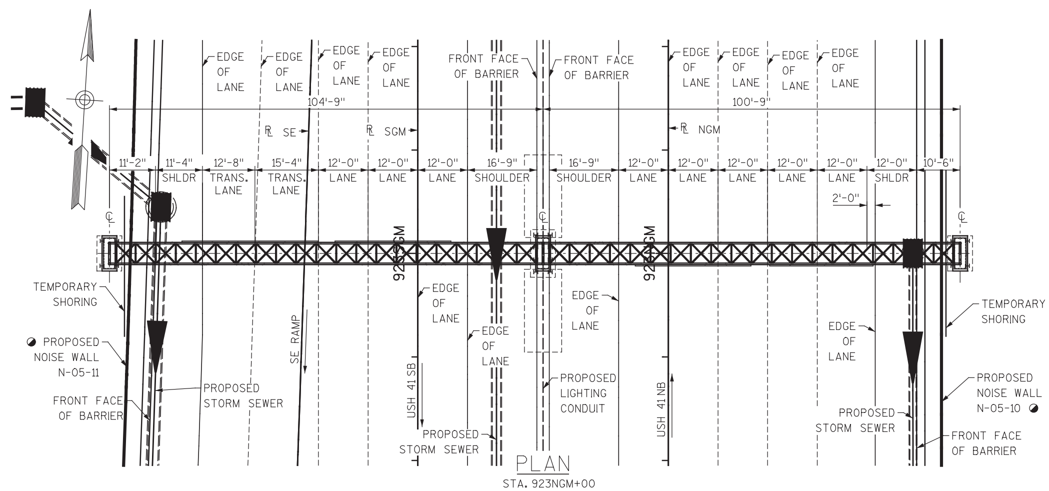

PLAN

STA. 923NGM+00

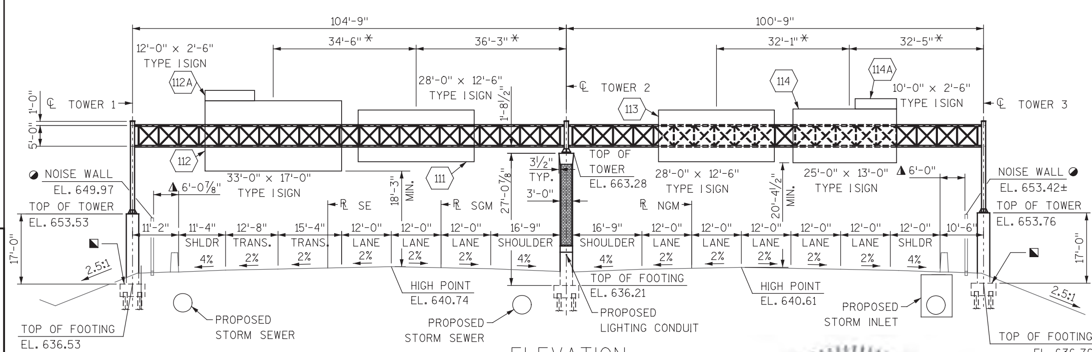

ELEVATION

(LOOKING NORTH AT FRONT FACE OF SIGN)

▲ MINIMUM LATERAL CLEARANCE

◪ CONTRACTOR TO VERIFY IF TEMPORARY SHORING IS NEEDED BEFORE FOOTING IS CONSTRUCTED.

WISCONSIN STEVEN J. MILLER 36937 MILWAUKEE, WI PROFESSIONAL ENGINEER

Steven J. Miller 2/15/2013

LIST OF DRAWINGS

1. PLAN & ELEVATION
2. CONCRETE TOWER 1 & 3 DETAIILS
3. CONCRETE TOWER 2 FOUNDATION DETAILS
4. CONCRETE TOWER 2 DETAILS
5. GALVANIZED STEEL SIGN BRIDGE
6. SIGN BRIDGE DETAILS
7. CONCRETE TOWER 1 & 3 AESTHETIC DETAILS
8. CONCRETE TOWER 2 AESTHETIC DETAILS
9. SUBSURFACE EXPLORATION

ULTIMATE DESIGN STRESSES:

TOWER

CONCRETE: ....f'c = 3,500 psi
HIGH STRENGTH BAR
STEEL REINFORCEMENT: ....fy = 60,000 psi

SIGN BRIDGE

STEEL COLUMN PIPE: ....fy = 42,000 psi
A.P.I. SPEC 5L GRADE X42
STEEL PIPE MEMBERS OF TRUSS: ....fy = 42,000 psi
A.P.I. SPEC 5L GRADE X42
PLATES, BARS, STRUCTURAL ANGLES: ....fy = 36,000 psi
A.S.T.M. A709 GRADE 36
STEEL ANCHOR BOLTS: ....fy = 55,000 psi
A.A.S.H.T.O. M314-90 GRADE 55
ALL BOLTED CONNECTIONS: ¾" ϕ A325 BOLTS, GALVANIZED A.S.T.M. A153, CLASS C

DESIGN DATA

DEAD LOAD - WT. OF SIGN AND SUPPORTING STRUCTURE. NO PROVISIONS HAVE BEEN INCLUDED FOR A CATWALK OR LIGHTING.
LIVE LOAD - NONE.
ICE LOAD - 3 P.S.F. TO 1 FACE OF SIGN & AROUND SURFACE OF MEMBERS.
WIND PRESSURE - 90 M.P.H. (3-SECOND GUST SPEED) TO SIGN AREA & EXPOSED MEMBERS.

WIND COMPONENTS	NORMAL	TRANSVERSE
COMBINATION 1	1.0	0.2
COMBINATION 2	0.6	0.3

GROUP LOADS	% OF ALLOWABLE STRESS
1. DEAD	100
2. DEAD + WIND	133
3. DEAD + ICE + ½ (WIND‡)	133

‡ MIN. VALUE OF 25 PSF FOR GR. 3

TYPE I SIGN DESIGN DATA

MAX DESIGN SIGN AREA (SQ. FT.)	MAX. TYPE I SIGN DEPTH	SPAN
978	17'-0"	SOUTHBOUND
1152	16'-0"	NORTHBOUND

GENERAL NOTES

DRAWINGS SHALL NOT BE SCALED.

ELEVATIONS ARE IN FEET UNLESS OTHERWISE SHOWN OR NOTED.

ALL STRUCTURAL STEEL MEMBERS SHALL BE GALVANIZED.

CENTER SIGNS VERTICALLY ON CHORD/TRUSS.

CONTRACTOR SHALL VERIFY DIMENSIONS PRIOR TO FABRICATION OF CONCRETE TOWERS AND SIGN BRIDGE.

EXCAVATION REQUIRED TO CONSTRUCT THE CONCRETE TOWER FOUNDATION ON THE PILES SHALL BE CONSIDERED INCIDENTAL TO THE BID ITEM "SIGN SUPPORTS CONCRETE MASONRY".

THE LOCATION OF EXISTING OR PROPOSED UTILITIES AS NOTED ON THE PLANS ARE APPROXIMATE. THERE MAY BE OTHER UTILITY INSTALLATIONS WITHIN THE PROJECT AREA THAT ARE NOT SHOWN. UTILITY SERVICES ARE NOT SHOWN.

PROVIDE AN IDENTIFICATION PLAQUE FOR THE SIGN BRIDGE IN ACCORDANCE WITH SDD STRUCTURE IDENTIFICATION PLAQUES, SIGN BRIDGES AND OVERHEAD SIGN SUPPORT. FASTEN THE IDENTIFICATION PLAQUE TO THE TOWER USING 3 - ¼" DIAMETER BY 1¾" LONG STAINLESS STEEL CONCRETE SCREWS. THIS WORK SHALL BE CONSIDERED INCIDENTAL TO THE BID ITEM "SIGN BRIDGE S-05-168 " "

SIGNS OR BLANKS SHALL BE INSTALLED ON THE TRUSS AT THE TIME OF ERECTION. BLANKS SHALL BE ¼ THE LENGTH OF THE BRIDGE, 2'-0" DEEPER THAN CENTER TO CENTER OF CHORDS & SHALL BE CENTERED ON THE BRIDGE. SIGNS SHALL BE AS DESIGNATED IN PLANS. SIGN BLANKS AND MOUNTING HARDWARE SHALL BE INCIDENTAL TO "SIGN BRIDGE S-05-168" "

THE UPPER 12" OF ANCHOR BOLTS, NUTS AND WASHERS SHALL BE GALVANIZED IN ACCORDANCE WITH THE A.A.S.H.T.O. SPECIFICATION AS STATED IN SECTION 641. OF THE WISDOT STANDARD SPECIFICATIONS. WELD TEST AS PER AWS D1.1.

WELDED CONNECTIONS CAN BE USED IN LIEU OF BOLTED CONNECTIONS, IF UNIT CAN BE GALVANIZED IN ONE PIECE.

THE SIGN SUPPORTS CONCRETE MASONRY QUANTITY IS BASED ON THE OUT-TO-OUT CONCRETE DIMENSIONS. NO DEDUCTIONS IN QUANTITY FOR THE ARCHITECTURAL SURFACE TREATMENT RELIEF HAVE BEEN MADE.

PROVIDE A ¾" CHAMFER OR 1" RADIUS ON ALL EXPOSED CONCRETE EDGES.

(##) - REPRESENTS THE SIGN NO. REFER TO THE PERMANENT SIGNING SHEETS.

* SIGN PANEL DIMENSIONS ARE TO THE CENTER OF THE SIGN PANEL. CONTRACTOR TO FIELD VERIFY SIGN PANEL DISPLAYS CORRELATE WITH ROADWAY LANE LAYOUT.

◕ REFER TO NOISE WALL PLANS FOR LATERAL CLEARANCE.

CONTACTS

BUREAU OF STRUCTURES CONTACT
BILL DREHER: (608) 266-8489

CONSULTANT CONTACT, COLLINS ENGINEERS, INC.
STEVE J. MILLER: (414) 282-6905

ESTIMATE OF QUANTITIES

ITEM NO.	ITEM DESCRIPTION	UNIT	TOTAL
206.6000.S	TEMPORARY SHORING	SF	640
550.1120	PILING STEEL HP 12-INCH X 53 LB	LF	1360
636.0100	SIGN SUPPORTS CONCRETE MASONRY	CY	70
636.1000	SIGN SUPPORTS STEEL REINFORCEMENT HS	LB	1610
636.1500	SIGN SUPPORTS STEEL COATED REINFORCEMENT HS	LB	7840
641.6600.959	SIGN BRIDGE S-05-168	LS	1
652.1350	CONDUIT RIGID METALLIC 3-INCH	LF	8
SPV.0165.500	ARCHITECTURAL SURFACE TREATMENT	SF	230
SPV.0165.501	STAINING CONCRETE	SF	1140
SPV.0165.502	STAINING CONCRETE BRICK	SF	230

NO.	DATE	REVISION	BY

COLLINS ENGINEERS INC.

STATE OF WISCONSIN
DEPARTMENT OF TRANSPORTATION

ACCEPTED William C. Dreher KAR 04/08/13
CHIEF STRUCTURES DESIGN ENGINEER — DATE

STRUCTURE S-05-168

DE PERE - SUAMICO

COUNTY BROWN — TOWN/CITY/VILLAGE ASHWAUBENON

DESIGN SPEC. AASHTO STANDARD SPECIFICATIONS

DESIGNED BY CES — DESIGN CK'D. SJM — DRAWN BY MJH — PLANS CK'D. CES

SHEET 1 OF 9

PLAN & ELEVATION

8

FILE NAME 15-05-168.dgn
PLOT DATE 12/15/2013 8:22:41 AM PLOT BY : Veronica Chovezvll DRV :Pdf_bw_HS.by level.plt PEN :CEL.TextSub_ScreenControlByLevel.tbl

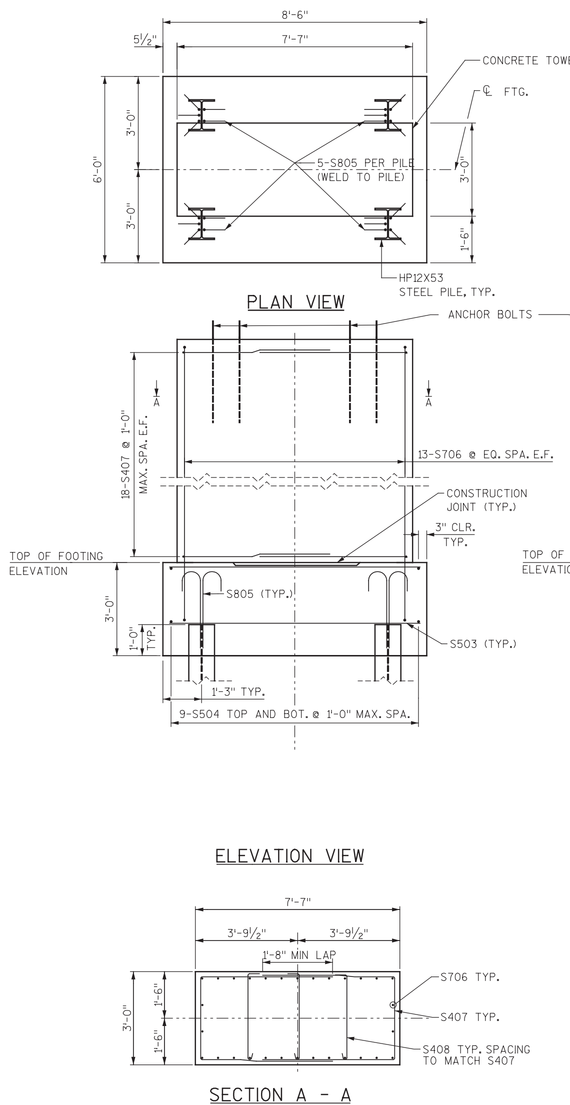

PLAN VIEW

ELEVATION VIEW

SECTION A - A

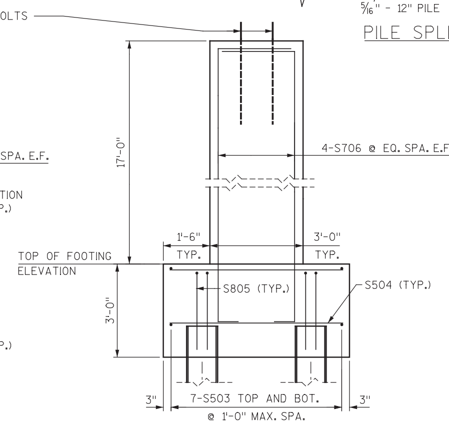

END VIEW

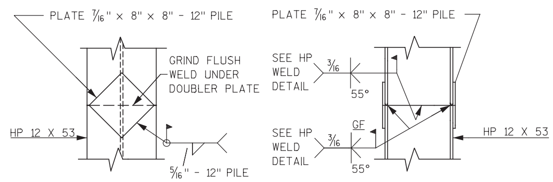

PILE SPLICE DETAIL

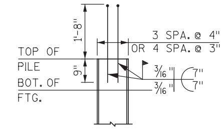

PILE HEAD DETAIL

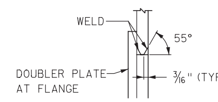

HP WELD DETAIL

FLANGE SHOWN, WEB SIMILAR

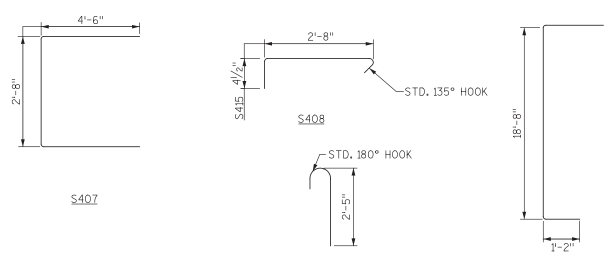

BILL OF BARS

NOTE: THE FIRST OR FIRST TWO DIGITS OF THE BAR MARK SIGNIFIES THE BAR SIZE.

BAR MARK	COAT	NO. REQ'D	LENGTH	BENT	BAR SERIES	LOCATION
S503		28	8'-0"			CAP LONGITUDINAL
S504		36	5'-6"			CAP TRANSVERSE
S805		40	3'-4"	▲		WELDED TO PILES
S706	X	60	22'-2"	▲		CAP BEAM VERTICAL
S407	X	72	11'-6"	▲		HORZ. STIRRUP, BOTTOM OF TOWER
S408	X	108	3'-4"	▲		HORZ. CROSSTIE, BOTTOM OF TOWER

TOWER NOTES

DRAWING SHALL NOT BE SCALED.

"E.F." SIGNIFIES EACH FACE.

BAR STEEL REINFORCEMENT SHALL BE EMBEDDED 2" CLEAR FROM THE FACE OF THE SMOOTH CONCRETE AND 2½" FROM THE FACE OF THE ARCHITECTURAL SURFACE TREATMENT, UNLESS OTHERWISE NOTED.

REFER TO THE RESPECTIVE PLAN AND ELEVATION SHEET FOR TOP OF TOWER ELEVATION.

ALL CONSTRUCTION JOINTS SHALL BE FORMED BY A 2" × 6" × 1'-6" LONG BEVELED KEYWAY.

FOUNDATION NOTES

DRAWING SHALL NOT BE SCALED.

"E.F." SIGNIFIES EACH FACE.

BAR STEEL REINFORCEMENT SHALL BE EMBEDDED 3" CLEAR, UNLESS OTHERWISE NOTED.

REFER TO THE RESPECTIVE PLAN AND ELEVATION SHEET FOR TOP OF FOOTING ELEVATIONS.

ALL CONSTRUCTION JOINTS SHALL BE FORMED BY A 2" × 6" × 1'-6" LONG BEVELED KEYWAY.

FOUNDATION DATA

SIGN BRIDGE TOWERS 1 AND 3 TO BE SUPPORTED ON HP12X53 STEEL PILING DRIVEN TO A REQUIRED DRIVING RESISTANCE OF 220 TONS** PER PILE AS DETERMINED BY THE MODIFIED GATES DYNAMIC FORMULA. BEDROCK IS EXPECTED TO BE ENCOUNTERED AT EL. 549.53 FOR TOWER 1 AND EL. 549.76 FOR TOWER 3. ESTIMATED LENGTH 85 FEET LONG FOR BOTH TOWERS.

**THE FACTORED AXIAL RESISTANCE OF PILES IN COMPRESSION USED FOR DESIGN IS THE REQUIRED DRIVING RESISTANCE MULTIPLIED BY A RESISTANCE FACTOR OF 0.5 USING THE MODIFIED GATES FORMULA TO DETERMINE DRIVEN PILE CAPACITY.

IF THE PILE OBTAINS A CAPACITY AT A LENGTH THAT IS MORE THAN 10 FEET SHORTER THAN THE ESTIMATED LENGTH, THE CONTRACTOR MUST NOTIFY THE ENGINEER FOR APPROVAL.

STEEL HP PILE MATERIAL SHALL BE A.S.T.M. A572, Fy=50,000 psi. PILE SPLICES (IF REQUIRED) SHALL BE MADE BY A CERTIFIED WELDER USING LOW HYDROGEN ELECTRODES.

WELDING OF THE REINFORCEMENT BARS TO THE PILES SHALL BE MADE BY A CERTIFIED WELDER USING LOW HYDROGEN ELECTRODES. THIS WORK SHALL BE CONSIDERED INCIDENTAL TO THE BID ITEM "PILING STEEL HP 12-INCH X 53 LB".

NO.	DATE	REVISION	BY

STATE OF WISCONSIN
DEPARTMENT OF TRANSPORTATION
STRUCTURES DESIGN SECTION

STRUCTURE S-05-168

DRAWN BY VC | PLANS CK'D. CES

CONCRETE TOWER 1 & 3 DETAILS

SHEET 2 OF 9

FILE NAME : S-05-168.dgn
PLOT DATE : 12/15/2013 8:22:43 AM PLOT BY : Veronica Chavez-Vill DRV : Pdf_bw_HS_by_level.plt PEN : CEI_TextSub_ScreenControlByLevel.tbl

STATE PROJECT NUMBER

1133-09-71

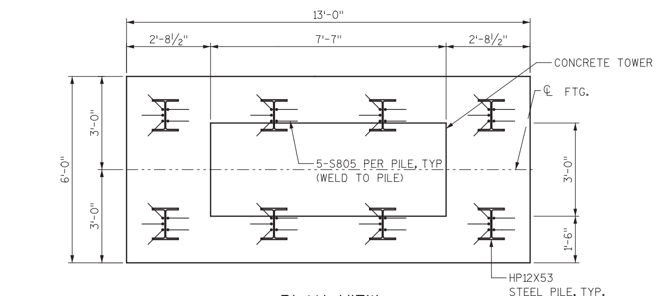

PLAN VIEW

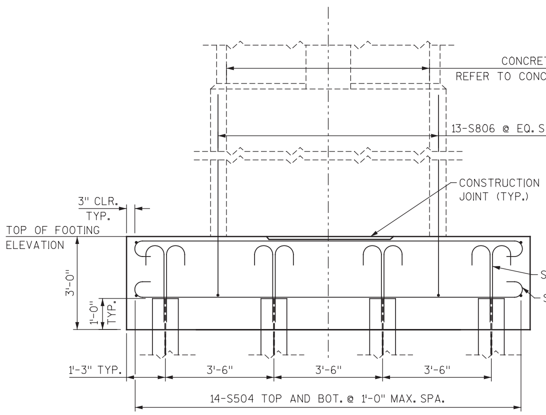

ELEVATION VIEW

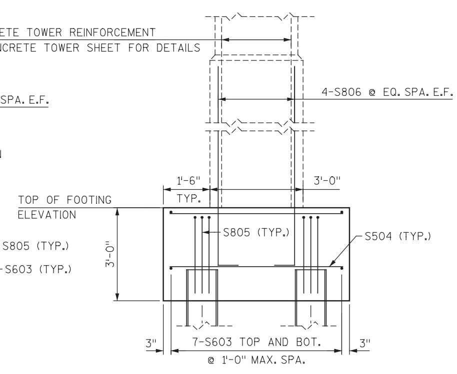

END VIEW

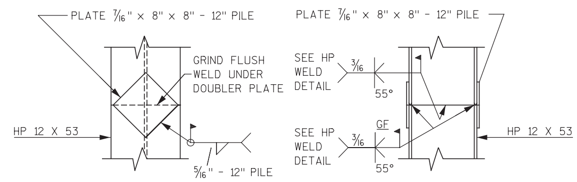

PILE SPLICE DETAIL

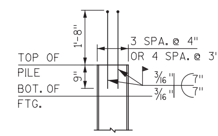

PILE HEAD DETAIL

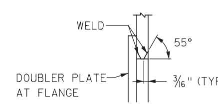

HP WELD DETAIL

FLANGE SHOWN, WEB SIMILAR

BAR SERIES TABLE

MARK	NO. REQ'D	LENGTH
S412	2 SERIES OF 4	12'-3" TO 12'-10"
S417	2 SERIES OF 4	3'-4" TO 3'-10"

BUNDLE AND TAG EACH SERIES SEPARATELY

BILL OF BARS

NOTE: THE FIRST OR FIRST TWO DIGITS OF THE BAR MARK SIGNIFIES THE BAR SIZE.

BAR MARK	COAT	NO. REQ'D	LENGTH	BENT	BAR SERIES	LOCATION
S603		14	13'-10"	▲		CAP LONGITUDINAL
S504		28	5'-6"			CAP TRANSVERSE
S805		40	3'-4"	▲		WELDED TO PILES
S806	X	30	12'-2"	▲		CAP BEAM VERTICAL
S507	X	20	12'-5"	▲		HORZ. STIRRUP, BOTTOM OF TOWER
S808	X	30	26'-10"			VERT. REINF., MIDDLE OF TOWER
S409	X	4	14'-10"			VERT. REINF., MIDDLE OF TOWER
S510	X	40	11'-6"	▲		HORZ. STIRRUP, MIDDLE OF TOWER
S411	X	32	5'-1"	▲		HORZ. STIRRUP, MIDDLE OF TOWER
S412	X	8	12'-7"	▲	△	HORZ. STIRRUP, TOP OF TOWER
S413	X	4	5'-0"	▲		VERT. REINF., TOP OF TOWER
S414	X	20	2'-4"			VERT. REINF., TOP OF TOWER
S415	X	30	3'-4"	▲		HORZ. CROSSTIE, BOTTOM OF TOWER
S416	X	60	2'-11"	▲		HORZ. CROSSTIE, MIDDLE OF TOWER
S417	X	8	3'-7"	▲	△	HORZ. CROSSTIE, TOP OF TOWER

FOUNDATION NOTES

DRAWING SHALL NOT BE SCALED.

"E.F." SIGNIFIES EACH FACE.

BAR STEEL REINFORCEMENT SHALL BE EMBEDDED 3" CLEAR, UNLESS OTHERWISE NOTED.

REFER TO THE RESPECTIVE PLAN AND ELEVATION SHEET FOR TOP OF FOOTING ELEVATIONS.

ALL CONSTRUCTION JOINTS SHALL BE FORMED BY A 2" × 6" × 1'-6" LONG BEVELED KEYWAY.

FOUNDATION DATA

SIGN BRIDGE TO BE SUPPORTED ON HP12X53 STEEL PILING DRIVEN TO A REQUIRED DRIVING RESISTANCE OF 220 TONS** PER PILE AS DETERMINED BY THE MODIFIED GATES DYNAMIC FORMULA. BEDROCK IS EXPECTED TO BE ENCOUNTERED AT EL. 550.21. ESTIMATED LENGTH 84 FEET LONG.

**THE FACTORED AXIAL RESISTANCE OF PILES IN COMPRESSION USED FOR DESIGN IS THE REQUIRED DRIVING RESISTANCE MULTIPLIED BY A RESISTANCE FACTOR OF 0.5 USING THE MODIFIED GATES FORMULA TO DETERMINE DRIVEN PILE CAPACITY.

IF THE PILE OBTAINS A CAPACITY AT A LENGTH THAT IS MORE THAN 10 FEET SHORTER THAN THE ESTIMATED LENGTH, THE CONTRACTOR MUST NOTIFY THE ENGINEER FOR APPROVAL.

STEEL HP PILE MATERIAL SHALL BE A.S.T.M. A572, Fy=50,000 psi. PILE SPLICES (IF REQUIRED) SHALL BE MADE BY A CERTIFIED WELDER USING LOW HYDROGEN ELECTRODES.

WELDING OF THE REINFORCEMENT BARS TO THE PILES SHALL BE MADE BY A CERTIFIED WELDER USING LOW HYDROGEN ELECTRODES. THIS WORK SHALL BE CONSIDERED INCIDENTAL TO THE BID ITEM "PILING STEEL HP 12-INCH X 53 LB".

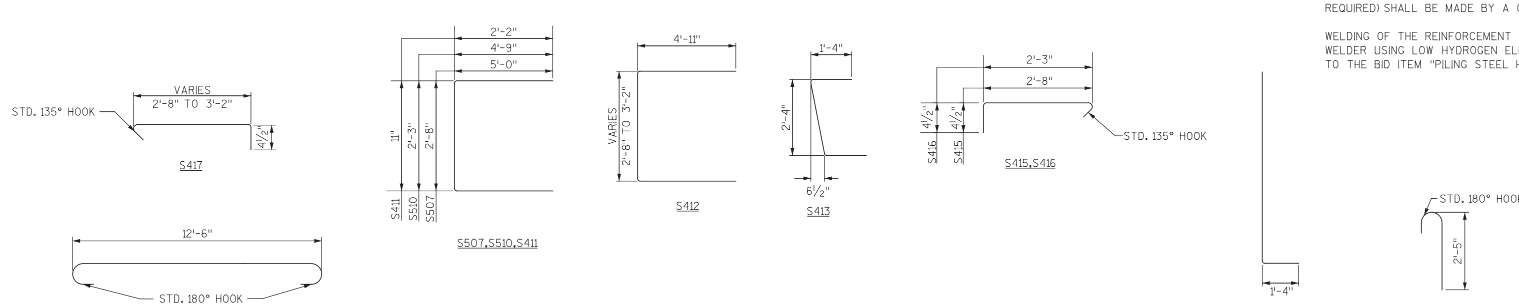

NO.	DATE	REVISION	BY

STATE OF WISCONSIN
DEPARTMENT OF TRANSPORTATION
STRUCTURES DESIGN SECTION

STRUCTURE S-05-168

DRAWN BY VC | PLANS CK'D. CES

CONCRETE TOWER 2
FOUNDATION
DETAILS

SHEET 3 OF 9

8

8

FILE NAME : S-05-168.dgn
PLOT DATE : 12/15/2013 8:22:45 AM PLOT BY : Veronica Chavezvill DRV :Pdf_bw_HS_by_level.plt PEN :CEL.TextSub_ScreenControlByLevel.tbl

STATE PROJECT NUMBER

1133-09-71

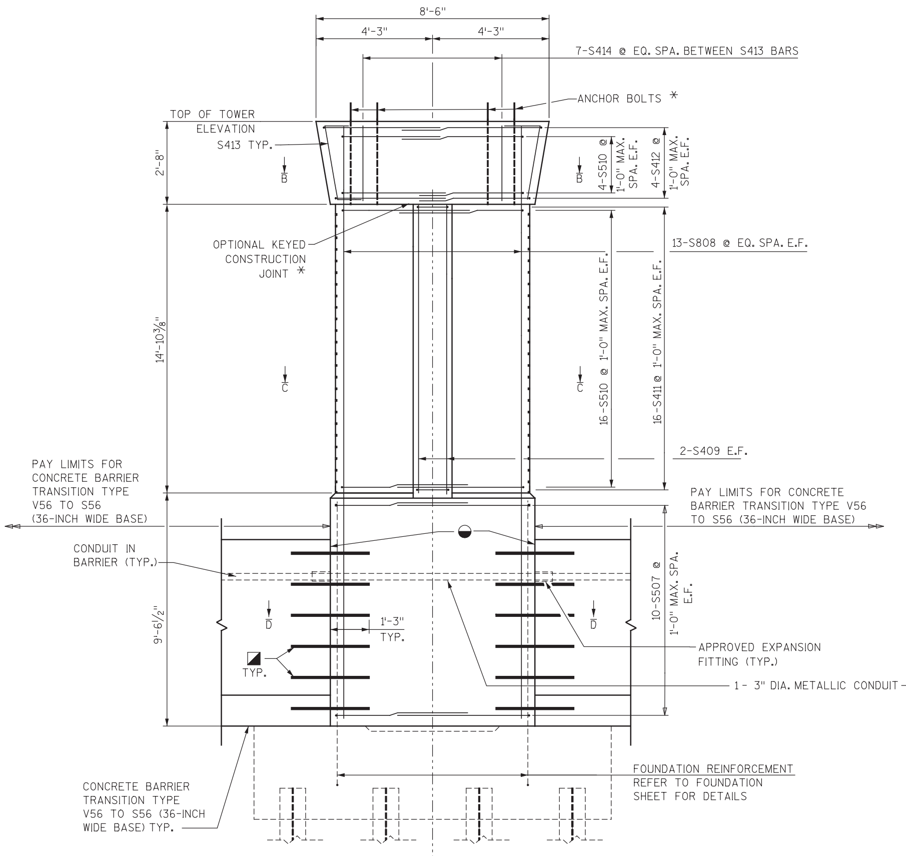

ELEVATION VIEW

S411, S415, S416, AND S417 NOT SHOWN FOR CLARITY. REFER TO SECTIONS

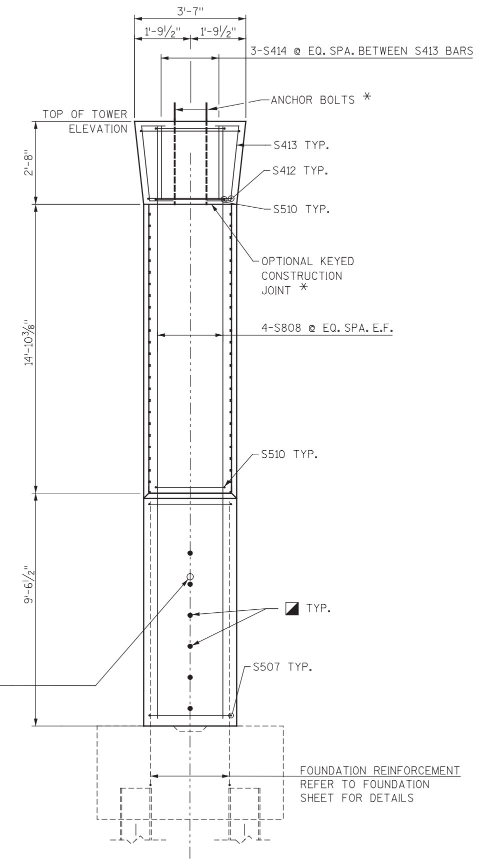

END VIEW

S411, S415, S416, AND S417 NOT SHOWN FOR CLARITY. REFER TO SECTIONS

TOWER NOTES

DRAWING SHALL NOT BE SCALED.

"E.F." SIGNIFIES EACH FACE.

BAR STEEL REINFORCEMENT SHALL BE EMBEDDED 2" CLEAR FROM THE FACE OF THE SMOOTH CONCRETE AND 2½" FROM THE FACE OF THE ARCHITECTURAL SURFACE TREATMENT, UNLESS OTHERWISE NOTED.

REFER TO THE RESPECTIVE PLAN AND ELEVATION SHEET FOR TOP OF TOWER ELEVATION.

ALL CONSTRUCTION JOINTS SHALL BE FORMED BY A 2" × 6" × 1'-6" LONG BEVELED KEYWAY.

APPROVED EXPANSION FITTING SHALL BE CAST INTO THE BARRIER OR TOWER CONCRETE, WHICH EVER ELEMENT IS CAST FIRST.

COORDINATE THE LOCATION OF THE ELECTRICAL CONDUIT IN THE TOWER TO MATCH THE LOCATION OF THE CONDUIT IN THE CONCRETE BARRIER.

SPACE S507 BARS TO MISS CONDUIT.

* PLACE ANCHOR BOLTS PRIOR TO POURING MIDDLE SECTION OF CONCRETE TOWER. OPTIONAL KEYED CONSTRUCTION JOINT MAY BE LOCATED AT A GROUT LINE BELOW THE ANCHOR ASSEMBLIES. THE FORMLINER PATTERN SHALL BE CONTINUOUS ACROSS THE CONSTRUCTION JOINT. OMIT JOINT BEVELED EDGES.

◪ PLACE 1" ϕ PLAIN (SMOOTH) ROUND DOWEL BARS, 2'-6" LONG BETWEEN BARRIER AND CONCRETE TOWER. USE DEBONDER ON EXTENSION INTO BARRIER. ASTM A36 MATERIAL MAY BE SUBSTITUTED FOR AASHTO M31. SPACE DOWELS AT 1'-0". COST OF ITEMS ARE TO BE INCLUDED IN THE BID ITEM "SIGN SUPPORTS CONCRETE MASONRY".

◒ PLACE 1/2" EXPANSION JOINT FILLLER BETWEEN TOWER AND BARRIER WALL, TYP. THE JOINT FILLER SHALL BE CONSIDERED INCIDENTAL TO THE BID ITEM "SIGN SUPPORTS CONCRETE MASONRY".

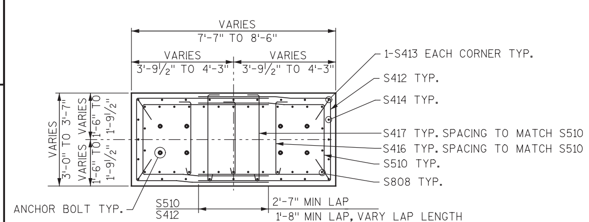

SECTION B - B

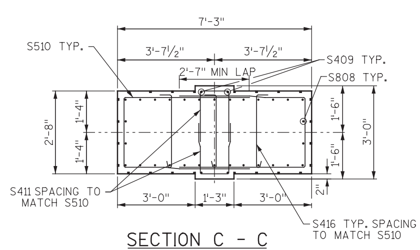

SECTION C - C

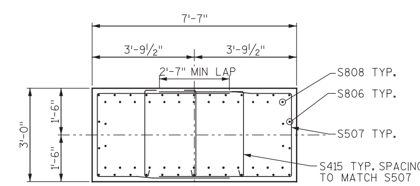

SECTION D - D

(DOWEL BARS OMITTED FOR CLARITY)

NO.	DATE	REVISION	BY

STATE OF WISCONSIN
DEPARTMENT OF TRANSPORTATION
STRUCTURES DESIGN SECTION

STRUCTURE S-05-168

DRAWN BY VC | PLANS CK'D. CES

CONCRETE TOWER 2 DETAILS

SHEET 4 OF 9

8

FILE NAME : S-05-168.dgn PLOT DATE : 12/16/2013 8:22:45 AM PLOT BY : Veronica Chavez/ll DRV :Pdf_bw_HS_by level.plt PEN :CEL.TextSub_ScreenControlByLevel.tbl

STATE PROJECT NUMBER

1133-09-71

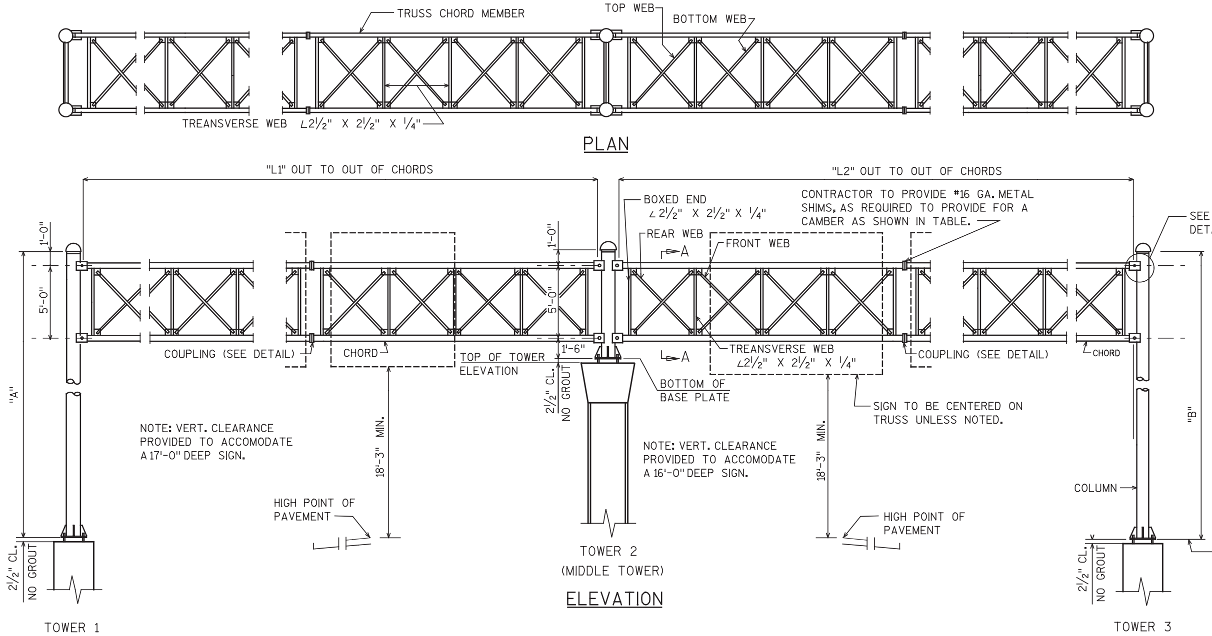

PLAN

ELEVATION

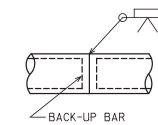

OPTIONAL COLUMN OR CHORD SPLICE DETAIL

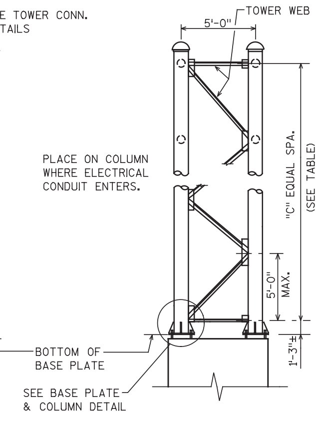

TOWER 3 END VIEW
(TOWER 1 OPPOSITE HAND)

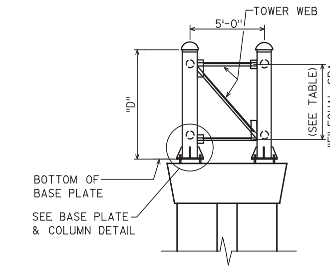

MIDDLE TOWER END VIEW
TOWER 2

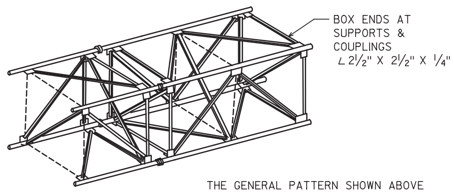

THE GENERAL PATTERN SHOWN ABOVE IS TO BE MAINTAINED WHEN ASSEMBLING TRUSSES. NOTE DIRECTION OF DIAGONALS AT JOINTS.

TYPICAL TRUSS SECTION

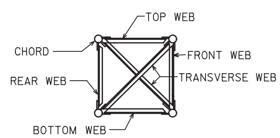

SECTION A

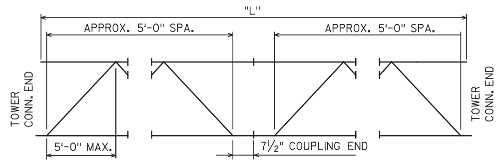

TRUSS ARRANGEMENT

FABRICATOR MAY MAKE TRUSSES ANY LENGTH KEEPING A SECTION A MINIMUM OF 20'-0" & A MULTPLE OF 5'-0". CHORD FIELD SPLICES SHALL BE MADE WITH COUPLINGS. CHORD SHOP SPLICE SHALL BE THE WELDED SPLICE SHOWN ABOVE.

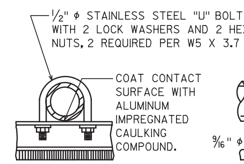

SECTION B

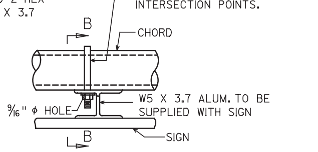

TYPICAL SIGN CONNECTION

NOTE: FOR 17' SIGN DEPTH, W5 X 3.7 ALUM. BEAMS TO BE SPACED NO MORE THAN 5 FEET APART WITH A MAXIMUM END OVERHANG OF 2.5 FEET.

GENERAL NOTES

DRAWING SHALL NOT BE SCALED.

REFER TO THE RESPECTIVE PLAN AND ELEVATION SHEET FOR TOP OF TOWER ELEVATION.

STRUCTURE MEMBER TABLE

A	B	C	D	E	CHORDS O.D. X THK.	TOP & BOTTOM WEB	FRONT & REAR WEB	COUPLING PLATE D1 & "T"	BOLT CIRCLE DIA. "D2"	NO. OF BOLTS IN COUPLING	CAMBER	COLUMN O.D. X THK.	TOWER WEBS	"L1"	"L2"
17'-3"	17'-0¼"	3	7'-6"	1	4.5" X 0.337"	3"X3"X5/16"	3"X3"X5/16"	10.5" × 1.375"	7.5"	6	2 ⅛"	12.75"×0.406"	3"x3"x5/16"	103'-5¼"	99'-5¼"

NO.	DATE	REVISION	BY

STATE OF WISCONSIN
DEPARTMENT OF TRANSPORTATION
STRUCTURES DESIGN SECTION

STRUCTURE S-05-168

DRAWN BY VC | PLANS CK'D. CES

GALVANIZED STEEL SIGN BRIDGE

SHEET 5 OF 9

8

FILE NAME : S-05-168.dgn
PLOT DATE : 12/15/2013 8:22:46 AM PLOT BY : Veronica Chavezvill DRV : Pdf_bw_HS_by_level.plt PEN : CEI_TextSub_ScreenControlByLevel.tbl

STATE PROJECT NUMBER
1133-09-71

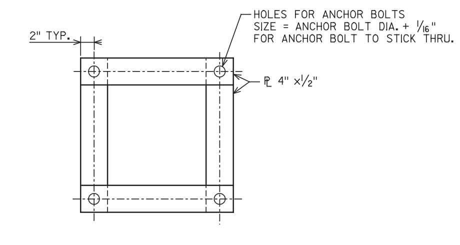

ANCHOR PLATE/TEMPLATE PLAN

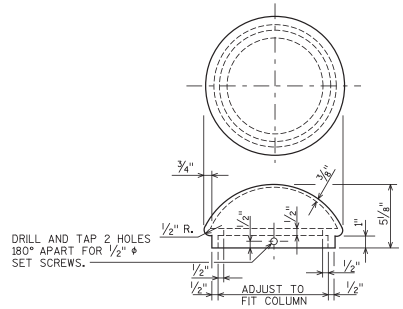

TOWER CAP DETAIL

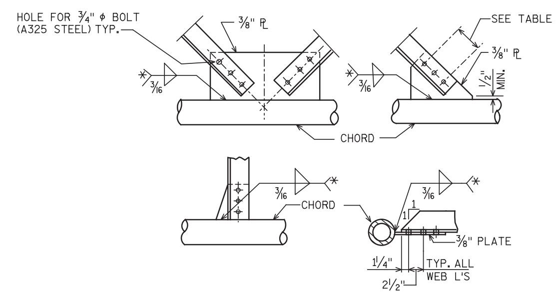

TYPICAL TRUSS CONNECTION DETAILS

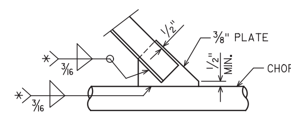

TYPICAL WELDED ALTERNATE

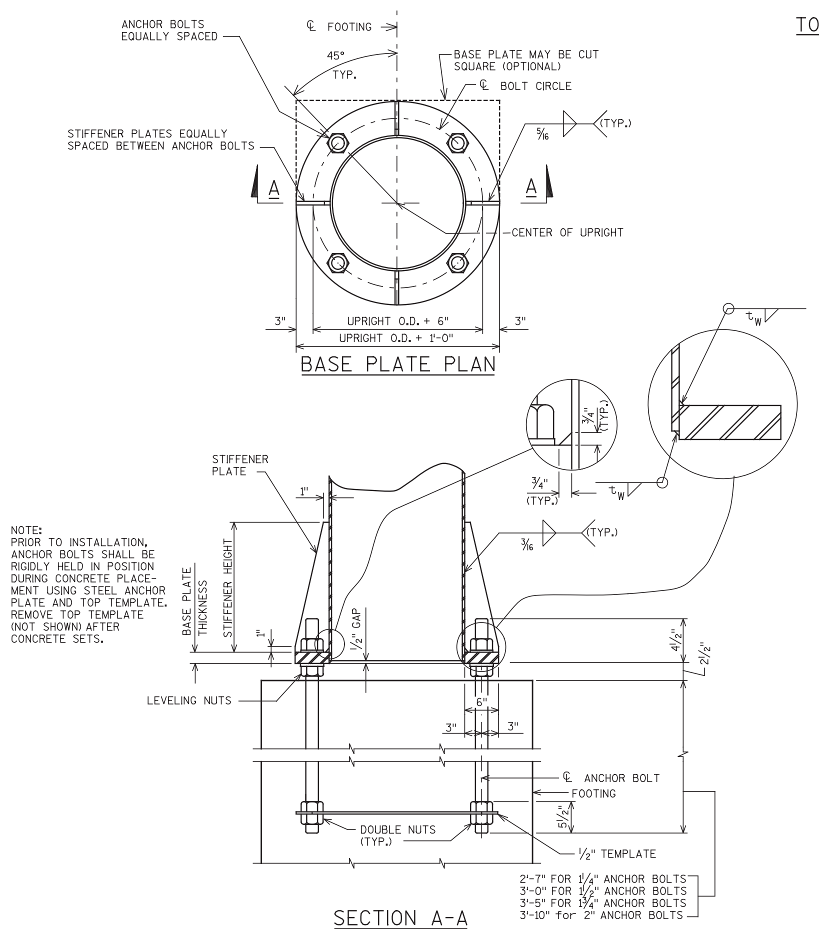

NOTE:
PRIOR TO INSTALLATION, ANCHOR BOLTS SHALL BE RIGIDLY HELD IN POSITION DURING CONCRETE PLACEMENT USING STEEL ANCHOR PLATE AND TOP TEMPLATE. REMOVE TOP TEMPLATE (NOT SHOWN) AFTER CONCRETE SETS.

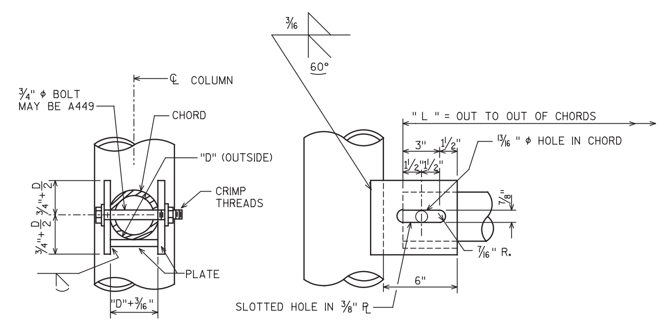

TOWER CONNECTION DETAIL

*ANGLE	WELD LENGTH	NO. OF BOLTS
● 2 1/2"x2 1/2"x1/4"	11"	3
3"x3"x3/16"	10"	3
3"x3"x1/4"	13"	4
3"x3"x5/16"	16 1/2"	5
3"x3"x3/8"	19 1/2"	6
4"x4"x1/4"	18"	5
4"x4"x5/16"	22"	6
4"x4"x3/8"	26"	8
4"x4"x7/16"	30"	9
4"x4"x1/2"	34"	10

● ONLY USED FOR BOXED END AND TRANSVERSE BRACING.

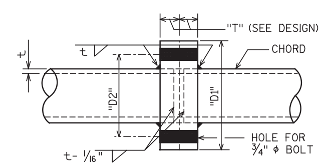

COUPLING DETAIL
(CONNECTION BOLTS OMITTED FOR CLARITY)

BASE PLATE & UPRIGHT COLUMN DETAILS

COLUMN O.D. X THK.	ANCHOR BOLTS	BASE PLATE THICKNESS (IN.)	STIFFENER PLATE THICKNESS (IN.)	STIFFENER PLATE HEIGHT (IN.)	t_W (IN.)
12.75"X0.406"	2"	2"	1"	13"	3/8"

NO.	DATE	REVISION	BY

STATE OF WISCONSIN
DEPARTMENT OF TRANSPORTATION
STRUCTURES DESIGN SECTION

STRUCTURE S-05-168

DRAWN BY VC | PLANS CK'D. CES

GALVANIZED STEEL SIGN BRIDGE DETAILS

SHEET 6 OF 9

8

FILE NAME 15-05-168.dgn PLOT DATE 12/15/2013 8:22:47 AM PLOT BY : Veronica Chavezv8 DRV :Pdf_bw_HS_by level.plt PEN :CEL.TextSub_ScreenControlByLevel.tbl

STATE PROJECT NUMBER
1133-09-71

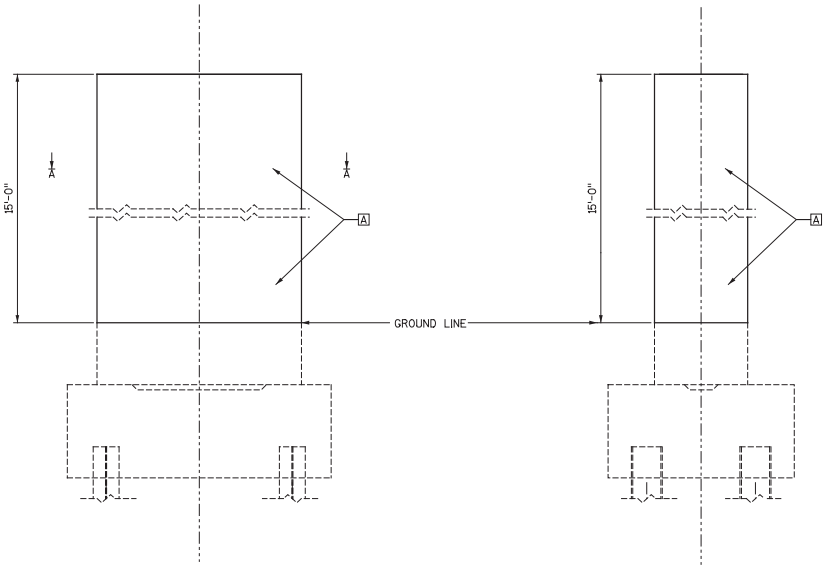

ELEVATION VIEW

END VIEW

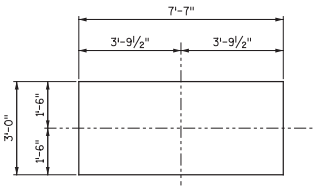

SECTION A - A

CONCRETE STAINING SCHEDULE

MARK	COLOR
A	BASE COLOR
B	ACCENT COLOR #1
D	ACCENT COLOR #3
E	ACCENT COLOR #4
F	ACCENT COLOR #5

*STAIN ALL BRICK PATTERN AREAS WITH BASE COLOR PRIOR TO STAINING WITH THE THREE BRICK ACCENT COLORS.

NO.	DATE	REVISION	BY

STATE OF WISCONSIN
DEPARTMENT OF TRANSPORTATION
STRUCTURES DESIGN SECTION

STRUCTURE S-05-168

DRAWN BY VC | PLANS CK'D. CES

CONCRETE TOWER 1 & 3 AESTHETIC DETAILS

SHEET 7 OF 9

A-8

8

8

FILE NAME :\S-05-168.dgn
PLOT DATE :12/8/2015 8:22:47 AM PLOT BY : Veronica Chavez-Vil DRV :Plot_bw_MS.by jewel.plt PEN :\CELTextSub_ScreenControlByLevel.tbl

STATE PROJECT NUMBER
1133-09-71

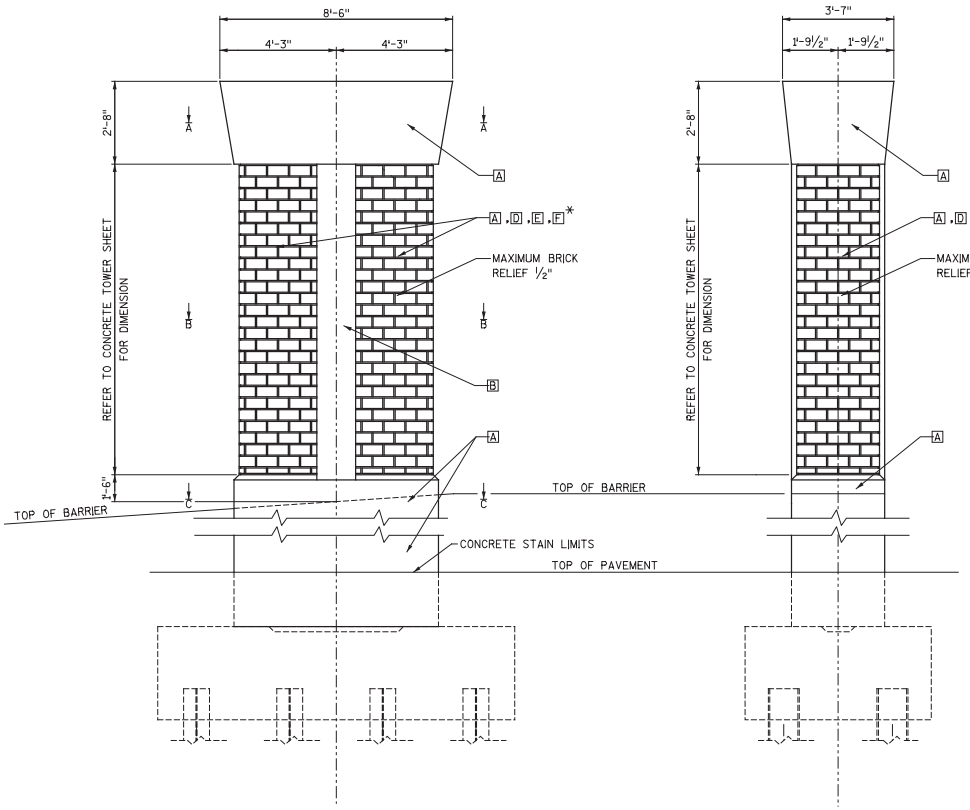

ELEVATION VIEW

END VIEW

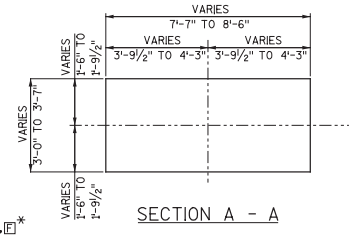

SECTION A - A

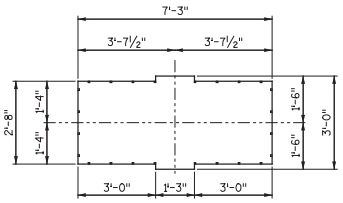

SECTION B - B

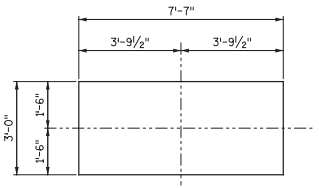

SECTION C - C

CONCRETE STAINING SCHEDULE

MARK	COLOR
A	BASE COLOR
B	ACCENT COLOR #1
D	ACCENT COLOR #3
E	ACCENT COLOR #4
F	ACCENT COLOR #5

*STAIN ALL BRICK PATTERN AREAS WITH BASE COLOR PRIOR TO STAINING WITH THE THREE BRICK ACCENT COLORS.

NO.	DATE	REVISION	BY

STATE OF WISCONSIN
DEPARTMENT OF TRANSPORTATION
STRUCTURES DESIGN SECTION

STRUCTURE S-05-168

DRAWN BY VC | PLANS CK'D. CES

CONCRETE TOWER 2 AESTHETIC DETAILS

SHEET 8 OF 9

A-9

8

8

FILE NAME :S-05-168.dgn
PLOT DATE :12/8/2015 8:22:47 AM PLOT BY : Veronica Chavez-R DRV :Plot_bw_MS.tbv levels.plt PEN :C:\EL_Text\Sub_Screen Control\ByLevel.tbl

USH-41 (S-05-168)
05-BROWN, WI

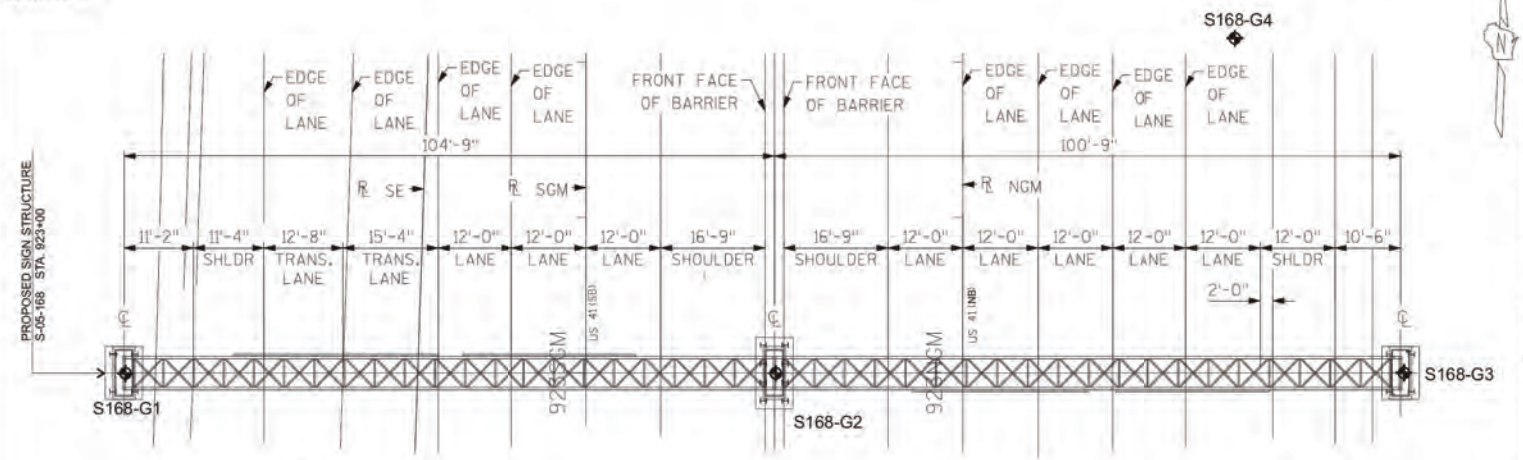

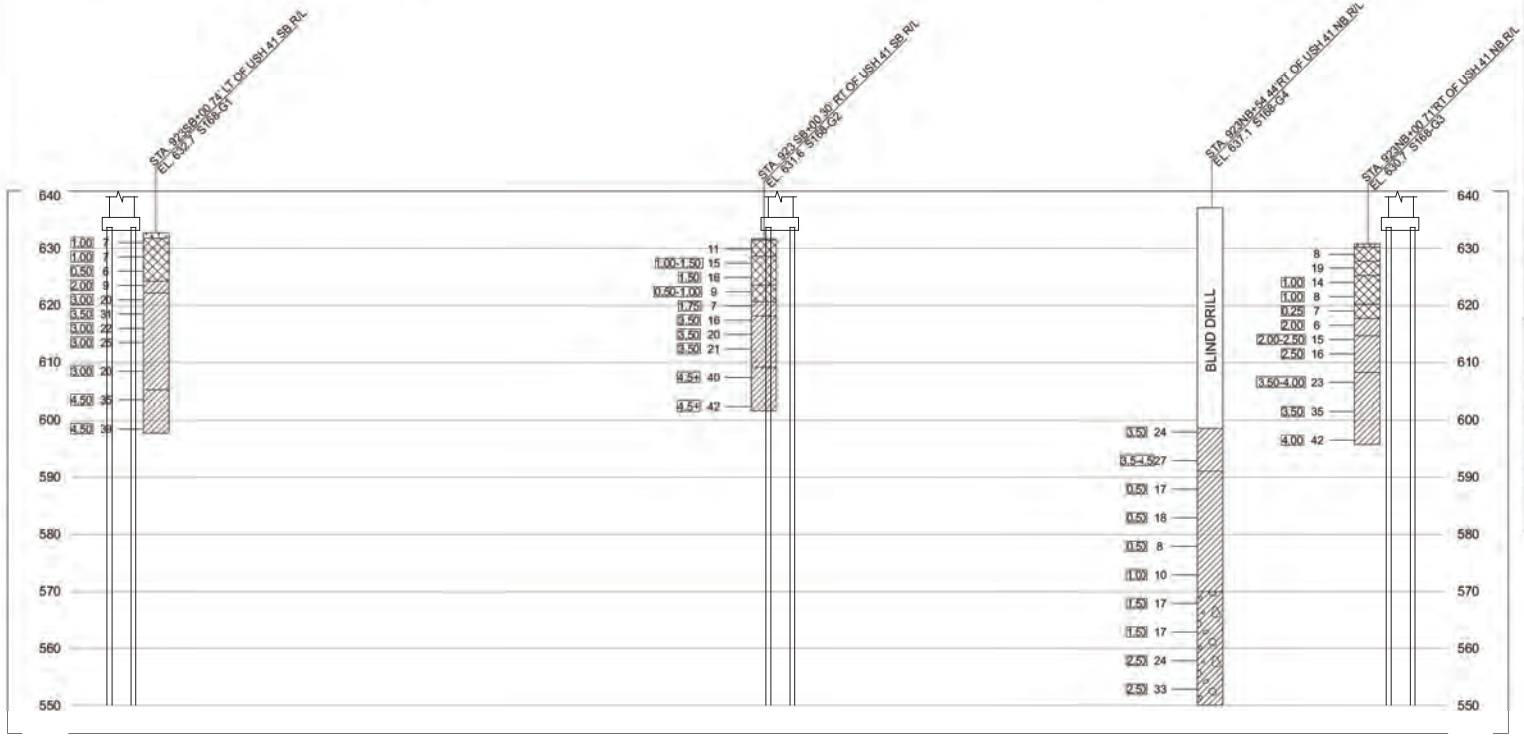

NOTE: BORING S168-G4 WAS TERMINATED DUE TO REFUSAL ON BOULDER OR POSSIBLE BEDROCK.

STATE PROJECT NUMBER

1133-09-71

ABBREVIATIONS

F — FINE M — MEDIUM C — COARSE
WS — WEATHERED SO — SOUND

MATERIAL SYMBOLS

TOPSOIL, SILT, FAT CLAY, SAND, PEAT, DOLOMITE, GRAVEL, CLAY, FILL

LEGEND OF PROBING

PROBING NO.
STA.
ELEVATION
7 AVERAGE BLOWS PER FOOT
REFUSAL 95/6

95/6=95 BLOWS FOR 6" PENETRATION
PROBING TAKEN WITH A 350# WT. FALLING 18" ON A 2" O.D. POINT.

LEGEND OF BORING

BORING NO.
ELEV.
STA.
UNCONFINED STRENGTH — 7.7
BLOWS PER FT. USING 140# WT. FALLING 30"
WASH SAMPLE
SHELBY TUBE — S.T.
GROUND WATER ELEVATION
NO GROUND WATER OBSERVED ABOVE THIS ELEVATION
SANDY GRAVEL
F. BOULDERS OR COBBLES
SAND
SILTY CLAY
SO LIMESTONE

UNLESS OTHERWISE SPECIFIED, THE BLOWS PER FOOT AT THE LOCATIONS INDICATED ARE BASED ON DRIVING A 2" O.D. X 1.4" I.D. SPLIT SPOON SAMPLER WITH A 140# HAMMER HAVING A FREE FALL OF 30". THE BLOW COUNT IS TAKEN IN UNDISTURBED SOIL IMMEDIATELY BELOW A CASED OR OPEN HOLE ELIMINATING SIDE FRICTION ON THE DRIVE PIPE.

SUBSURFACE EXPLORATION FOR FOUNDATION DESIGN AND BIDDERS INFORMATION

TO OBTAIN RELATIVE DATA CONCERNING THE CHARACTER OF MATERIAL IN AND UPON WHICH THE FOUNDATION MIGHT BE BUILT, BORINGS AND/OR SOUNDINGS WERE MADE AT POINTS APPROXIMATELY AS INDICATED ON THIS DRAWING. THE DATA PRESENTED HEREIN REPRESENTS THE FINDINGS OF THE SUBSURFACE EXPLORATIONS MADE. HOWEVER, BECAUSE THE DEPTHS INVESTIGATED ARE LIMITED AND THE AREA OF THE BORINGS AND/OR SOUNDINGS IS VERY SMALL IN RELATION TO THE ENTIRE AREA, THE WISCONSIN DEPARTMENT OF TRANSPORTATION DOES NOT WARRANT CONDITIONS BELOW THE DEPTHS INVESTIGATED OR THAT THE CLASSIFICATION OF MATERIAL ENCOUNTERED IN THESE INVESTIGATIONS IS NECESSARILY TYPICAL OF THE ENTIRE SITE.

NO.	DATE	REVISION	BY

STATE OF WISCONSIN
DEPARTMENT OF TRANSPORTATION
STRUCTURES DESIGN SECTION

STRUCTURE S-05-168

DRAWN BY RH | PLANS CK'D. DB

SUBSURFACE EXPLORATION

SHEET 9 OF 9

SCALE 1"=20'

SUMMARY OF CALCULATION PROCEDURES

The purpose of these calculations was to provide the structural design for the sign structure. The calculations were carried out under the direct supervision of a professional engineer registered in Wisconsin.

The design was completed under the following codes:

AASHTO Standard Specifications for Structural Supports for Highway Signs, Luminaires and Traffic Signals
AASHTO Standard Specifications for Highway Bridges, 17th Edition
Wisconsin Bridge Manual
Wisconsin Facilities Development Manual

The following publications were used as references:

ACI 318-05 Building Code and Commentary

The following material strengths were used in the calculations:

Concrete,	f'c = 3,500 psi
HS Reinforcement Bars,	fy = 60,000 psi

The following design loads were used in the calculations:

Dead loads are in accordance with shown physical structure.
Ice load – 3 psf to 1 face of the signs and around the full surface of the structural members.
Wind Load – 90 mph (3-second gust speed).

The soil properties used in the foundation design were as recommended in the geotechnical report.

All elements were designed based on the above and the supporting calculations are provided in this book.

Pile Group Analysis

Job: 6099
Description: Outside Towers 1 and 3
Time: 9:00 AM 10/31/2012

Designed By: CES
Checked By:
Program: Pile Group Analysis 2.2

P I L E G R O U P D A T A

```
Number of Piles                 : 4
Piles Fixed At Top?             : No
Piles Fixed At Bottom?          : No
Pile Width                      : 12.00 In
     Depth                      : 12.00 In
     Perimeter                  : 71.00 In
     Shaft Area                 : 18.40 In^2
     Point Area                 : 18.40 In^2
     Modulus, E                 : 3000.00 K/In^2
     Inertia, Ix                : 472.00 In^4
     Inertia, Iy                : 153.00 In^4
     Torsion, J                 : 1.80 In^4
Vertical Group Factor           : 1.00
Horizontal Group Factor         : 1.00

Horizontal Soil Data
     As                         : 150.00 K/Ft^3
     Bs                         : 200.00 K/Ft^3
     Exponent                   : 0.67

Vertical Soil Data
     Pile Point Subgrade Modulus : 200.00 K/Ft^3
     Skin Friction
          From :    0.000  Ft    To :    4.500  Ft     Shear :    1.000   K/Ft ^2    Slip :    0.100 In
                    4.500                 9.000                     1.000                       0.100
                    9.000                13.500                     1.000                       0.100
                   13.500                18.000                     1.000                       0.100
                   18.000                22.500                     1.000                       0.100
                   22.500                27.000                     1.000                       0.100
                   27.000                31.500                     1.000                       0.100
                   31.500                36.000                     1.000                       0.100
                   36.000                40.500                     1.000                       0.100
                   40.500                45.000                     1.000                       0.100
```

P I L E L O C A T I O N S

No.	X	Y	Z	Length	Bearing	Batter
Units:	Ft	Ft	Ft	Ft	Deg	
1	0.000	0.000	0.000	45.000	0.000	0.000
2	3.500	0.000	0.000	45.000	0.000	0.000
3	0.000	0.000	6.000	45.000	0.000	0.000
4	3.500	0.000	6.000	45.000	0.000	0.000

A P P L I E D F O R C E S

```
C.G. of Forces : 1.75 Ft (X), 0.00 Ft (Y), 3.00 Ft (Z)

Loads
          PX : 4.00 K
          PY : -90.00 K
          PZ : 25.00 K
          MX : 777.00 Ft-K
          MY : 21.00 Ft-K
          MZ : 124.00 Ft-K
```

A N A L Y S I S R E S U L T S

PILE NO	ELEM NO	MAX AXIAL	MAX MOMENT X	MAX MOMENT Y	MAX TORSION	POINT LOAD	MAX SKIN FRIC	DISPLACEMENTS DX	DZ	DY
Units:		K	K-Ft	K-Ft	K-Ft	K	K-Ft ^2	In	In	In
1	1	24.536	10.005	0.190	0.000	-0.001	-0.45574	-0.013	0.317	0.046
2	46	59.964	7.559	0.190	0.000	-0.003	-1.11381	-0.013	0.239	0.111
3	91	-104.964	10.005	-1.756	0.000	0.005	1.94967	0.120	0.317	-0.195
4	136	-69.536	7.559	-1.756	0.000	0.004	1.29160	0.120	0.239	-0.129

Vertical Equilibrium Check:
Sum of vertical load at top of piles: -90.000 (Compression)
Sum of vertical forces supported by skin friction: -89.996 (Compression)
Sum of vertical forces supported by the pile points: -0.005 (Compression)
Sum of vertical forces supported by 'horizontal' subgrade: 0.000 (Tension)

Pile Group Analysis

Job: 6099
Description: Outside Towers 1 and 3
Time: 9:57 AM 11/27/2012

Designed By: CES
Checked By:
Program: Pile Group Analysis 2.2

P I L E G R O U P D A T A

```
Number of Piles                 : 4
Piles Fixed At Top?             : No
Piles Fixed At Bottom?          : No
Pile Width                      : 12.00 In
     Depth                      : 12.00 In
     Perimeter                  : 71.00 In
     Shaft Area                 : 18.40 In^2
     Point Area                 : 18.40 In^2
     Modulus, E                 : 3000.00 K/In^2
     Inertia, Ix                : 472.00 In^4
     Inertia, Iy                : 153.00 In^4
     Torsion, J                 : 1.80 In^4
Vertical Group Factor           : 1.00
Horizontal Group Factor         : 1.00

Horizontal Soil Data
     As                         : 150.00 K/Ft^3
     Bs                         : 200.00 K/Ft^3
     Exponent                   : 0.67

Vertical Soil Data
     Pile Point Subgrade Modulus : 200.00 K/Ft^3
     Skin Friction
          From :    0.000  Ft    To :    4.500  Ft     Shear :    1.000   K/Ft ^2    Slip :    0.100 In
                    4.500                 9.000                     1.000                       0.100
                    9.000                13.500                     1.000                       0.100
                   13.500                18.000                     1.000                       0.100
                   18.000                22.500                     1.000                       0.100
                   22.500                27.000                     1.000                       0.100
                   27.000                31.500                     1.000                       0.100
                   31.500                36.000                     1.000                       0.100
                   36.000                40.500                     1.000                       0.100
                   40.500                45.000                     1.000                       0.100
```

P I L E L O C A T I O N S

No.	X	Y	Z	Length	Bearing	Batter
Units:	Ft	Ft	Ft	Ft	Deg	
1	0.000	0.000	0.000	45.000	0.000	0.000
2	3.500	0.000	0.000	45.000	0.000	0.000
3	0.000	0.000	6.000	45.000	0.000	0.000
4	3.500	0.000	6.000	45.000	0.000	0.000

A P P L I E D F O R C E S

```
C.G. of Forces : 1.75 Ft (X), 0.00 Ft (Y), 3.00 Ft (Z)

Loads
          PX : 5.00 K
          PY : -96.00 K
          PZ : 13.00 K
          MX : 400.00 Ft-K
          MY : 11.00 Ft-K
          MZ : 148.00 Ft-K
```

A N A L Y S I S R E S U L T S

PILE NO	ELEM NO	MAX AXIAL	MAX MOMENT X	MAX MOMENT Y	MAX TORSION	POINT LOAD	MAX SKIN FRIC	DISPLACEMENTS DX	DZ	DY
Units:		K	K-Ft	K-Ft	K-Ft	K	K-Ft ^2	In	In	In
1	1	-11.810	5.207	-0.469	0.000	0.001	0.21936	0.032	0.165	-0.022
2	46	30.476	3.926	-0.469	0.000	-0.002	-0.56608	0.032	0.124	0.057
3	91	-78.476	5.207	-1.488	0.000	0.004	1.45767	0.102	0.165	-0.146
4	136	-36.190	3.926	-1.488	0.000	0.002	0.67222	0.102	0.124	-0.067

Vertical Equilibrium Check:
Sum of vertical load at top of piles: -96.000 (Compression)
Sum of vertical forces supported by skin friction: -95.995 (Compression)
Sum of vertical forces supported by the pile points: -0.005 (Compression)
Sum of vertical forces supported by 'horizontal' subgrade: 0.000 (Tension)

Pile Group Analysis

Job: 6099
Description:
Time: 3:53 PM 11/28/2012

Designed By: VC
Checked By:
Program: Pile Group Analysis 2.2

PILE GROUP DATA

```
Number of Piles                 : 8
Piles Fixed At Top?             : No
Piles Fixed At Bottom?          : No
Pile Width                      : 12.00 In
     Depth                      : 12.00 In
     Perimeter                  : 71.00 In
     Shaft Area                 : 18.40 In^2
     Point Area                 : 18.40 In^2
     Modulus, E                 : 3000.00 K/In^2
     Inertia, Ix                : 472.00 In^4
     Inertia, Iy                : 153.00 In^4
     Torsion, J                 : 1.80 In^4
Vertical Group Factor           : 1.00
Horizontal Group Factor         : 1.00

Horizontal Soil Data
     As                         : 150.00 K/Ft^3
     Bs                         : 200.00 K/Ft^3
     Exponent                   : 0.67

Vertical Soil Data
     Pile Point Subgrade Modulus : 200.00 K/Ft^3
     Skin Friction
          From :    0.000  Ft    To :    4.500  Ft     Shear :    1.000  K/Ft ^2    Slip :    0.100 In
                    4.500                 9.000                    1.000                      0.100
                    9.000                13.500                    1.000                      0.100
                   13.500                18.000                    1.000                      0.100
                   18.000                22.500                    1.000                      0.100
                   22.500                27.000                    1.000                      0.100
                   27.000                31.500                    1.000                      0.100
                   31.500                36.000                    1.000                      0.100
                   36.000                40.500                    1.000                      0.100
                   40.500                45.000                    1.000                      0.100
```

PILE LOCATIONS

No.	X	Y	Z	Length	Bearing	Batter
Units:	Ft	Ft	Ft	Ft	Deg	
1	0.000	0.000	0.000	45.000	0.000	0.000
2	3.500	0.000	0.000	45.000	0.000	0.000
3	0.000	0.000	3.500	45.000	0.000	0.000
4	3.500	0.000	3.500	45.000	0.000	0.000
5	0.000	0.000	7.000	45.000	0.000	0.000
6	3.500	0.000	7.000	45.000	0.000	0.000
7	0.000	0.000	10.500	45.000	0.000	0.000
8	3.500	0.000	10.500	45.000	0.000	0.000

APPLIED FORCES

C.G. of Forces : 1.75 Ft (X), 0.00 Ft (Y), 5.25 Ft (Z)

Loads

```
PX : 6.00 K
PY : -144.00 K
PZ : 72.00 K
MX : 2338.00 Ft-K
MY : 200.00 Ft-K
MZ : 152.00 Ft-K
```

ANALYSIS RESULTS

PILE NO	ELEM NO	MAX AXIAL	MAX MOMENT X	MAX MOMENT Y	MAX TORSION	MAX POINT LOAD	MAX SKIN FRIC	DISPLACEMENTS DX	DZ	DY
Units:		K	K-Ft	K-Ft	K-Ft	K	K-Ft ^2	In	In	In
1	1	71.343	16.533	4.824	0.000	-0.004	-1.32517	-0.329	0.523	0.133
2	46	93.057	8.759	4.824	0.000	-0.005	-1.72850	-0.329	0.277	0.173
3	91	4.543	16.533	1.217	0.000	0.000	-0.08438	-0.083	0.523	0.008
4	136	26.257	8.759	1.217	0.000	-0.001	-0.48772	-0.083	0.277	0.049
5	181	-62.257	16.533	-2.391	0.000	0.003	1.15640	0.163	0.523	-0.116
6	226	-40.543	8.759	-2.391	0.000	0.002	0.75307	0.163	0.277	-0.075
7	271	-129.057	16.533	-5.999	0.000	0.007	2.39718	0.409	0.523	-0.240
8	316	-107.343	8.759	-5.999	0.000	0.005	1.99385	0.409	0.277	-0.200

Vertical Equilibrium Check:
Sum of vertical load at top of piles: -144.000 (Compression)
Sum of vertical forces supported by skin friction: -143.993 (Compression)
Sum of vertical forces supported by the pile points: -0.007 (Compression)
Sum of vertical forces supported by 'horizontal' subgrade: 0.000 (Tension)

COLLINS ENGINEERS INC

PROJECT 5-05-166 Outside Towers
CLIENT

JOB
SHEET NO. OF
BY MJH DATE
CHKD. BY DATE

Loads (Max Case DL+W)

① 24.6 (Uplift)
② 60.0 (Uplift)
③ -105.0
④ -69.6

(Max Case DL+WL+JL)

① -11.9
② 30.5 (Uplift)
③ -78.5
④ -36.2

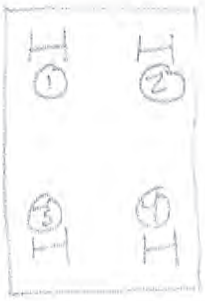

→ Max Uplift = 60.0 kips

Use 4 #4 bars = 75.8 kips > 60.0 kips ✓

→ Max Pile Loads = 78.5 + 11.9 = 90.4 kips << 665 kips

So #5 top & bottom ok for bending

COLLINS ENGINEERS INC

PROJECT 3' Deep Footing Shear
CLIENT

JOB
SHEET NO. OF
BY MJH DATE 11/28/12
CHKD. BY DATE

$d_p \approx 3' - 1' - 4'' \approx 20'' \rightarrow \frac{d_p}{2} = 10''$

$b_1 = 3'-0'' + 20'' = 4'-8'' = 56''$

$b_2 = 7'-7'' + 20'' = 9'-3'' = 111''$

$A_p = 2(b_1 + b_2)\,d = 2(4'-8'' + 9'-3'')\,20'' = 6680\ in^2$

$V_u = \frac{P_u - R}{A_p}$

$P_u = \Sigma$ Pile Loads

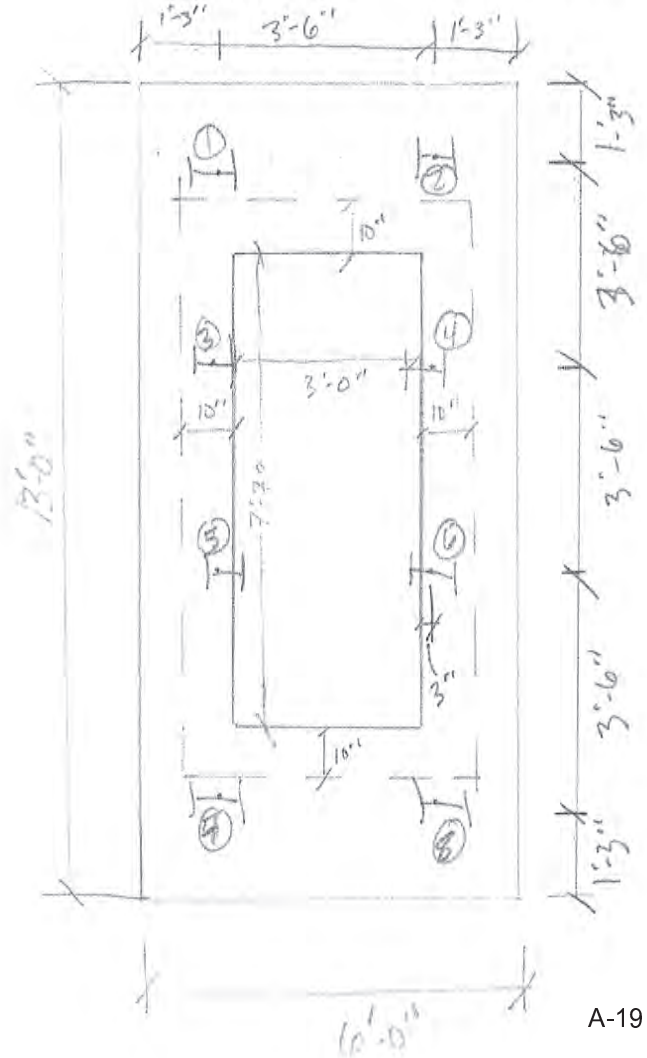

DL+WL Case		D
①	71.4	71.4
②	93.1	93.1
③	4.6	(0.3) 1.4
④	26.3	(0.3) 7.9
⑤	-62.3	(0.3) 18.7
⑥	-40.6	(0.3) 12.2
⑦	-129.1	129.1
⑧	-107.4	107.4

$\Sigma = 441.2$

Interpolation Factor $= \frac{3''}{15''} = 0.3$

$P_u = 1.3P = 1.3(441.2) = \boxed{573.6k}$

Appendix B – Construction Plans

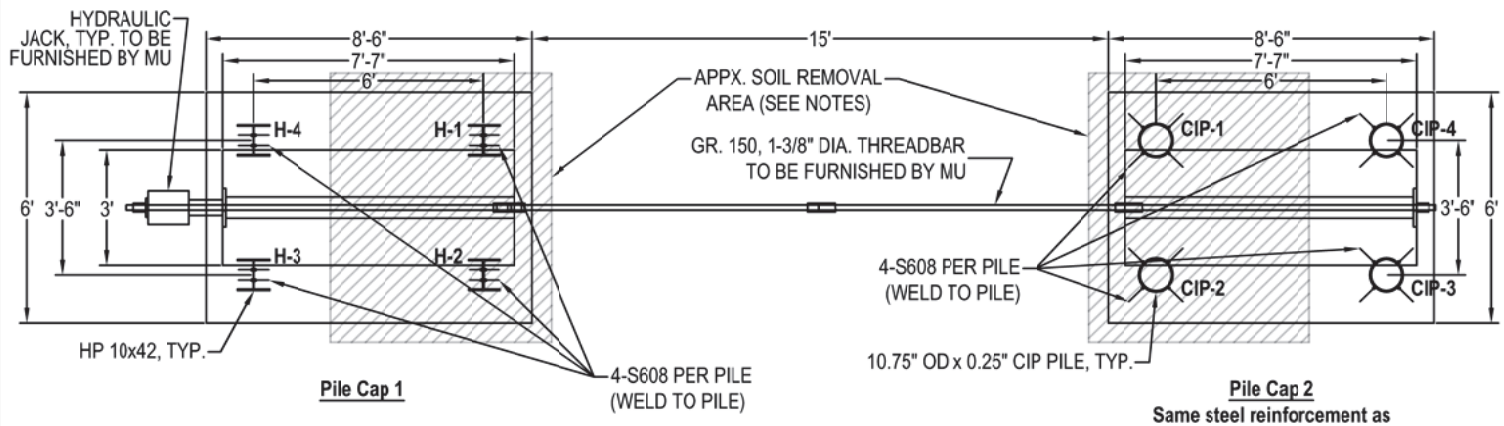

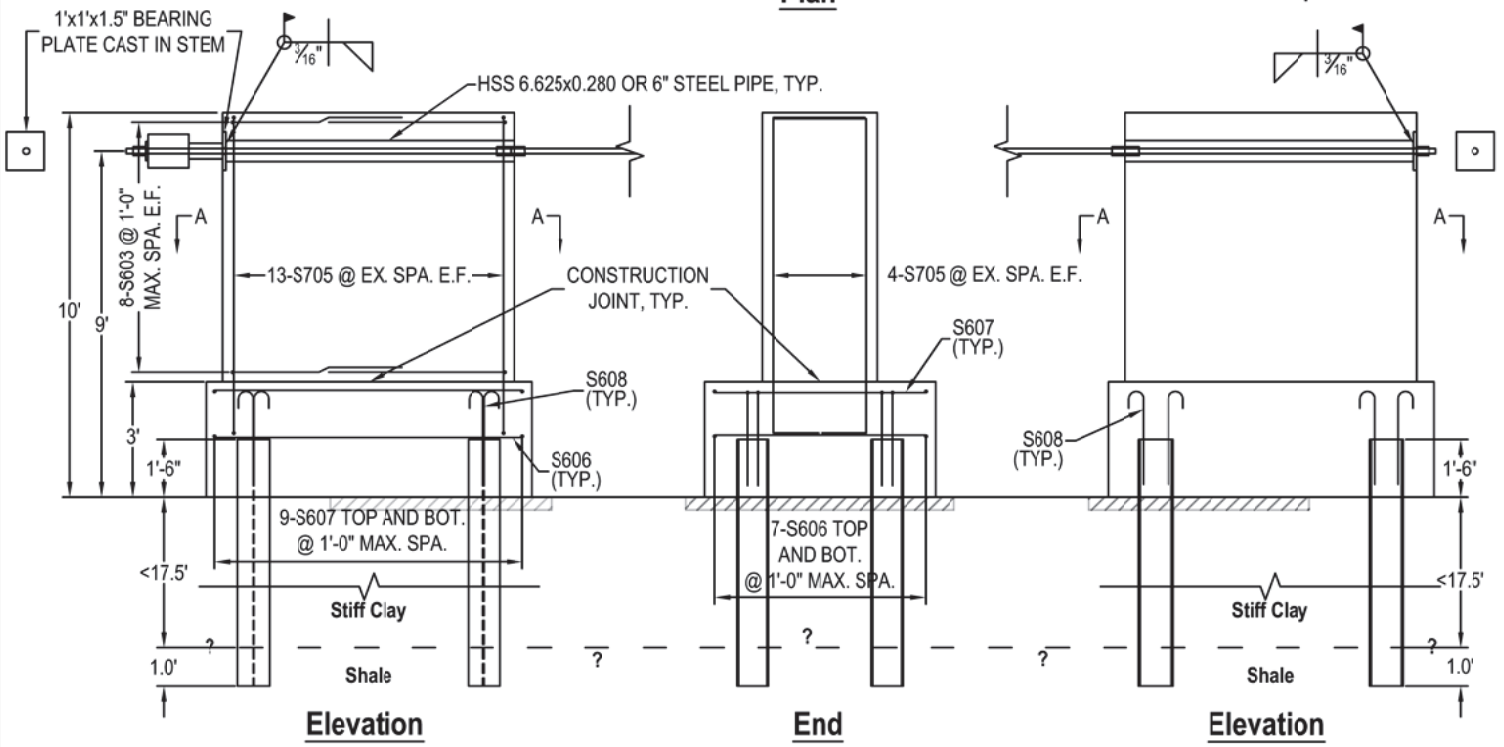

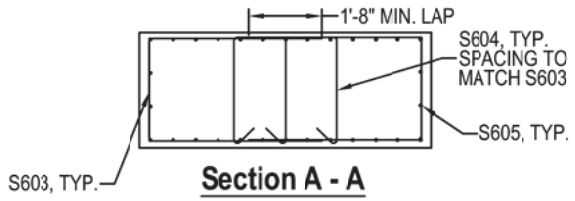

Notes

Drawing shall not be scaled.
"E.F." = each face.
Construction Joints: All construction joints shall be formed by a 2" x 6" x 1'-6" long beveled keyway.
Concrete: All concrete shall have f'c = 4,000 psi. Use 3" concrete cover for pile caps unless otherwise specified.
Steel Reinforcement: Use Grade 60 (fy = 60,000 psi) reinforcing steel. Steel reinforcement scheme is shown for Pile Cap 1. The same scheme shall be applied to Pile Cap 2. Details of reinforcement are on Sheet 2.
Driven H-Piles: Four HP10x42 piles shall be driven to depth shown on plans to support Pile Cap 1. See "Pile Driving" section below. Steel HP pile material shall be ASTM A572, fy = 50,000 psi. One 1-in. Sch. 40 steel pipe to be supplied by university shall be tack welded to the inside corner of each H-Pile by the contractor prior to driving.
Driven CIP Piles: Four 10.75" OD closed-ended steel pipe piles shall be driven to the depth shown on plans to support Pile Cap 2. Steel pipe piles shall be ASTM A252, Grade 2, and steel pipe pile thickness shall be 0.25". An oversized steel plate with minimum thickness of 0.75" shall be welded to bottom of pipe piles. CIP piles shall be filled with a neat cement grout per the pile driving note below.
Pile Driving:
General: 20-ft long piles shall be driven 1 ft into shale. The top of shale is estimated to be no more than 17 ft deep. Piles shall be driven with a single-acting diesel hammer. University engineer shal approve hammer specifications prior to construction. University engineer shall be on site during pile driving and may terminate driving before piles reach plan depth.
Order of Pile Driving: University to apply instrumentation to piles with welding by Contractor between steps below:
1. CIP-1
2. H-1
3. CIP-2, CIP-3 CIP-4
4. H-2, H-3, H-4

Pile Cutoff and CIP Pile Pouring: After driving, any extra length shall be removed to establish 1'-6" pile head embedment into pile cap for all piles. After driving CIP piles, University will place 1-in. instrumented steel pipe into the center of each CIP pile. The contractor shall fill the CIP with a neat cement grout after the instrumented pipe is in place.
Soil Removal: After pile driving, approximately 4 in. of soil shall be removed from the ground surface as shown in drawing. Hole shall be filled with sand during placement of concrete. Sand shall be blown out from under cured caps to maintain a gap between the lowered ground surface and the cap in the soil removal area shown in the drawing.
Welding: Welding of reinforcement bars to the piles and of steel pipe to bearing plates shall be made by a certified welder using low hydrogen electrodes.
Forms: Contractor shall design and supply forms for construction of concrete piles caps and stems.
Instrumentation: University engineer will apply instrumentation devices to H-Piles with welding by Contractor and to instrumented pipe within CIP per note above. Application of instrumentation is anticipated to cause delays in pile driving operation. Devices to be supplied by University.

B-2

5 4 3 2 1 0 5
1" = 5'

Piles and Pile Caps for Lateral Load Test
WisDOT Performance of Pile Supported Sign Structures
Date: April 16, 2014
Sheet 1 of 2

University of Missouri
Civil and Environmental Engineering

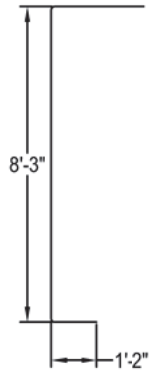

S705

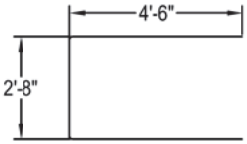

S603

S604

Bill of Bars

Note: The first digit of the bar mark signifies the bar size.

BAR MARK	TOTAL NO. REQ'D**	LENGTH	BENDS	LOCATION
S603	32	11'-8"	2 @ 90-deg.	STEM HORZ. STIRRUP
S604	48	3'-0 1/2"	1 @ 90-deg.; 1 @ 135-deg.	STEM HORZ. CROSSTIE
S705	60	11'-9"	2 @ 90-deg.	STEM VERTICAL
S606	28	8'-0"		CAP LONGITUDIAL
S607	36	5'-6"		CAP TRANSVERSE
S608	32	3'-1"	1 @ 180-deg.	WELDED TO PILE

**Total is for both pile caps and stems.

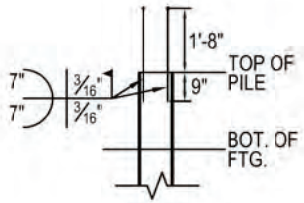

CIP Pile

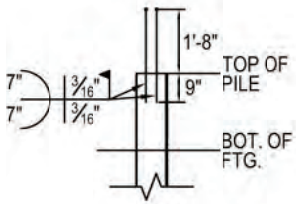

H-Pile

Pile Head Details

Form T-737+(RMA)
Rev. 05/01

MISSOURI DEPARTMENT OF TRANSPORTATION
Construction and Materials

BORING DATA (CORE & SPT)

Sheet 7 of 9c

Job No.:	TMTIPR03				
County:	Johnson	**Route:**	I3	**Design:**	MTI-WAR-8
Over:	Route 50 over Route 13			**Skew:**	Right Angles
Logged by:	R. Todd			**Operator:**	Donahoe
Equipment:	Failing 1500			**Drillers Hole No.:**	H-09-75
Hole Stab. by:	Drilling Fluids			**Date of Work:**	12/2/2009
Automatic Hammer Efficiency:	80 %			**Drill No.:**	G-7888

Bent	Station	Location	Surface Elevation, ft.
MTI-WAR-8	209+77.7	179.5' LT.	781.2
Longitude:	-93.688409W	Latitude:	38.773849N

TEST DATA

Depth, ft.	Sample No.	Shelby Tube	P.P., tsf	Tv., tsf	Wn%
3.0	9MRNT633	3"	4.0	0.85	17.8
6.0	9MRNT634	3"	2.5	--	--
13.5	9MRNT635	3"	6.0	0.9+	12.9

LOG OF MATERIALS*

0.0-10.0'	Grayish-brown mottled fat clay, scattered gravel, moist, very stiff.
10.0-14.5'	Brown mottled fat clay, trace shale, scattered gravel, moist, very stiff.
14.5-19.5'	Tan to gray thinly laminated shale, soft.
19.5-28.0'	Gray thinly laminated shale, soft.
28.0-35.0'	Gray shale, thinly laminated, soft.
35.0-35.2'	Coal.
35.2-39.5'	Gray poorly laminated clay shale, soft, (underclay).
39.5-53.3'	Gray thinly laminated shale.
53.3-54.1'	Black shale, soft.
54.1-57.5'	Coal.
57.5-60.1'	Black shale, soft.
60.1-64.5'	Gray poorly laminated clay shale, soft, (underclay).

CORING LOG (NX Double Tube Barrel)

From	To	Run	Rec	Loss	% RQD	Notes
14.5	19.5	5.0	5.0	0.0	Shale	
19.5	24.5	5.0	5.0	0.0	Shale	
24.5	29.5	5.0	4.8	0.2	Shale	
29.5	34.5	5.0	4.4	0.6	Shale	
34.5	39.5	5.0	5.0	0.0	Shale	
39.5	44.5	5.0	5.0	0.0	Shale	
44.5	49.5	5.0	4.2	0.8	Shale	
49.5	54.5	5.0	4.8	0.2	Shale	
54.5	59.5	5.0	5.0	0.0	Shale	
59.5	64.5	5.0	5.0	0.0	Shale	

WATER TABLE OBSERVATIONS

Date	Time Change	Depth Hole Open	Depth To Water

Coordinate System:	Geographic	**Coordinate Zone:**	
Coordinate Datum:	NAD 83 (CONUS)	**Coordinate Units:**	U.S. Survey Feet **Coordinate Projection Factor:**

$N_{60} = (Em/60)Nm$

N_{60} - Corrected N value for standard 60% SPT efficiency.
Em - Measured transfer efficiency in percent.
Nm - Observed N-value.

* Persons using this information are cautioned that the materials shown are determined by the equipment used and accuracy of the "log of materials" is limited thereby and by judgment of the operator.
THIS INFORMATION IS FOR DESIGN PURPOSES ONLY

5 4 3 2 1 0 5
1" = 5'

Piles and Pile Caps for Lateral Load Test
WisDOT Performance of Pile Supported Sign Structures
Date: April 16, 2014 Sheet 2 of 2

University of Missouri
Civil and Environmental Engineering

Appendix C – Driven Pile Logs

DRIVEN PILE LOG

PROJECT: WisDOT Sign Foundations **PROJECT NO.:**

PILE CONTRACTOR: Boone Construction Co.

WEATHER: 80s, sunny **DATE:** 6/2/2014

BRIDGE NO.: N/A	**DESIGN LOAD (TONS):** 50-60
BENT NO. CIP Cap	
PILE NO.: CIP-1	**PILE TYPE:** CIP (Cast-in-Place; 10.75" OD x 0.25" wall closed-ended pipe backfilled with concrete)

Depth (ft)	Blow ft.	Depth (ft)	in. 5 blows
1	4	13.75	2.5
2	6	13.96	1.875
3	7	14.11	1.625
4	10		
5	8		
6	8		
7	8		
8	8		
9	8		
10	9		
11	8		
12	12		
13	10		
14	17		
15	*44*	<----11 for 3"	
16			
17			
18			
19			
20			
21			
22			
23			
24			
25			
26			
27			
28			
29			
30			
31			
32			
33			
34			
35			
36			
37			
38			
39			
40			

Hammer: ICE 32-S
- rated energy **26,000** ft-lbs
- weight of ram **3,000** lbs
- striker plate **200** lbs
- helmet **610** lbs
- pile cap **605** lbs

Original pile length **20 ft**
- Pile Tip Depth 14'-3"
- Stick-Up Length 5'-9"
- Date Cast/Poured 6/2/14
- Date Driven 6/2/14
  - Time Start 12:49
  - Time Stop 12:54
- Driving Delay Time 1 min
- Actual Driving Time ~4 mins

Termination Parameters
- Ram Stroke 7.5'
- Pile Set 0.325"

ENR Capacity

53 tons

REMARKS:

DRIVEN PILE LOG

PROJECT: WisDOT Sign Foundations **PROJECT NO.:**

PILE CONTRACTOR: Boone Construction Co.

WEATHER: 80s, sunny **DATE:** 6/2/2014

BRIDGE NO.: N/A	**DESIGN LOAD (TONS):** 50-60
BENT NO. CIP Cap	
PILE NO.: CIP-2	**PILE TYPE:** CIP (Cast-in-Place; 10.75" OD x 0.25" wall closed-ended pipe backfilled with concrete)

Depth (ft)	Blow ft.	Depth (ft)	in. 5 blows
1	9	13.04	4.5
2	7	13.42	3.75
3	6	13.73	3
4	11	13.98	2.25
5	10	14.17	2
6	10		
7	7		
8	8		
9	7		
10	8		
11	9		
12	10		
13	11		
14	12		
15	*48*	<----16 for 4"	
16			
17			
18			
19			
20			
21			
22			
23			
24			
25			
26			
27			
28			
29			
30			
31			
32			
33			
34			
35			
36			
37			
38			
39			
40			

Hammer: ICE 32-S
- rated energy **26,000** ft-lbs
- weight of ram **3,000** lbs
- striker plate **200** lbs
- helmet **610** lbs
- pile cap **605** lbs

Original pile length **20 ft**
- Pile Tip Depth 14'-4"
- Stick-Up Length 5'-8"
- Date Cast/Poured 6/2/14
- Date Driven 6/2/14
  - Time Start 12:39
  - Time Stop 12:45
- Driving Delay Time 2 mins
- Actual Driving Time ~4 mins

Termination Parameters
- Ram Stroke 7.5'
- Pile Set 0.4"

ENR Capacity

45 tons

REMARKS:

DRIVEN PILE LOG

PROJECT: WisDOT Sign Foundations **PROJECT NO.:**

PILE CONTRACTOR: Boone Construction Co.

WEATHER: 80s, sunny **DATE:** 6/2/2014

BRIDGE NO.: N/A	**DESIGN LOAD (TONS):** 50-60
BENT NO. CIP Cap	
PILE NO.: CIP-3	**PILE TYPE:** CIP (Cast-in-Place; 10.75" OD x 0.25" wall closed-ended pipe backfilled with concrete)

Depth (ft)	Blow ft.	Depth (ft)	in. 5 blows
1	5	13.90	2.5
2	5	14.10	1.75
3	8	14.25	1.625
4	10		
5	10		
6	10		
7	8		
8	7		
9	7		
10	8		
11	9		
12	11		
13	11		
14	16		
15	*36*	<----14 for 4-5/8"	
16			
17			
18			
19			
20			
21			
22			
23			
24			
25			
26			
27			
28			
29			
30			
31			
32			
33			
34			
35			
36			
37			
38			
39			
40			

Hammer: ICE 32-S
- rated energy **26,000** ft-lbs
- weight of ram **3,000** lbs
- striker plate **200** lbs
- helmet **610** lbs
- pile cap **605** lbs

Original pile length **20 ft**
- Pile Tip Depth 14'-4-5/8"
- Stick-Up Length 5'-7-3/8"
- Date Cast/Poured 6/2/14
- Date Driven 6/2/14
  - Time Start 12:57
  - Time Stop 13:01
- Driving Delay Time 0 min
- Actual Driving Time ~4 mins

Termination Parameters
- Ram Stroke 7.5'
- Pile Set 0.325"

ENR Capacity

53 tons

REMARKS:

DRIVEN PILE LOG

PROJECT: WisDOT Sign Foundations **PROJECT NO.:**

PILE CONTRACTOR: Boone Construction Co.

WEATHER: 80s, sunny **DATE:** 6/2/2014

BRIDGE NO.: N/A	**DESIGN LOAD (TONS):** 50-60
BENT NO. CIP Cap	
PILE NO.: CIP-4	**PILE TYPE:** CIP (Cast-in-Place; 10.75" OD x 0.25" wall closed-ended pipe backfilled with concrete)

Depth (ft)	Blow ft.	Depth (ft)	in. 5 blows
1	5	13.48	3.5
2	4	13.77	3
3	6	14.02	2.5
4	11	14.23	2
5	10	14.40	1.75
6	10		
7	9		
8	9		
9	11		
10	11		
11	11		
12	12		
13	14		
14	16		
15	*35*	<----19 for 6-1/2"	
16			
17			
18			
19			
20			
21			
22			
23			
24			
25			
26			
27			
28			
29			
30			
31			
32			
33			
34			
35			
36			
37			
38			
39			
40			

Hammer: ICE 32-S
- rated energy **26,000** ft-lbs
- weight of ram **3,000** lbs
- striker plate **200** lbs
- helmet **610** lbs
- pile cap **605** lbs

Original pile length **20 ft**
- Pile Tip Depth 14'-6-1/2"
- Stick-Up Length 5'-5-1/2"
- Date Cast/Poured 6/2/14
- Date Driven 6/2/14
  - Time Start 13:06
  - Time Stop 13:09
- Driving Delay Time 0 min
- Actual Driving Time ~3 mins

Termination Parameters
- Ram Stroke 7.5'
- Pile Set 0.35"

ENR Capacity

50 tons

REMARKS:

DRIVEN PILE LOG

PROJECT: WisDOT Sign Foundations **PROJECT NO.:**

PILE CONTRACTOR: Boone Construction Co.

WEATHER: low 90s, sunny **DATE:** 6/3/2014

BRIDGE NO.: N/A	**DESIGN LOAD (TONS):** 50-60
BENT NO. H-Pile Cap	
PILE NO.: HP-1	**PILE TYPE:** HP10x42

Depth (ft)	Blow ft.	Depth (ft)	in. 5 blows
1	4	13.39	3.5
2	5	13.68	3.25
3	5	13.95	2.75
4	8	14.18	1.875
5	10		
6	8		
7	8		
8	9		
9	8		
10	9		
11	10		
12	10		
13	12		
14	15		
15	*39*	<----13 for 4"	
16			
17			
18			
19			
20			
21			
22			
23			
24			
25			
26			
27			
28			
29			
30			
31			
32			
33			
34			
35			
36			
37			
38			
39			
40			

Hammer: ICE 32-S
- rated energy **26,000** ft-lbs
- weight of ram **3,000** lbs
- striker plate **200** lbs
- helmet **610** lbs
- pile cap **605** lbs

Original pile length **19'-5"**
- Pile Tip Depth 14'-4"
- Stick-Up Length 5'-1"
- Date Cast/Poured N/A
- Date Driven 6/3/14
  - Time Start 12:57
  - Time Stop 13:00
- Driving Delay Time 0 mins
- Actual Driving Time 3 mins

Termination Parameters
- Ram Stroke 7.5'
- Pile Set 0.375"

ENR Capacity

47 tons

REMARKS:

DRIVEN PILE LOG

PROJECT: WisDOT Sign Foundations **PROJECT NO.:**

PILE CONTRACTOR: Boone Construction Co.

WEATHER: low 90s, sunny **DATE:** 6/3/2014

BRIDGE NO.: N/A	**DESIGN LOAD (TONS):** 50-60
BENT NO. H-Pile Cap	
PILE NO.: HP-2	**PILE TYPE:** HP10x42

Depth (ft)	Blow ft.	Depth (ft)	in. 5 blows
1	4		
2	5		
3	5		
4	8		
5	8		
6	7		
7	7		
8	6		
9	7		
10	7		
11	9		
12	9		
13	10		
14	15		
15	*24*	<----10 for 5"	
16			
17			
18			
19			
20			
21			
22			
23			
24			
25			
26			
27			
28			
29			
30			
31			
32			
33			
34			
35			
36			
37			
38			
39			
40			

Hammer: ICE 32-S
- rated energy **26,000** ft-lbs
- weight of ram **3,000** lbs
- striker plate **200** lbs
- helmet **610** lbs
- pile cap **605** lbs

Original pile length **23'-8"**
- Pile Tip Depth 14'-5"
- Stick-Up Length 9'-3"
- Date Cast/Poured N/A
- Date Driven 6/3/14
  - Time Start 12:41
  - Time Stop 12:44
- Driving Delay Time 0 mins
- Actual Driving Time 3 mins

Termination Parameters
- Ram Stroke 7.5'
- Pile Set ?? 0.4" ??

ENR Capacity

45 ?? tons

No marks were made on pile before refusal. AZB noticed abrupt increase in stroke and decrease in observed pile set and quickly indicated to crew to terminate driving.

REMARKS:

DRIVEN PILE LOG

PROJECT: WisDOT Sign Foundations **PROJECT NO.:**

PILE CONTRACTOR: Boone Construction Co.

WEATHER: low 90s, sunny **DATE:** 6/3/2014

BRIDGE NO.: N/A	**DESIGN LOAD (TONS):** 50-60
BENT NO. H-Pile Cap	
PILE NO.: HP-3	**PILE TYPE:** HP10x42

Depth (ft)	Blow ft.	Depth (ft)	in. 5 blows
1	5	14.35	2.5
2	5	14.56	2.75
3	5	14.79	3
4	7	15.04	2.75
5	7	15.27	2.75
6	6		
7	7		
8	8		
9	7		
10	8		
11	8		
12	9		
13	10		
14	17		
15	*21*	<----31 for 1'6"	
16	*21*	<----31 for 1'6"	
17			
18			
19			
20			
21			
22			
23			
24			
25			
26			
27			
28			
29			
30			
31			
32			
33			
34			
35			
36			
37			
38			
39			
40			

Hammer: ICE 32-S

rated energy **26,000** ft-lbs

weight of ram **3,000** lbs

striker plate **200** lbs

helmet **610** lbs

pile cap **605** lbs

Original pile length **20'-5"**

Pile Tip Depth 15'-6"

Stick-Up Length 4'-11"

Date Cast/Poured N/A

Date Driven 6/3/14

Time Start 12:32

Time Stop 12:36

Driving Delay Time 0 mins

Actual Driving Time 4 mins

Termination Parameters

Ram Stroke 7.5'

Pile Set 0.55"

ENR Capacity

35 tons

REMARKS:

DRIVEN PILE LOG

PROJECT: WisDOT Sign Foundations **PROJECT NO.:**

PILE CONTRACTOR: Boone Construction Co.

WEATHER: low 90s, sunny **DATE:** 6/3/2014

BRIDGE NO.: N/A	**DESIGN LOAD (TONS):** 50-60
BENT NO. H-Pile Cap	
PILE NO.: HP-4	**PILE TYPE:** HP10x42

Depth (ft)	Blow ft.	Depth (ft)	in. 5 blows
1	4	13.33	2.5
2	5	13.54	2.5
3	4	13.75	2.5
4	8	13.96	3
5	9	14.21	1.5
6	6		
7	5		
8	7		
9	6		
10	10		
11	7		
12	10		
13	10		
14	16		
15	18		
16	*108*	<----18 for 2"	
17		BUT right after restarting hammer	
18		(BPF likely less if had kept driving.)	
19			
20			
21			
22			
23			
24			
25			
26			
27			
28			
29			
30			
31			
32			
33			
34			
35			
36			
37			
38			
39			
40			

Hammer: ICE 32-S
- rated energy **26,000** ft-lbs
- weight of ram **3,000** lbs
- striker plate **200** lbs
- helmet **610** lbs
- pile cap **605** lbs

Original pile length **18'-9"**
- Pile Tip Depth 15'-2"
- Stick-Up Length 3'-7"
- Date Cast/Poured N/A
- Date Driven 6/3/14
  - Time Start 12:18
  - Time Stop 12:25
- Driving Delay Time 4 mins
- Actual Driving Time 3 mins

Termination Parameters
- Ram Stroke 6.5'
- Pile Set 0.3"

ENR Capacity

49 tons

Driving delay to remove hanger for instrument cables, which was about to hit ground.

Only saw one ring on ram -- stroke less.

REMARKS:

Wisconsin Highway Research Program
University of Wisconsin – Madison
1415 Engineering Drive
Madison, WI 53706
http://wisdotresearch.wi.gov/whrp